INTEGRATED SEISMIC RISK ANALYSIS FOR EARTH DAMS

by

M. K. Yegian
E. A. Marciano
V. G. Ghahraman

Report No. CE - 88 - 15

Department of Civil Engineering
Northeastern University
Boston, Massachusetts, 02115

Sponsored by the National Science Foundation
Grant No. DFR - 8412124
December 1988

50272-101

REPORT DOCUMENTATION PAGE	1. REPORT NO. CE-88-15	2.	3. Recipient's Accession No.

4. Title and Subtitle

Integrated Seismic Risk Analysis for Earth Dams

5. Report Date

December 1988

6.

7. Author(s)

M.K.Yegian, E.A.Marciano, V.G.Ghahraman

8. Performing Organization Rept. No.

9. Performing Organization Name and Address

Department of Civil Engineering
Northeastern University
Room 420 Snell Engineering Center
Boston, MA 02115

10. Project/Task/Work Unit No.

11. Contract(C) or Grant(G) No.

(C)

(G) DFR - 8412124

12. Sponsoring Organization Name and Address

Earthquake Hazard Mitigation Program
National Science Foundation
Washington, D.C. 20550

13. Type of Report & Period Covered

Final

14.

15. Supplementary Notes

16. Abstract (Limit: 200 words)

There are many sources of uncertainty involved in the seismic design or safety evaluation of an earth dam. Even when conservative assumptions and selections of design parameters are made, there will always be a probability that the performance of the dam during its lifetime may not be as predicted.

To evaluate the overall seismic risk of damage to or failure of earth dams an Integrated Seismic Risk Analysis procedure was developed. The analysis combines the probabilistic prediction of occurrence of seismic events with probabilistic prediction of the performance of a dam experiencing these events and provides estimates of seismic risk. In this research techniques were employed to express the Seismic Hazard Analysis results in terms of joint occurrence of peak ground acceleration and earthquake magnitude or associated number of equivalent cycles. Furthermore, a probabilistic procedure for the calculation of permanent deformation of earth dams was developed in which the seismic event is characterized in terms of acceleration, number of cycles and predominant period of motion.

The application of these procedures provides estimates of relative risks, which are useful in design and decision analysis, where trade-offs are made between the cost of increasing the seismic resistance and the risks associated with the consequences of seismic damage. In addition, risk-based safety evaluation enables identification of the most important parameters, assumptions, hypotheses and safety criterion affecting the evaluation of the safety of the dam and avoids compounding of conservatism.

17. Document Analysis a. Descriptors

*Earth Dams
*Risk Analysis
*Probability
*Seismic Risk
*Permanent Deformations

b. Identifiers/Open-Ended Terms

*Soil Dynamics
*Earthquake Engineering
*Damage Probabilities

c. COSATI Field/Group

18. Availability Statement	19. Security Class (This Report)	21. No. of Pages
Release Unlimited	Unclassified	142
	20. Security Class (This Page) Unclassified	22. Price

Integrated Seismic Risk Analysis For Earth Dams

ABSTRACT

There are many sources of uncertainty involved in the seismic design or safety evaluation of an earth dam. Even when conservative assumptions and selections of design parameters are made, there will always be a probability that the performance of the dam during its lifetime may not be as predicted.

To evaluate the overall seismic risk of damage to or failure of earth dams an Integrated Seismic Risk Analysis procedure was developed. The analysis combines the probabilistic prediction of occurrence of seismic events with probabilistic prediction of the performance of a dam experiencing these events and provides estimates of seismic risk. In this research techniques were employed to express the Seismic Hazard Analysis results in terms of joint occurrence of peak ground acceleration and earthquake magnitude or associated number of equivalent cycles. Furthermore, a probabilistic procedure for the calculation of permanent deformation of earth dams was developed in which the seismic event is characterized in terms of acceleration, number of cycles and predominant period of motion.

The application of these procedures provides estimates of relative risks, which are useful in design and decision analysis, where trade-offs are made between the cost of increasing the seismic resistance and the risks associated with the consequences of seismic damage. In addition, risk-based safety evaluation enables identification of the most important parameters, assumptions, hypotheses and safety criterion affecting the evaluation of the safety of the dam and avoids compounding of conservatism.

Acknowledgement

The research described in this report was sponsored by the National Science Foundation through Grant No. DFR-84-12124 for research on Integrated Seismic Risk Analysis for Earth Dams. The authors gratefully acknowledge this support and extend appreciation to the Program Directors, Drs. K. Thirumalai and Clifford Astill at the National Science Foundation.

TABLE OF CONTENTS

LIST OF TABLES

LIST OF FIGURES

INTEGRATED SEISMIC RISK ANALYSIS FOR EARTH DAMS

I. INTRODUCTION

Over the past two decades, significant developments have been made in the understanding of dynamic response of earth dams. Analytical procedures have been developed of varying degrees of sophistication ranging from the simple application of Newton's second law to three-dimensional finite element analyses. Notwithstanding these developments, the estimation of the likelihood of seismically-induced failure, or conversely, the reliable performance of an earth dam, during the period of its functional life remains a challenge.(61)

Seismic safety evaluation of an earth dam involves the identification and determination of various parameters, including the seismic loads on the dam and the resistance to these loads. There are many uncertainties that need to be considered for a realistic evaluation of the seismic risk associated with a dam. Uncertainty is introduced in the parameters defining the seismicity and geology of the site, in the parameters describing the strength of the foundation and dam materials, and in the methods of dynamic analysis employed for the dam.

In the current practice of seismic safety evaluation of an earth dam, a deterministic approach is generally followed in which conservative selections of parameters and assumptions are made to account for the various uncertainties involved in the seismic safety evaluation of the dam. Typically, in this type of an investigation, a minimum required factor of safety or a limiting level of permanent strain or deformation is adopted. If it is satisfied, then the

dam is considered to be safe. This approach can render the design of a new earth dam economically unfeasible due to the compounding of conservatism. More seriously, in the seismic safety evaluation of existing earth dams, the deterministic approach can lead to the conclusion that most existing dams are unsafe. A more realistic evaluation of the seismic safety, using reasonable assumptions and parameters and accounting for their uncertainties using probabilistic procedures, may indicate that the level of risk is acceptable to all parties concerned.

This report describes a probabilistic approach to the seismic safety evaluation of earth dams. The method involves the integration of the seismological and geotechnical inputs and their uncertainties in a consistent manner to yield the likelihoods of seismically induced damage and catastrophic failure of the dam. The application of these procedures provides estimates of relative risks, which are useful in design and decision analysis, where trade-offs are made between the cost of increasing the seismic resistance and the risks associated with the consequences of seismic damage. In addition, risk-based safety evaluation enables identification of the most important parameters, assumptions, hypotheses and safety criterion affecting the evaluation of the safety of the dam and avoids compounding of conservatism.

II METHODOLOGY

The evaluation of the risk of seismic damage or failure of a facility requires two analyses hereafter referred to as the Seismic Hazard Analysis (SHA) and the Seismic Performance Analysis (SPA). The estimation of seismic risk involves the following steps which are also illustrated in Figure 1.

Step 1. Seismic Hazard Analysis considers the various seismic sources and the frequency content and other characteristics of the seismic excitations that can be generated by these sources. It yields probabilistic statements of the recurrence of levels of seismic hazard defined in terms of ground motion parameters at the site of the facility.

Step 2. Seismic Performance Analysis considers the seismic resistance of the facility, providing probabilistic statements regarding the performance of the facility, conditional upon a given level of seismic excitation.

Step 3. Seismic Risk Analysis integrates the results of the Seismic Hazard Analysis and the Seismic Performance Analysis to yield the overall risk of damage or failure. Figure 2 is a schematic representation of the integration involved in the Seismic Risk Analysis.

The methodology described is applicable to any type of facility (70). In this research, procedures were developed to apply this methodology specifically to earth dams. The framework for performing these procedures is illustrated in Figure 3. A matrix approach is used to display the results of the three steps of the risk analysis.

The advantages of the matrix approach over closed-form formulations are:

1. The damage probability matrices compiled from the Seismic Performance Analysis are in themselves useful information. They indicate the adequacy of current design practices in relation to expected damages for different levels of seismic excitation.

2. The integration of the results from Seismic Hazard Analysis and Seismic Performance Analysis to obtain estimates of risk can be done in a simple manner with the use of a hand

calculator. This makes it more convenient to repeat analyses to assess the effects of different assumptions and different design alternatives.

3. Permits the use of simple or rigorous state-of-the-art analyses. For example, the Seismic Performance Analysis can be performed empirically, subjectively, using simple analytical procedures, or using complex three-dimensional finite element analyses.

Sections III and IV describe the procedures developed for conducting the SHA and SPA.

III SEISMIC HAZARD ANALYSIS (SHA)

Damage to or failure of an earth dam can occur as the result of different failure mechanisms, hereafter referred to as modes. For the seismic analysis of earth dams consisting of materials that progressively lose shearing resistance during seismic excitations, the pseudo-static analysis is no longer considered a reliable approach (24, 57, 65). Seismic safety evaluation of earth dams requires assessment of the potential for permanent deformations, which can result in loss of freeboard and consequently, failure by overtopping.

The first mode of failure considered is the progressive accumulation of residual displacements during the course of the earthquake. Newmark (1965) proposed a simple sliding-block model for the calculation of permanent deformation using a rigid-plastic force-displacement relationship. In recent years, other analytical procedures (1, 3, 12, 14, 18, 21, 22, 23, 25, 26, 32, 37, 39, 40, 42, 46, 47, 56, 60, 62, 66, 69) have been developed for calculating permanent deformations. These have been essentially extensions of Newmark's simple concept. A review of these methodologies indicates that the characteristics of the

seismic excitation plays an important role in the estimation of permanent deformations in earth dams. The peak ground acceleration, frequency content and duration, as well as the random nature of the ground motions, affect the magnitude of the accumulated permanent deformation.

The second mode of failure considered is associated with post-earthquake instability due to reduction in shearing resistance of the dam and the foundation soil during shaking. The potential for this mode of failure depends not only upon the characteristics of the soil, but also on the severity of the seismic excitations.

In this research, a simple procedure for calculating the permanent deformations of an earth dam was developed. The parameters selected to describe the seismic event are peak ground acceleration, predominant period of motion, and number of equivalent cycles of seismic load application, N_{eq}. The selection of number of equivalent cycles as one of the parameters is consistent with the procedures for post-earthquake instability analysis involving the cyclic shear strength of soils.

For a specific level of peak ground acceleration, the probability of exceeding a specified permanent deformation and the probability of post-earthquake instability will be significantly lower for a smaller number of cycles, all other factors being the same. Therefore, the Seismic Hazard Analysis procedure must provide not only the annual number of events causing acceleration to exceed a specified level, but also the distribution of these events with respect to the number of cycles of excitation.

Current Seismic Hazard Analysis procedures typically provide only the number of events causing acceleration to exceed a certain level (2, 15, 32, 45, 49, 73). The results from such an

analysis are expressed in terms of annual number of events causing acceleration A to exceed 'a', $\lambda(A \geq a)$. The total number of events contributing to exceeding 'a' will generally cover a range of Richter magnitudes, M, due to varying site-to-source distances. It is important to identify the distribution of Richter magnitudes expected for the events giving $\lambda(A \geq a)$. For example, if $\lambda(A \geq a)$ is equal to 10, it is necessary to determine how many of these 10 events have magnitudes between four and five, five and six, six and seven and so forth, or more specifically how many of the 10 events will cause 0 to 5 cycles, 5 to 10 cycles and so on. The mathematical formulation that permits the calculation of the distribution of $\lambda(a, \Delta M)$ or $\lambda(a, \Delta N_{eq})$, where ΔM and ΔN_{eq} are the ranges of earthquake magnitude and number of cycles, respectively, is provided in Appendix A. The number of earthquakes causing acceleration at a site to exceed 'a' and having magnitudes between the minimum value of interest, m_o and a selected value m_i can be obtained through the use of computer programs currently used in conventional probabilistic Seismic Hazard Analysis, provided that the following input parameter modifications are made.

(a) The maximum credible magnitude m_{max} to be read in to the computer would be m_i

and

(b) the number of events causing magnitude to exceed m_o to be read into the computer would be equal to

$$\lambda(m_o)\left[\frac{1 - e^{-\beta(m_i - m_o)}}{1 - e^{-\beta(m_{max} - m_o)}}\right]$$

where, β is the magnitude-frequency parameter, and $\lambda(m_o)$ is the total number of events having magnitude between m_o and m_{max}.

With the use of these modified parameters the results of the computer analysis will

correspond to $\lambda(a, \Delta M_i)$, the total number of events causing acceleration to exceed 'a' and having magnitudes greater than m_0 but less than m_i. By selecting various values of m_i, it is possible to generate a histogram of events $\lambda(a, \Delta M)$ for various intervals of magnitude.

To establish the joint occurrence of acceleration and number of cycles, $\lambda(a, \Delta N_{eq})$, a relationship between Richter magnitude, M, and number of equivalent cycles, N_{eq}, is required. Appendix B presents various relationships based on the research of different investigators. Using these relationships, the distributions of $\lambda(a, \Delta N_{eq})$ can be determined from the distribution of $\lambda(a, \Delta M)$.

III-1 Example Application of SHA

An example is presented herein to demonstrate the application of the Seismic Hazard Analysis that provides the joint distribution of $\lambda(a, \Delta M)$ and $\lambda(a, \Delta N_{eq})$. Figure 4 shows the seismic sources used for the example site, which is located near Boston. Appendix C presents the relevant seismic data used and the steps followed in the analysis. The computer program developed by Schumacker and Whitman (1978) was used for the Seismic Hazard Analysis. Figure 5 shows the result obtained from the application of conventional Seismic Hazard Analysis. The plot provides the annual number of events that cause acceleration A to exceed 'a'. However, it does not provide the magnitudes associated with these events. Using the procedure described in the previous section (and Appendix C) the number of events having accelerations and magnitudes between selected ranges, $\lambda(\Delta A, \Delta M)$, were computed and the results presented in a matrix form as shown in Table 1. Table 2 shows a comparable SHA matrix with the results expressed in terms of N_{eq} rather than M. The relationship between M and N_{eq} proposed by Seed et. al. (1983), described in

Appendix C, was used to calculate the results shown in Table 2.

Figure 6 shows a histogram of the number of events as a function of M and N_{eq} for peak accelerations exceeding 0.15g. It can be seen that the magnitude, M, and the number of cycles, N_{eq}, associated with an acceleration of 0.15g will most likely be small. This information is extremely useful in the analysis of permanent deformations and evaluation of post-earthquake shearing resistance of the embankment soils.

IV SEISMIC PERFORMANCE ANALYSIS (SPA)

The objective of a Seismic Performance Analysis is to provide the probabilities of damage and failure of an earth dam conditional upon the occurrence of a specified level of seismic loading. As described earlier, damage or failure of an earth dam can occur during or shortly after a seismic event. During shaking, a section of the dam will experience substantial permanent deformation if the earthquake induced shear stresses exceed the shearing resistance of the embankment or foundation materials. The dam may suffer limited damage or may experience total failure due to overtopping, if the available freeboard is lost. This potential mode of damage and failure is hereafter referred to as Mode 1. If the embankment or its foundation material are susceptible to loss of shear strength due to application of seismic excitation, then the potential for post-earthquake instability of the dam needs to be evaluated. This type of failure mechanism is hereafter referred to as Mode 2. Sections IV-1 and IV-2 describe the procedures for the Seismic Performance Analysis for Modes 1 and 2, respectively. The combination of the contribution of the two modes to the overall risk is discussed in Section IV-3.

IV-1 Earthquake-Induced Permanent Deformations, Mode 1

Earthquake-induced permanent deformations of an earth dam can be estimated by a number of approaches, varying in their degree of sophistication. On the one hand, Newmark (1965) and Makdisi and Seed (1978) developed empirical charts to estimate the permanent deformation. On the other hand, two dimensional finite element analysis combined with cyclic simple shear or triaxial compression test results on undisturbed or reconstituted soil samples have also been used to evaluate the strain potentials and permanent deformations within a dam subjected to seismic excitations (12, 22, 37, 38, 42, 43, 46, 52, 53, 60, 66).

In the development of the Seismic Performance Analysis procedures described in this report, an analytical model was developed for the calculation of permanent deformation that satisfies the following criteria:

(a) The seismological input for both Mode 1 and Mode 2 analyses and the parameters describing the output of the Seismic Hazard Analysis are consistent with each other.

(b) The permanent deformation model is simple enough to be conveniently applied in design practice, yet accounts for all the pertinent seismic and material parameters.

(c) The model allows for the application of probability theory to estimate the likelihood of the permanent deformation exceeding specified values.

(d) The model parameters can be evaluated in simple approximate ways or using rigorous sophisticated procedures as dictated by need.

The following section describes the procedure that was developed to estimate permanent deformations.

IV-1.1 Procedure for Calculating Permanent Deformations

Calculation of earthquake-induced permanent deformation can be made using Newmark's sliding block model shown in Figure 7. In this approach, a rigid-plastic response is assumed, such that if the acceleration of the block representing a section of an earth dam exceeds a limiting yield level, K_y, then a relative displacement, D_r, will be initiated representing a permanent deformation of the dam section. An illustration of the motions of the block and the base for a triangular base excitation is presented in Figure 7. The derived mathematical formulation for D_r, given triangular base motion, is presented in Appendix D. In addition, derived expressions for sinusoidal and rectangular base excitations are also presented. Based on these derivations for D_r, the following observations are made:

(a) The expression for D_r is of the form:

$$D_r = f\left(\frac{K_y}{K_a}\right) N_{eq} K_a T^2 \qquad (1)$$

in which f( ) is a function that depends on the type of base motion considered, K_y is the yield acceleration, K_a is the peak acceleration of the base, T is the period of the motion, and N_{eq} is the number of cycles of the base motion.

(b) The permanent deformation, D_r, can be normalized with respect to the peak acceleration of the base, K_a, and the square of the period, T, of the base motion and the number of the

uniform cycles, N_{eq}, as shown in Equation 2.

$$D_n = \frac{D_r}{K_a N_{eq} T^2} = f\left(\frac{K_y}{K_a}\right) \tag{2}$$

where D_n is referred to as the normalized permanent deformation and is a function of only K_y, K_a, and type of base motion.

Figure 8 shows plots of D_n versus K_y/K_a for each of the three simple base motions considered, i.e. triangular, sinusoidal, and rectangular. It is clear that the shape of the base motion has an important effect on the permanent deformation, especially if K_y/K_a is nearly 1.0. Recognizing that none of these motions properly depict the random nature of earthquake-induced ground motions, a more realistic determination of the function f( ) of Equation 2 was made by considering actual earthquake records. Table 3 summarizes the permanent deformations computed by Franklin and Chang (1977) using 86 actual recorded acceleration time-histories for the base motion in Newmark's sliding-block analysis. In this research, their computed permanent deformations were normalized according to Equation 2 in order to establish the functional relationship between D_n and K_y/K_a.

Table 4 presents the normalized permanent deformation, D_n, for each of the three ratios of K_y/K_a considered by Franklin & Chang (1977). The peak ground accelerations and the predominant periods for these records were obtained from Chang (1978), and their number of equivalent cycles of ground motion from Asturias & Dobry (1982). A plot of the data from Table 4 for the three K_y/K_a values of 0.02, 0.1 and 0.5 is shown in Figure 9. The determination of the permanent deformation function using these data is described in the following section.

IV-1.2 Function for Permanent Deformations

To establish the function f( ) of Equation 2 based on actual earthquake records a third degree polynomial was fitted to the data plotted in Figure 9, using Lagrange interpolation. The polynomial was fitted through the median values of the plotted data points at K_y/K_a = 0.02, 0.1, and 0.5 thus, deemphasizing the effect of the few extreme points at the high end, which are orders of magnitude different than the next highest values. In addition, D_n was assigned a very small value (10^{-5}) at $K_y/K_a = 1.0$, in order to account for the fact that the displacement should be zero if $K_y/K_a = 1.0$. This value was selected in order to obtain for f( ) in the range of $0.5 < K_y/K_a < 1.0$ (where data is lacking) a shape consistent with that of the triangular base motion which appears to be more representative of actual earthquake motion than the sinusoidal or the rectangular base motions (see Figure 11). The resulting polynomial curve is shown in Figure 10, and its mathematical expression is:

$$\log D_n = \log f(K_y/K_a)$$

$$= g(K_y/K_a) = 0.22 - 10.12(K_y/K_a) + 16.38(K_y/K_a)^2 - 11.48\,(K_y/K_a)^3 \qquad (3)$$

where $$D_n = \frac{D_r}{K_a N_{eq} T^2} = f\left(\frac{K_y}{K_a}\right)$$

IV-1.3 Comparison of the Proposed Function With Other Models

In Figure 11, the polynomial curve proposed for the calculation of seismically induced permanent deformations is compared with the deformation functions of the triangular, sinusoidal, and rectangular pulses. For $K_y/K_a < 0.1$ these simple base motions yield

significantly lower values of D_n than obtained based on Franklin and Chang's integration of recorded time histories. Conversely, for $K_y/K_a > 0.1$, the sine and rectangular base motions yield significantly higher values of D_n. For $K_y/K_a > 0.1$ the assumption of a triangular pulse yields deformations that are generally in agreement with Franklin and Chang's data and thus with the established performance function for permanent deformations.

Figure 11 also shows values of D_n estimated based on the results of Makdisi and Seed (1978) for Richter magnitudes of 6.5, 7.5, and 8.25. These values of D_n were obtained by normalizing the displacements computed by Makdisi and Seed with respect to the peak acceleration of the potential sliding mass of the dam, K_a, the square of the first mode fundamental period of the dam, T, and the number of equivalent cycles of the ground motion, N_{eq}. The data thus obtained plot slightly below the proposed function. This could be explained by the fact that the periods of the dams used to normalize Makdisi and Seed data are larger than the period of the motion of the dam. Nevertheless, it is noted that Makdisi and Seed data plot within the range of data presented by Franklin and Chang.

IV-1.4 Uncertainty of the Proposed Function, $g(K_y/K_a)$

There is considerable scatter in the values of D_n computed using Franklin & Chang's (1977) data. The scatter of the resulting values of D_n for the 86 seismic records for K_y/K_a = 0.02, 0.1, and 0.5 is illustrated in Figure 9. This scatter is due to the random and stochastic nature of seismic ground motions. In other words, the random nature of the ground motions is not taken into account solely by the peak acceleration, N_{eq}, and predominant period. Two seismograms having essentially identical values for these parameters can, and generally do, have very different time histories, resulting in different

calculated permanent deformations. To account for the resulting uncertainty in the predicted value of D_n given by the proposed function, statistical analysis of the data shown in Figure 9 was made. The $\log D_n$ values of all the data were plotted on normal probability paper for $K_y/K_a = 0.02$, 0.1 and 0.5 and is illustrated in Figure 12. It is seen that the three sets of the data lie on nearly parallel straight lines between 10% and 99% probabilities of not exceeding D_n. The slope of these lines is about 0.45. Thus, the standard deviation of the $\log D_n$ within this range is 0.45 for all 3 values of K_y/K_a, and probability of exceeding any given value, d_n, of normalized permanent deformation can be obtained by:

$$P(D_n > d_n) = P\left(\frac{\log D_n - \mu_{\log D_n}}{\sigma_{\log D_n}} > \frac{\log d_n - \mu_{\log D_n}}{\sigma_{\log D_n}}\right) = P(S > s) = 1 - \Phi(s) \qquad (4)$$

where

Φ = the cumulative standard normal distribution function

$$S = \frac{\log D_n - \mu_{\log D_n}}{\sigma_{\log D_n}} \qquad (5)$$

and

$\mu_{\log D_n}$ = mean of $\log D_n$

= $g(K_y/K_a)$ as given by Equation 3

Rearranging Equation 5 gives

$$\log D_n = g(K_y/K_a) + S\sigma_{\log D_n} \qquad (6)$$

$$= g(K_y/K_a) + \Phi^{-1}\,[\,1 - P(D_n > d_n)\,]\,\sigma_{\log D_n}$$

where S is the standard normal variate, and has a mean of zero and a standard deviation of 1.0. It is convenient to introduce

$$\xi_{D_n} = \sigma_{\log D_n}$$

giving

$$\log D_n = g(K_y/K_a) + \Phi^{-1} [\, 1 - P(D_n > d_n) \,] \, \xi_{D_n} \qquad (7)$$

Equation 7 was used to calculate contours of D_n versus K_y/K_a for specified probabilities of exceeding d_n: namely, 0.90, 0.70, 0.50, 0.30, and 0.10. The resulting curves are shown in Figure 13.

An example of the application of Equations 4 through 7 follows.

Considering the following parameters:

K_a = 0.21g

K_y = 0.07g

N_{eq} = 12 cycles

T = 0.7 second

What is the probability of $D_r > 4$ feet ?

The value of D_n corresponding to $D_r = 4$ feet is

$$D_n = 4 / [0.21 \times 32.2 \times 12 \times (0.7)^2] = 0.10$$

and K_y / K_a = 0.07g/0.21g = 0.33

Entering Figure 13 with these two values yields the probability of D_r exceeding 4 feet equal to about 5%.

The above procedure considers the uncertainty in the deformation function introduced by the scatter in Franklin and Chang's data. Prediction of permanent deformations using the proposed function involves additional uncertainties associated with the parameters used in the function namely, K_a, K_y, N_{eq}, and T.

The evaluation of K_a involves significant uncertainty and professional judgement. The value of K_a depends upon the base motion of the dam and the dynamic response of the dam. Makdisi and Seed (1978) described a procedure for estimating K_a. The resulting value can vary substantially, depending upon the procedures selected, assumptions made and the values of the material properties used. This uncertainty can be considered by repeated Seismic Performance Analysis by varying K_a and then combining the results using Bayesian weighted average technique described by Yegian (1979). The uncertainty in K_a due to the uncertainty in the peak ground acceleration, A, is considered through the SHA. For this research, the uncertainty in the number of cycles, N_{eq}, is taken into account by determining its probability distribution in the Seismic Hazard Analysis as described in section III. The uncertainties in the yield acceleration K_y (or K_y/K_a) and the predominant period T can be considered as described in the following section.

IV-1.5 Uncertainty in K_y/K_a, T and $g(K_y/K_a)$

In order to facilitate the analysis of the uncertainty in the values of K_y/K_a, T, and the nature of the deformation function $g(K_y/K_a)$, Equations 2 and 6 were combined to yield

$$\log D_r = g(K_y/K_a) + S\xi_{D_n} + 2\log T + \log(N_{eq}.K_a) \quad (8)$$

In this study, the probability of $D_r > d_r$, or alternatively $\log D_r > \log d_r$, conditional upon specified values for N_{eq} and K_a, is determined by numerical integration of the joint probability density function of T, K_y/k_a, and S over the region defined by

$$g(K_y/k_a) + S\xi_{D_n} + 2\log T + \log(n_{eq}\, k_a) > \log d_r \quad (9)$$

where n_{eq} and k_a are the specified values of N_{eq} and K_a.

Appendix E presents the details of the formulation of the numerical integration that provides the probability of D_r exceeding a specified value, d_r, given values for N_{eq} and K_a. Details of these calculations are discussed in Appendix C and in the Example Problem. A computer program (NIMPED), was developed to perform the integration. The program requires the following input parameters:

d_r = a specified value of displacement.

k_a = specified value for the peak acceleration of the dam cross-section analyzed.

n_{eq} = specified value for the number of uniform cycles of motion for the dam.

μ_T = mean value estimate of the predominant period of the motion,T.

σ_T = the standard deviation of T.

μ_{K_y} = mean value estimate of the yield acceleration of the cross-section of the dam under consideration.

σ_{K_y} = the standard deviation of K_y.

ξ_{D_n} = the standard deviation associated with the random nature of seismic ground motions (as discussed in Section IV-1.4).

The values of K_a and μ_T can be obtained from the peak ground acceleration by appropriate dynamic response analysis. This will be illustrated in the forthcoming example.

The output of the analysis provides the probability of the permanent deformation exceeding the specified value d_r. The standard deviations of T and K_y are obtained based on statistical evaluations or subjective judgement of the investigator. Appendix F describes a relationship between the coefficient of variation of K_y (c.o.v.$_{K_y}$), and the coefficient of variation of T (c.o.v.$_T$), for both cohesionless and cohesive soils. The formulation suggests that c.o.v.$_T$ can be assumed to be on the order of one half of c.o.v.$_{K_y}$ for a flexible dam on a rigid foundation.

The computer program was used to develop standardized (non-dimensional) plots which provide the exceeding probabilities without the need of a computer analysis. They are illustrated in Figures 14 and 15. Each plot corresponds to specified values of c.o.v.$_T$ and c.o.v.$_{K_y}$, with c.o.v.$_T$ equal to 1/2(c.o.v.$_{K_y}$). An example of the use of these plots follows.

Given

d_r = 4 feet

K_a = 0.21g

μ_{K_y} = 0.07g

N_{eq} = 12 cycles

μ_T = 0.7 seconds

$$c.o.v._{K_y} = 50\%$$

$$c.o.v._{T} = 25\%$$

$$\xi_{D_n} = 0.45$$

The probability of permanent deformation exceeding 4 feet, $P[D_r > 4 \text{ feet}]$, is obtained by computing

$$D_n = 4/[0.21 \times 32.2 \times 12 \times (0.7)^2] = 0.10$$

and $$\mu_{K_y}/K_a = 0.07g/0.21g = 0.33$$

and using Figure 15. The probability contour line on which the point plots, as shown in Figure 16, defines the probability of displacement exceeding 4 feet. For the example problem this probability is equal to about 20%. Note that if the uncertainty in K_y and T were not considered, the probability of displacement exceeding 4 feet would be about 5% as demonstrated earlier and shown by the plots in Figure 13.

The plots of Figures 13, 14, and 15 can be used to determine the complementary cumulative distribution curve for D_r, conditional upon prespecified values of K_a and N_{eq}. Figure 17 shows the resulting distribution for the example. This curve can be used to determine the probabilities of the occurrence of different damage states. For example, if a permanent deformation greater than 4 feet is considered catastrophic because of potential overtopping of the dam, and if deformations of less than 1 foot are considered inconsequential then, the following damage states with their corresponding probabilities can be defined from Figure 17.

$$P[0] = P[\text{minor or no}] = P[D_r \leq 1'] = 0.55$$

$$P[H] = P[\text{heavy}] = P[1' < D_r \leq 4'] = 0.25$$

$$P[C] = P[\text{catastrophic}] = P[D_r > 4'] = 0.20$$

The results of the Seismic Performance Analysis can be conveniently displayed in a damage probability matrix. Table 5 shows a typical SPA matrix for Mode 1 type failure, i.e. due to earthquake induced permanent deformation. The damage probabilities obtained from the above example are displayed as a single column in this matrix (for the range where $0.15g \leq A < 0.2g$). In order to perform the overall risk analysis, SPA computations need to be repeated for different combinations of N_{eq} and A to fill in the entire matrix. An example application of the Mode 1 type of SPA for an earth dam will be presented in section VI.

IV-2 Post-Earthquake Instability, Mode 2

Reliable performance of an earth dam depends not only upon its survival during a seismic event but also its survival at the aftermat of the event. If the dam or foundation soils are susceptible to loss of shear strength due to shaking, a post-earthquake instability of the dam can ensue. This type of failure mechanism (Mode 2) contributes to the overall seismic risk of the dam. The following section describes the seismic risk estimation associated with Mode 2.

The analsysis of the post-earthquake stability of earth dams typically is performed by conventional slope stability analysis using the shear strenghts corresponding to the end of the earthquake conditions (28, 33, 38, 44, 52, 59). For the past decade, procedures have been developed that provide estimates of post-earthquake shear strengths and pore water

pressures based on empirical, experimental, and analytical approaches (8, 10, 34, 35, 44, 59, 74, 75). In addition, probabilistic procedures have been developed to account for the uncertainties in the parameters used in the slope stability analysis and to estimate the probability of failure of a slope (5, 6, 7, 8, 11, 28, 64, 68, 71, 72). Any combination of these existing procedures can be used to estimate the probability of post-earthquake failure of an earth dam.

In as much as the post-earthquake shearing resistance depends upon the peak ground acceleration and the number of cycles of the seismic motion, it is suggested that the probability results from Mode 2 analysis be presented in a matrix format as shown in Table 6. The use of this matrix format permits the calculation of the failure probabilities, P[F], or the probabilities of survival, P[S] = (1 - P[F]), as a function of the two seismic parameters: acceleration, A, and number of cycles, N_{eq}, which have density functions determined through the Seismic Hazard Analysis described in Section III. Also the use of matrix format for Mode 2 facilitates the combining of the contributions of Mode 1 and Mode 2 to the overall seismic risk. Section VI also presents an example application of Mode 2 type of Seismic Performance Analysis.

IV-3 Combined Seismic Performance Analysis: Mode 1 and Mode 2

In section IV.1 the SPA procedure was described, which provides damage probabilities associated with the Mode 1 type failure mechanism. The integration of this SPA matrix with the SHA results provides the seismic risk of a dam associated with Mode 1. Similar risk calculations using the SPA matrix obtained considering Mode 2 type of failure provides the risk of a post-earthquake instability failure. The evaluation of seismic risk due

to Modes 1 and 2 combined, requires the calculation of an overall (combined) damage probability matrix.

Figure 18 describes an event tree of Seismic Performance Analysis that presents possible outcomes associated with the occurences of an event with acceleration A and N_{eq}. Note that the joint occurrence of any given pair of values of A and Neq is in itself one of many possible outcomes, from the Seismic Hazard Analysis. Given any pair of A and N_{eq}, following outcomes need to be considered

Possible outcomes for Mode 1

O	None to little permanent deformation
H	Permanent deformation leading to heavy damage
C	Permanent deformation leading to catastrophic damage

Possible outcomes for Mode 2

S	Safe under post-earthquake conditions
F	Failure due to post-earthquake conditions

Thus, overall there are six possible outcomes due to the combination of Mode 1 and Mode 2. The outcomes for Modes 1 and 2 and their combinations are schematically illustrated in Figure 19a.

To facilitate the prediction and evaluation of the performance of the earth dam, the following damage states are defined in terms of the above described outcomes.

Damage State, DS	Description	Probabilistic Notation
I	None to minor Damage	$O \cap S$, i.e. the joint occurrence of O and S
II	Heavy Damage	$H \cap S$, i.e. the joint occurrence of H and S
III	Catastrophic Damage	$C \cup F$, i.e. the occurrence of either C or F or both

The damage states are schematically illustrated in Figure 19b in correspondence with the outcomes in Figure 19a. If statistical independence is assumed between the Mode 1 and the Mode 2 outcomes, then the probability of occurrence for each damage state is as given below.

$$
\begin{aligned}
P(I) &= P(O)\,P(S) \\
P(II) &= P(H)\,P(S) \\
P(III) &= P(O)\,P(F) + P(H)\,P(F) + P(C) \\
&= 1 - \{P(O)\,P(S) + P(H)\,P(S)\}
\end{aligned}
$$

Thus the two damage probability matrices associated with Mode 1 and Mode 2 can be combined into a single matrix which have the three damage states shown above and which will describe the overall results from the SPA. This matrix will then be the SPA input to the Seismic Risk Analysis.

V INTEGRATED SEISMIC RISK ANALYSIS

In Section III the Seismic Hazard Analysis procedure was described, which provides the expected number of annual occurrences of seismic events having a range of peak ground acceleration ΔA, and a range of number of cycles, ΔN_{eq}. The results are presented in a matrix form as shown in Table 2. Section IV described the Seismic Performance Analysis, which provides the probabilities of an earth dam experiencing various specified damage states conditional upon ΔA and ΔN_{eq}. These probabilities are displayed in a matrix form similar to that of the results of the SHA. Table 5 shows a typical SPA matrix. The calculation of the overall risk of damage or failure of the dam requires integration of the results of the SHA and the SPA. The use of matrices to display the results from the SHA and the SPA facilitates the integration to be performed numerically employing either hand calculator or the computer, using the following expression:

$$\lambda(DS_i) = \Sigma_{\text{all } A} \Sigma_{\text{all } N_{eq}} \lambda(\Delta A, \Delta N_{eq})\, P(DS_i|\Delta A, \Delta N_{eq}) \qquad (9)$$

where

$\lambda(DS_i)$ = annual number of events causing damage state DS_i

$\lambda(\Delta A, \Delta N_{eq})$ = annual number of events having acceleration range of ΔA and number of equivalent cycles of ΔN_{eq}. (from the SHA matrix)

$P(DS_i|\Delta A, \Delta N_{eq})$ = probability of damage state DS_i occurring, conditioned on ΔA and ΔN_{eq}. (from the SPA matrix)

and

i = I, II, III referring to damage states

Equation 9 gives the annual number of events associated with each damage state (DS). Next, the probability of at least one event causing a specified level of damage to the dam during the design life of the dam is calculated assuming a Poisson arrival process. For example, the probability of at least one catastrophic failure occurring in t years can be obtained from

$$P[\text{Failure in t years}] = 1 - e^{-\lambda(DS_{III})t} \tag{10}$$

where $\lambda(DS_{III})$ is the annual number of events causing catastrophic failure of the dam and is calculated using Equation 9.

The following section presents a comprehensive example of the application of the Integrated Seismic Risk Analysis described in this report.

VI EXAMPLE APPLICATION OF INTEGRATED SEISMIC RISK ANALYSIS FOR EARTH DAMS

To illustrate the various steps that are involved in the application of the Integrated Seismic Risk Analysis, an earth dam located near Boston was selected for investigation.

VI-1 Description of the Dam

Figure 20 shows a typical cross section of the dam. The upstream shell consists of medium dense to dense sands. The downstream section consists primarily of loose to medium dense sands and gravel with a loose sand layer near the base of the dam. The dam is founded on glacial till overlying bedrock. A field investigation indicated a layer of loose silty sands with blow counts as low as 4 blows per foot at about 40 feet below the crest of the dam, extending under the entire downstream shell of the dam. The hatched region is a proposed fill that would increase the available freeboard of the dam. The following analysis was performed for the dam with the proposed fill assumed to be already placed. The analysis utilizes the results of the SHA example in Section III.

VI-2 Seismic Hazard Analysis - SHA

The SHA gives the annual number of joint occurences of acceleration and magnitude and thus of acceleration and equivalent number of cycles. The seismicity of the region of the dam is illustrated in Figure 4 of Section III. Tables 7 and 8 provide the resulting annual number of events, $\lambda(\Delta A, \Delta M)$ or $\lambda(\Delta A, \Delta N_{eq})$, for selected ranges of acceleration and

magnitude and thus of acceleration and equivalent number of cycles.

VI-3 Seismic Performance Analysis - SPA

The overall risk of failure of the dam is affected by both Modes 1 and 2 which were described in Section VI. Mode 2 is involved due to the fact that the loose sand layer is susceptible to the development of excess pore water pressure during the seismic excitations.

VI-3-1 Permanent Deformations (Mode 1)

Figure 21 indicates the procedures followed to estimate the earthquake-induced permanent deformations of the dam. The average lateral earthquake-induced acceleration, K_a, for a critical sliding mass was estimated by performing dynamic response analysis of the dam cross-section. Specifically the computer program, SHAKE, was used to analyze two idealized soil columns, one at the crest and the other near the toe of the dam. The acceleration-time record applied at bedrock level was generated using the design response spectrum considered appropriate for the region. The average lateral acceleration, K_a, of the critical sliding mass shown in Figure 20 was computed using the results from SHAKE analysis and the equation shown in Figure 21. Figure 22 shows a plot of K_a versus the peak ground acceleration of the bedrock. From Figure 22, the values of K_a for each of the selected acceleration ranges, shown on Table 8, were estimated and the results are tabulated in Table 9.

The yield acceleration, K_y, of the critical wedge shown in Figure 20 was estimated through the use of slope stability analysis in which the lateral acceleration coefficient was varied and the factors of safety were computed. The lateral acceleration corresponding to a factor of safety of one defined the yield acceleration, K_y. The stability analysis was performed for different levels of pore water pressure buildup, in the loose sand layer, yielding different values of K_y. Based on the results of these analyses the following expression for K_y was derived.

$$K_y = -0.091 + 0.571\,(1 - R_u)\tan\phi \qquad \text{for } R_u < 0.7 \qquad (11)$$

$$K_y = 0 \qquad \text{for } R_u > 0.7$$

where $R_u = \Delta u / \bar{\sigma}_v$

Δu = the excess pore water pressure in the loose sand layer

$\bar{\sigma}_v$ = the vertical effective stress in the loose sand layer.

Figure 23 shows a plot of K_y versus R_u corresponding to a mean value of $\phi=28^\circ$ for the friction angle of the loose sand. The mean values of K_y for the example dam were estimated from Figure 23 using values of R_u that were estimated empirically for each level of seismic input (ΔA, ΔM) following the procedures proposed by Yegian and Vitelli (1981). The calculated values of R_u are shown in Table 10. Table 9 presents the resulting mean values of K_y. However, uncertainty exists in the predicted values of K_y due to uncertainties in the values of R_u and ϕ used in Equation 11. To calculate the standard deviation of K_y, σ_{K_y}, the Taylor series expansion of Equation 11 was used and σ_{K_y} was related to the standard deviations of R_u and ϕ as shown in Equation 12.

$$\sigma^2_{K_y} = \left[0.571\,(1 - r_u)\right]^2 \sigma^2_{TAN\phi} + \left[0.571\tan\phi\right]^2 \sigma^2_{R_u} \qquad (12)$$

The standard deviation of R_u was estimated from the upper and lower bound curves developed by Yegian & Vitelli (1981). The standard deviation of tan ϕ was taken as 0.15 (31). Using Equation 12, the standard deviation of K_y was estimated to be constant and equal to about 0.06 for all combination of K_a and the Richter magnitude, M.

The period of the motion, T, of the sliding mass was estimated from the dynamic response analyses and is tabulated in Table 11. The standard deviation of T, σ_T, was estimated to be 0.08.

For a rigid plastic mass, permanent deformation is imminent if the yield acceleration, K_y, is smaller than the average lateral acceleration, K_a. The probability that the permanent deformation, D_r, will exceed a certain specified limit, d_r, conditional upon the occurrence of a seismic event, can be obtained from normalized plots such as shown in Figures 14 and 15, or the computer program NIMPED. For this example, three conditional probabilities of exceeding the permanent deformation were obtained using the program NIMPED and the input parameters shown in Table 11. To illustrate this example application of Seismic Performance Analysis (Mode 1), the following damage states were defined

$$[\text{No or Minor Damage}] = [d_r \leq 2']$$

$$[\text{Heavy Damage}] = [2' < d_r \leq 10']$$

$$[\text{Catastrophic Damage}] = [d_r > 10']$$

Table 12 summarizes the conditional probabilities for each damage state and for the varying ranges of acceleration and equivalent number of cycles. This matrix provides the Seismic Performance Analysis results associated with Mode 1 type failure mechanism.

VI-3-2 Post-Earthquake Instability (Mode 2)

The results shown in Table 12 are the probabilities associated with Mode 1. However, generation of excess pore water pressure in the loose sand layer during an earthquake may cause reduction in the post-earthquake static shear strength of the sand. Depending upon the magnitude of the excess pore pressure, the post-earthquake stability of the dam can be of concern. Consequently, post-earthquake static stability analyses of the dam were made and the values of the factor of safety were calculated as a function of the pore pressure ratio, r_u, and the friction angle ϕ of the loose sand. Figure 24 shows the stability results which suggest the following relationship between the post-earthquake factor of safety, F.S., R_u and ϕ.

$$F.S. = 0.66 + 2(1 - R_u)\tan\phi \tag{13}$$

Equation 13 can be used to estimate the mean value of F.S. from the mean values of R_u and ϕ. The calculation of the probability of post-earthquake slope failure requires the estimation of the standard deviation of F.S. Using the Taylor series expansion for Equation 13, the standard deviation of F.S. can be obtained by the resulting expression:

$$\sigma^2_{F.S.} = \left[2\,(1 - r_u)\right]^2\ \sigma^2_{TAN\phi} + \left[2\,(-\tan\phi)\right]^2\ \sigma^2_{R_u} \tag{14}$$

Using the estimated mean value of F.S. and $\sigma_{F.S.}$, for each seismic event, the probability of failure was calculated assuming the factor of safety to be a normally distributed random variable. Table 13 provides the resulting damage probability matrix for Mode 2.

VI-3-3 Damage Probability Matrix (Mode 1 and Mode 2 Combined)

Assuming statistical independence between Mode 1 and Mode 2 failure mechanisms (for each seismic event) the damage probabilities of these two modes were combined as described in Section VI. Table 14 provides the combined damage probabilities which assumes that the catastrophic damage from Mode 1 and failure from Mode 2 have the same loss function thus, limiting the number of combined damage states to three.

VI-4 Integrated Seismic Risk Analysis

The results shown in the SHA and SPA matrices were integrated to provide the annual number of seismic events that would cause a specified damage state. Equation 15 indicates the integration expressed in terms of discrete intervals of A and N_{eq}.

$$\lambda(DS_i) = \Sigma_{\text{all } A}\Sigma_{\text{all } N_{eq}} \lambda(\Delta A, \Delta N_{eq})\, P(DS_i|\Delta A, \Delta N_{eq}) \qquad (15)$$

For each of the damage states, the annual number of events for Mode 1 and Mode 2 are illustrated in Tables 15 and 16, respectively. Similar results are illustrated in Table 17, considering the combined effect of Mode 1 and Mode 2. The annual probability of at least one occurance of a damage state can be obtained assuming the Poisson arrival process. Thus

$$P(\text{III}) = 1 - e^{-\lambda(DS_{III})} = 1 - e^{-(0.001060)} = 1.060\text{x}10^{-3} \quad \text{(Annual Probability)}$$

$$P(\text{II}) = 1 - e^{-[\lambda(DS_{II}) + \lambda(DS_{III})]} - P(\text{III})$$

$$= 1 - e^{-(0.001104)} - 1.060\text{x}10^{-3} = 0.043\text{x}10^{-3}$$

$$P(\text{I}) = 1 - [P(\text{II}) + P(\text{III})] = 0.9989$$

These risk estimates are based on a set of assumptions in both Seismic Hazard and Seismic Performance Analyses. Repeated applications of the Integrated Seismic Risk Analysis described in this example, and varying the assumptions, can reveal the importance of these assumptions and the parameters of most concern that may require special considerations.

REFERENCES

1. Abdel-Ghaffar A.M., Scott R.F., *"Analysis of Earth Dam Response to Earthquakes,"* Journal of the Geotechnical Engineering Division, ASCE, Vol. 105, GT12, Dec., 1979, pp. 1379-1404.

2. Algermissen S.T., *"Seismic Risk Studies in the United States,"* Proc. of the 4th World Conference on Earthquake Engineering, Santiago, Chile, 1969, Vol. 1, pp. 14-27.

3. Ambraseys N.N., Sarma S.K., *"The Response of Earth Dams to Strong Earthquakes,"* Geotechnique, Vol. 17, 1967, pp. 181-213.

4. Asturias R.W., Dobry R., *"The Equivalent Number of Cycles of Recorded Accelerograms for Soil Liquefaction Studies,"* Report No. CE-82-5, Department of Civil Engineering, R.P.I., Troy, New York, April, 1982.

5. A-Grivas D., Howland J., Tolcser P., *"A Probabilistic Model for Seismic Slope Stability Analysis,"* Report No. CE-78-5, Department of Civil Engineering, R.P.I., Troy, New York, June, 1979.

6. A-Grivas D., *"Probabilistic Evaluation of Safety of Soil Structures,"* Journal of the Geotechnical Engineering Division, ASCE, Vol. 105, No. GT9, Sept., 1979, pp. 1091-1095.

7. A-Grivas D., Asaoka A., *"Slope Safety Prediction Under Static and Seismic Loads,"* Journal of the Geotechnical Engineering Division, ASCE, Vol. 108, No. GT5, May, 1982, pp. 713-729.

8. Bergado D.T., Anderson L.R., *"Stochastic Analysis of Pore Pressure Uncertainty for the Probabilistic Assessment of the Safety of Earth Slopes,"* Soils and Foundations, Vol. 25, June, 1985, pp. 87-105.

9. Bolognesi A.J.L., *"Peculiarities of the Seismic-Resistant Analysis of Earth Dams with Pervious Gravelly Shells,"* Dams and Earthquakes, Proc. of the Conference at Institute of Civil Engineers, London, U.K., 1980, pp. 89-95.

10. Castro G., *"Comments on Seismic Stability Evaluation of Embankment Dams,"* Proc. of the Engineering Foundation Conference on the Evaluation of Dam Safety, Pacific Grove, Calif., Nov., 1976, pp. 377-390.

11. Catalan J.M., Cornell C.A., *"Earth Slope Reliability by a Level-Crossing Method,"* Journal of the Geotechnical Engineering Division, Vol. 102, No. GT6, June, 1976, pp. 591-604.

12. Chaney R.C., *"Earthquake Induced Deformations in Earth Dams,"* Proc. of the 2nd U.S. National Conference on Earthquake Engineering, Stanford Univ., Calif., 1979, pp. 633-642.

13. Chang F.K., *"Catalogue of Strong Motion Earthquake Records, Volume I, Western United States, 1933-1971,"* State of the Art for Assessing Earthquake Hazards in the United States, Report 9, U.S. Army Engineer Waterways Experiment Station, Misc. Paper No. S-73-1, April, 1978.

14. Constantinou M., Gazetas G., *"Probabilistic Seismic Sliding Deformations of Earth Dams and Slopes,"* Proc. of Specialty Conference on Probabilistic Mechanics and Structural Reliability, Berkeley, Calif., 1984, pp. 318-321.

15. Cornell C.A., *"Engineering Seismic Risk Analysis,"* Bulletin of the Seismological Society of America, Vol. 58, No. 4, Oct., 1968, pp. 1583-1606.

16. Cornell C.A., Vanmarcke E. H., *"The Major Influences on Seismic Risk,"* Proc. of the 4th World Conference on Earthquake Engineering, Santiago, Chile, Jan., 1969, Vol. I, pp. 69-83.

17. Cornell C.A., Merz H.A.,*"A Seismic Risk Analysis of Boston,"* Seismic Design Decision Analysis, Report No.11, MIT, Cambridge, Apr., 1974

18. Dakoulas P., Gazetas G., *"Contributions to Seismic Analysis of Earth Dams,"* Ph.D. Dissertation, Department of Civil Engineering, R.P.I., Troy, New York, May, 1985.

19. Donovan N.C., *"A Statistical Evaluation of Strong Motion Data, Including the February 9, 1971, San Fernando Earthquake,"* Proc. of the 5th World Conference on Earthquake Engineering, Rome, Italy, June, 1973, pp. 1252-1261.

20. Dunn I.S., Anderson L.R., Kiefer F.W., *"Fundamentals of Geotechnical Analysis,"* J. Wiley and Sons, New York, 1980.

21. Elgamal A.W., Abdel-Ghaffar A.M., Prevost J.H., *"2-D Elastoplastic Seismic Shear Response of Earth Dams: Theory,"* Journal of the Geotechnical Engineering Division, ASCE, Vol. 113, No. 5, May, 1987, pp. 689-701.

22. Elgamal A.W., Abdel-Ghaffar A.M., Prevost J.H., *"2-D Elastoplastic Seismic Shear Response of Earth Dams: Application,"* Journal of the Geotechnical Engineering Division, ASCE, Vol. 113, No. 5, May, 1987, pp. 702-719.

23. Franklin A.G., Chang F.K., *"Permanent Displacements of Earth Embankments by Newmark Sliding Block Analysis,"* Earthquake Resistance of Earth and Rock-Fill Dams, Report 5, U.S. Army Engineering Waterways Experiment Station, Misc. Paper No. S-71-17, Nov., 1977.

24. Gazetas G., Debchaudhury A., Gasparini D.A., *"Random Vibration Analysis for the Seismic Response of Earth Dams,"* Geotechnique, Vol. 31, No. 2, 1981, pp. 261-277.

25. Gazetas G., *"Seismic Response of Earth Dams: Some Recent Developments,"* Soil Dynamics and Earthquake Engineering, Vol. 6, No. 1, 1987, pp. 2-47.

26. Goodman R.E., Seed H.B., *"Earthquake-Induced Displacements in Sand Embankments,"* Journal of the Soil Mechanics and Foundations Division, ASCE, Vol. 92, No. SM2, Mar., 1966, pp. 125-146.

27. Gutenberg B., Richter C.F., *"Seismicity of the Earth,"* Princeton Univ. Press, 1954.

28. Hadj-Hamou T., Kavazanjian E., *"Probabilistic Seismic Stability of a Cohesionless Slope of Limited Extent,"* Proc. of the 8th World Conference on Earthquake Engineering, San Francisco, 1984.

29. Haldar A., Tang W.H., *"Probabilistic Evaluation of Liquefaction Potential,"* Journal of the Geotechnical Engineering Division, ASCE, Vol. 105, No. GT2, Feb., 1979, pp. 145-163.

30. Haldar A., Tang W. H., *"Statistical Study of Uniform Cycles in Earthquakes,"* Journal of the Geotechnical Engineering Division, ASCE, Vol. 107, No. GT5, May, 1981, pp. 577-589.

31. Harr M., *"Mechanics of Particulate Media,"* McGraw-Hill, New York, 1977.

32. Idriss I.M., *"Evaluating Seismic Risk in Engineering Practice,"* Proc. of the 11th International Conference on Soil Mechanics and Foundation Engineering, San Francisco, Calif., 1985, Vol. 1, pp. 255-320.

33. Ishihara K., *"Post-Earthquake Failure of a Tailing Dam Due to Liquefaction of the Pond Deposit,"* Proc. of the International Conference on Case Histories in Geotechnical Engineering, University of Missouri, Rolla, 1984, Vol. III, pp. 1129-1143.

34. Kikusawa M., Hasegawa T., *"Analysis of Model Embankment Dam by Shaking Table Test,"* Soils and Foundations, Vol. 25, No. 1, 1985, pp. 1-14.

35. Klohn E.J., Maartman C.M., Lo R.C.Y., Finn W.D.L., *"Simplified Seismic Analysis for Tailing Dams,"* Proc. of Specialty Conference on Earthquake Engineering and Soil Dynamics, ASCE, Pasadena, Calif., 1978, pp. 540-556.

36. Lee K.L., Chan K., *"Number of Equivalent Significant Cycles in Strong Motion Earthquakes,"* Proc. of the Microzonation Conference, Seattle, Wash., 1972, Vol. II, pp. 609-634.

37. Lee K.L., *"Seismic Permanent Deformations in Earth Dams,"* Report No. UCLA-ENG-7497, School of Engineering and Applied Sciences, U.C.L.A., Calif., Dec., 1974.

38. Lee K.L., *"Seismic Stability Analysis of Hawkins Hydraulic Fill Dam,"* Journal of the Geotechnical Engineering Division, ASCE, Vol. 103, No. GT6, June, 1977, pp. 627-644.

39. Lin J.S., Whitman R.V., *"Earthquake Induced Displacements of Sliding Blocks,"* Journal of the Geotechnical Engineering Division, ASCE, Vol. 112, No. 1, Jan., 1986, pp. 44-59.

40. Makdisi F.I., Seed H.B., *"Simplified Procedure for Estimating Dam and Embankment Earthquake-Induced Deformations,"* Journal of the Geotechnical Engineering Division, ASCE, Vol. 104, No. GT7, July, 1978, pp. 849-867.

41. Newmark N.M., *"Effects of Earthquakes on Dams and Embankments,"* Geotechnique, Vol. 15, No. 2, June, 1965, pp. 139-160.

42. Paskalov T.A., *"Permanent Displacement Estimation on Embankment Dams Due to Earthquake Excitations,"* Proc. of the 8th World Conference on Earthquake Engineering, San Francisco, 1984, pp. 327-334.

43. Prevost J.H., Abdel-Ghaffar A.M., Lacy S.J., *"Non-Linear Dynamic Analysis of an Earth Dam,"* Journal of the Geotechnical Engineering Division, ASCE, Vol. 111, No. 7, July, 1985, pp. 882-897.

44. Ramanujam N., Holish L.L., Chen W.W.H., *"Post Earthquake Stability Analysis of Earth Dams,"* Proc. of Specialty Conference on Earthquake Engineering and Soil Dynamics, ASCE, Pasadena, Calif., 1978, pp. 762-776.

45. Reiter L., Jackson R.E., *"Seismic Hazard Review for the Systematic Evaluation Program - A Use of Probability in Decision Making,"* U.S. Nuclear Regulatory Commission, NUREG-0967, Mar., 1983.

46. Resendiz D., Romo M.P., *"Analysis of Embankment Deformations,"* Proc. of Specialty Conference on Performance of Earth and Earth-Supported Structures, ASCE, Purdue Univ., Indiana, June, 1972, Vol. I, Part I, pp. 817-776.

47. Sarma S.K., *"Seismic Stability of Earth Dams and Embankments,"* Geotechnique, Vol. 25, No. 4, 1975, pp. 743-761.

48. Schnabel P.B., Lysmer J., Seed H.B., *"SHAKE - A Computer Program For Earthquake Response Analysis of Horizontally Layered Sites,"* Earthquake Engineering Research Center, University of California, Berkeley, Report No. EERC 72-12, 1972.

49. Schumacker B., Whitman R.V., *"Preliminary Seismic Risk Study of Orinoco Delta and Computer Program for Seismic Risk,"* Research Report No. R78-39, MIT, Cambridge, Aug., 1978.

50. Seed H.B., Idriss I.M., " *Soil Moduli and Damping Factors for Dynamic Response Analysis,*" Report No. EERC 70-10, University of California, Berkeley, Dec., 1970.

51. Seed H.B., Idriss I.M.,*"Simplified Procedures for Evaluating Soil Liquefaction Potential,"* Journal of the Soil Mechanics and Foundations Division, ASCE, Vol. 97, No. SM9, Sept., 1971, pp. 1249-1273.

52. Seed H.B., Lee K.L., Idriss I.M., Makdisi F.I., *"The Slides in the San Fernando Dams During the Earthquake of February 9, 1971,"* Journal of the Geotechnical Engineering Division, ASCE, Vol. 101, No. GT7, July, 1975, pp. 651-688.

53. Seed H.B., Idriss I.M., Lee K.L., Makdisi F.I., *"Dynamic Analysis of the Slide in the Lower San Fernando Dam During the Earthquake of February 9, 1971,"* Journal of the Geotechnical Engineering Division, ASCE, Vol. 101, No. GT9, Sept., 1975, pp. 889-911.

54. Seed H.B., Idriss I.M., Makdisi F., Banerjee N., *"Representation of Irregular Stress Time Histories by Equivalent Uniform Stress Series in Liquefaction Analysis,"* Report No. EERC 75-29, College of Engineering, Univ. of California, Berkeley, Oct., 1975.

55. Seed H.B., *"Evaluation of Soil Liquefaction Effects on Level Ground During Earthquakes,"* Liquefaction Problems in Geotechnical Engineering, Annual Convention and Exposition, Specialty Session, ASCE, 1976.

56. Seed H.B., Makdisi F.I., DeAlba P., *"Performance of Earth Dams During Earthquakes,"* Journal of the Geotechnical Engineering Division, ASCE, Vol. 104, No. GT7, July, 1978, pp. 967-994.

57. Seed H.B., *"Considerations in the Earthquake-Resistant Design of Earth and Rockfill Dams,"* Geotechnique, Vol. 29, No. 3, 1979, pp. 215-263.

58. Seed H.B., Idriss I.M., Arango I., *"Evaluation of Liquefaction Potential Using Field Performance Data,"* Journal of the Geotechnical Engineering Division, ASCE, Vol. 109, No. 3, Mar., 1983, pp. 458-482.

59. Seed H.B., " *Design Problems in Soil Liquefaction,*" Journal of the Geotechnical Engineering Division, ASCE, Vol. 113, No. GT8, Aug., 1987, pp. 827-845.

60. Serff N., Seed H.B., Makdisi F.I., Chang C.Y., *"Earthquake Induced Deformation of Earth Dams,"* Report No. EERC 76-4, Univ. of California, Berkeley, Sept., 1976.

61. Sewell R.T., *"Simplified Seismic Reliability Analysis of Earth Dams,"* Ph.D. Dissertation, Department of Civil Engineering, Stanford Univ., Calif., Sept., 1984.

62. Shieh W.Y.J., Huang R.J., *"Permanent Deformation of Earth Dams Under Earthquakes,"* Proc. of the International Conference on Recent Advances in Geotechnical Earthquake Engineering and Soil Dynamics, Univ. of Missouri, Rolla, Apr., 1981, Vol. I, pp.453-458.

63. Singh L.P., *"Attenuation Relationship for Number of Equivalent Cycles of Earthquake Induced Motions,"* Master of Science Report, Department of Civil Engineering, Northeastern University, Boston, Mass., Apr., 1984.

64. Singh M.P., Khatua T.P., *"Stochastic Seismic Stability Prediction of Earth Dams,"* Proc. of Specialty Conference on Earthquake Engineering and Soil Dynamics, ASCE, Pasadena, Calif., 1978, pp. 875-889.

65. U.S. Army Corps of Engineers, *"Earthquake Design and Analysis For Corps of Engineers Projects,"* ER 1110-2-1806, 16 May, 1983.

66. Taniguchi E., Whitman R.V., Marr W.A., *"Prediction of Earthquake-Induced Deformation of Earth Dams,"* Soils and Foundations, Vol. 23, No. 4, Dec., 1983, pp. 126-132.

67. Tong W.H., Schumacker B., Cornell C.A., Whitman R.V., *"Seismic Hazard Maps for Massachusetts,"* Seismic Design Decision Analysis Series, Internal Report No. 52, Department of Civil Engineering, MIT, Cambridge, 1975.

68. Vanmarcke E.H., *"Reliability of Earth Slopes,"* Journal of the Geotechnical Engineering Division, ASCE, Vol. 103, No. GT 11, Nov., 1977, pp. 1247-1265.

69. Von Thun J.L., Harris C.W., *"Estimation of Displacements of Rockfill Dams Due to Seismic Shaking,"* Proc. of the International Conference on Recent Advances in Geotechnical Earthquake Engineering and Soil Dynamics, Univ. of Missouri, Rolla, Apr., 1981, Vol. 1, pp. 417-423.

70. Whitman R.V., *"Evaluating Calculated Risk in Geotechnical Engineering,"* Journal of the Geotechnical Engineering Division, ASCE, Vol. 110, No. GT2, Feb., 1984, pp. 145-188.

71. Wu T.H., Kraft L.M., *"Safety Analysis of Slopes,"* Journal of the Soil Mechanics and Foundations Division, ASCE, Vol. 96, No. SM2, Mar., 1970, pp. 609-630.

72. Wu T.H., Kraft L.M., *"Seismic Safety of Earth Dams,"* Journal of the Soil Mechanics and Foundations Division, ASCE, Vol. 96, No. SM6, Nov., 1970, pp. 1987-2006.

73. Yegian M.K., *"Probabilistic Seismic Hazard Analysis,"* State-of-the-Art for Assessing Earthquake Hazards in the United States, Report 13, U.S. Army Engineer Waterways Experiment Station, July, 1979.

74. Yegian M.K., Vitelli B.M., *"Probabilistic Analysis for Liquefaction,"* Research Report No. CE-81-1, Civil Engineering Department, Northeastern Univ., Boston, Mar., 1981.

75. Yegian M.K., *"Probabilistic Seismic Hazard Analysis for Pore Pressure Build-up in Sands,"* Proc. of the 8th World Conference on Earthquake Engineering, San Francisco, Calif., July, 1984.

Peak Ground Acceleration / Magnitude	ANNUAL NUMBER OF EVENTS, λ X 10^{-4}					
	0.0g≤A<0.05g	0.05g≤A<0.1g	0.1g≤A<0.15g	0.15g≤A<0.2g	0.2g≤A<0.25g	A≥0.25g
$4.33 \leq M < 5.0$	1467.50	41.22	7.87	2.67	1.07	1.25
$5.0 \leq M < 5.5$	392.80	18.51	4.17	1.25	0.55	0.64
$5.5 \leq M < 6.0$	163.30	12.04	2.54	0.98	0.37	0.46
$6.0 \leq M < 6.5$	68.19	7.22	1.86	0.73	0.36	0.44
$6.5 \leq M < 6.8$	12.90	1.72	0.67	0.21	0.12	0.18
TOTAL	2113.69	80.71	17.11	5.84	2.47	2.97

TABLE 1 SEISMIC HAZARD ANALYSIS RESULTS FOR THE EXAMPLE SITE

Peak Ground Acceleration / Number of Cycles	ANNUAL NUMBER OF EVENTS, $\lambda \times 10^{-4}$					
	0.0g≤A<0.05g	0.05g≤A<0.1g	0.1g≤A<0.15g	0.15g≤A<0.2g	0.2g≤A<0.25g	A≥0.25g
$1 \leq N_{eq} < 2$	1467.50	41.22	7.87	2.67	1.07	1.25
$2 \leq N_{eq} < 3$	392.80	18.51	4.17	1.25	0.55	0.64
$3 \leq N_{eq} < 5$	163.30	12.04	2.54	0.98	0.37	0.46
$5 \leq N_{eq} < 8$	68.19	7.22	1.86	0.73	0.36	0.44
$8 \leq N_{eq} < 11$	12.90	1.72	0.67	0.21	0.12	0.18
TOTAL	2113.69	80.71	17.11	5.84	2.47	2.97

TABLE 2 SEISMIC HAZARD ANALYSIS RESULTS FOR THE EXAMPLE SITE

TABLE 3 SEISMIC DATA ANALYZED

Caltech File #	Peak Grd Acceler. cm/s^2	Peak Grd Velocity cm/s	Peak Grd Displ. cm	Period T sec	Neq cycles	Earthq. Magnitude	Epicent. Distance km	Standardized Displacement (*) Us (in) 0.02	for 0.1	Ky/Ka 0.5
1	341.7	33.4	10.9	0.25	7.3	6.7	9.3	230.9	55.6	1.9
1	210.1	36.9	19.8	0.50	12.37	6.7	9.3	138.2	41.6	1.38
4	175.9	17.7	9.2	0.45	11.72	7.7	43	294.3	74.8	2.37
4	152.7	15.7	6.7	0.35	7.64	7.7	43	268.7	85.3	2.09
5	128.6	19.3	5.8	0.90	10.25	7.7	89.5	192.9	70.1	3.61
5	87.8	11.8	4.6	0.50	2.55	7.7	89.5	366.2	136.2	3.1
8	252.7	29.4	14.1	0.40	7.28	6.5	24	143.5	41	2.7
8	164.5	31.6	12.4	0.40	7.23	6.5	24	157.9	31.4	1.7
9	155.7	35.6	14.2	0.40	2.5	6.5	40.4	167.7	53	5.2
9	197.3	26	9.6	0.80	5.28	6.5	40.4	187	52.3	3.2
15	81.8	4.9	2.3	0.25	4.74	5.3	11.8	125.8	23.6	1.07
18	175.7	17.1	8.8	0.40	16.74	5.6	40	164.7	36.5	0.65
21	130.6	28.7	15.5	0.30	2.92	6.3	47.8	115.7	22.6	0.66
25	142.5	13.3	3.7	0.30	4.79	6	6.6	94.6	23.8	1.08
29	274.6	17	10.4	0.35	17.93	7.1	16.8	582.9	127.1	0.5
34	425.7	25.4	7.1	0.35	2.57	5.6	32.4	198.7	41.9	0.02
35	269.6	11.8	3.9	0.20	3.04	5.6	34.1	363	69.8	1.45
37	340.8	22.5	5.5	0.35	2.5	5.6	31	100.6	26.3	0.73
48	250	30	14.9	0.65	7.89	6.6	22.4	398	126.1	1.26
51	122.7	21.9	11.6	0.45	6.4	6.6	42.8	172	38.6	1.47
54	147.1	17.4	11.8	0.45	4.8	6.6	41.9	247.7	60.7	2.88
54	117	17.3	11.8	0.25	8.54	6.6	41.9	215.9	58	0.31
56	309.4	16.5	4.2	0.35	3.35	6.6	28.6	223.3	50.7	0.17
57	103.8	17	8.6	0.25	12.76	6.6	37.1	210.1	62	1.55
57	148.2	19.4	13.1	0.25	8.13	6.6	37.1	284.2	87.7	1.46
58	167.3	16.5	8	0.25	14.4	6.6	37.1	237.6	53.3	1.28
59	133.8	9.6	7.5	0.15	6.56	6.6	39.8	479.9	85.6	0.99
62	130	17.6	6.9	0.25	15.03	6.6	42.8	231.2	63.9	2.77
65	146.7	18	10.3	0.30	3.55	6.6	40	155.9	34.7	0.39
72	82.2	20.8	14.7	0.55	11.48	6.6	39.5	117.7	49.3	0.64
75	133.8	22.3	11.4	0.30	9.92	6.6	40.1	207.2	48.8	2.17
78	126.5	23.2	13.7	0.35	5.54	6.6	42.5	179.5	36.2	2.18
81	198.3	6.2	4.6	0.55	8.29	6.6	32.9	505.5	63.2	3.27
83	158.2	18.3	9	0.30	13.5	6.6	40	228.3	64.3	1.75
86	104.6	17.4	14.8	0.45	5.47	6.6	49.4	306.8	62.2	2.36
88	209.1	23.5	5.3	0.20	8.37	6.6	34.1	276	117.5	4.62
89	139	20.7	11.6	0.15	5.12	6.6	44	181.4	44.3	0.18
98	236.4	21.8	13.2	0.20	3.34	6.6	42.7	218.9	21.3	0.14
103	120.5	5.4	2.4	0.15	14.56	6.6	45.4	605.1	161	2.95
104	103.1	6	2.3	0.20	2.34	6.6	52.2	180.1	36.7	1.21
105	83.1	8.3	4	0.20	12.04	6.6	38.7	338.5	55.8	1.49
106	188.6	11.6	5	0.25	6.04	6.6	36.1	204.1	53.9	4.07
107	107.3	14.3	7.3	0.45	8.36	6.6	39.8	257.9	78.3	0.94

(*) Standardized Displacement According to Franklin and Chang (1977)

TABLE 3 SEISMIC DATA ANALYZED

Caltech File #	Peak Grd Acceler. cm/s^2	Peak Grd Velocity cm/s	Peak Grd Displ. cm	Period T sec	Neq cycles	Earthq. Magnitude	Epicent. Distance km	Standardized Displacement (*) Us (in) 0.02	for 0.1	Ky/Ka 0.5
112	78.5	15.7	9.2	0.60	12.18	6.6	40.5	154.8	32.1	1.99
114	110.8	14	3.8	0.25	19.04	6.6	32.3	287.2	110.1	2.51
115	220.6	28.2	13.4	0.25	8.76	6.6	29.3	351.6	71.4	1.2
121	119.4	17.1	8.6	0.30	8.39	6.6	41.1	253.1	67.4	2.64
131	184.3	17.2	9.2	0.25	6.23	6.6	38.2	244.7	38.7	0.34
137	129	22.3	8.4	0.25	12.63	6.6	29	285.7	122.7	0.56
141	145.5	18	3.4	0.70	4.1	6.6	29.6	183.3	57.3	1.76
142	143.5	8.6	1.7	0.20	8.47	6.6	26.8	204.5	54.2	1.29
143	119.3	4.8	2	0.15	7.14	6.6	26.6	331.8	93.2	4.25
144	277.9	12.4	8.9	0.25	9.96	6.6	23.3	254.9	72.9	6.46
145	113.9	31.5	17.5	0.40	16.16	6.6	34.9	227.7	97.3	3.23
148	112	17.5	11.1	0.30	15.12	6.6	39.9	185	62.2	2.22
166	147.6	15	5.4	0.25	8.93	6.6	30.8	166.2	49.1	3.79
176	83.4	20.9	13.7	1.20	13.43	6.6	42.9	183	59.4	1.19
185	67.3	4.5	2.1	0.25	18.13	6.6	75.6	440.3	128.3	6.79
186	94.7	9.7	5	0.20	13.92	6.6	54.1	405.2	54.3	1.26
187	55.7	3.1	0.7	0.25	11.81	6.6	72.1	498	187.3	8.67
188	114.4	17	10.8	0.30	6.14	6.6	38.9	200.5	26.4	0.34
192	98.9	19.5	7.9	1.10	12.41	6.6	40.7	110.9	33.3	0.54
198	176	20.5	7.28	0.25	5.21	6.6	34	174.5	34.1	1.92
217	108	14.7	9.94	0.45	8.77	6.6	40	294	88.1	1.6
221	165	6.66	5.91	0.15	9.37	6.6	43.3	231.7	63.5	1.73
223	69.7	4.6	2.07	0.20	6.51	6.6	65	327.4	71.4	1.86
233	243	31.5	18.3	0.30	14.42	6.6	29.3	257.6	66.5	1.68
233	197	17.8	9.46	0.20	13.51	6.6	29.3	371	89.2	2.58
236	167	13.4	6.13	0.20	8.67	6.6	34.9	372.1	77.6	1.94
239	119	17.2	9.79	0.20	16.1	6.6	38	255.9	63.5	2.48
239	161	19.1	11.6	0.30	4.76	6.6	38	297.7	54.3	1.49
241	86.8	17.9	9.22	0.25	20.35	6.6	41.8	160.7	52.4	1.42
241	138	19.6	9.98	0.25	3.29	6.6	41.8	221.8	50.4	1.75
244	149	18.3	9.8	0.40	2.94	6.6	41.9	191.8	45.6	1.69
246	115	16.7	8.29	0.30	7.65	6.6	35.7	198.4	57.2	1.49
251	188	18.7	9.49	0.45	3.6	6.6	41.8	189.6	34.8	0.18
253	242	19.2	11.4	0.25	3.77	6.6	42	280.2	64.5	1.44
255	123	22.5	15.8	0.35	11.27	6.6	38.9	206.4	61.5	0.69
261	97.7	18.3	12.2	0.35	11.25	6.6	39.6	200.1	56.5	0.83
262	68.3	25.7	16.5	0.35	11	6.6	39	100.8	47.4	1.46
262	93.6	27.8	13.7	0.45	5.71	6.6	39	118.6	42	1.57
265	125	18.2	12.6	0.15	8.19	6.6	39.9	200.1	51.7	0.43
266	129	21.4	11.6	0.25	10.06	6.6	40	175.6	60.2	0.74
267	55.5	13.5	8.49	0.70	11.55	6.6	52	157.9	40.3	0.7
267	61.5	13.8	9.38	0.20	8.23	6.6	52	218.9	58.6	0.25
312	232	11.9	1.66	0.15	2.57	5.8	30.6	108.4	9.2	0

(*) Standardized Displacement According to Franklin and Chang (1977)

TABLE 4 NON-DIMENSIONAL NORMALIZED PERMANENT DEFORMATIONS, Dn

Caltech File #	(1) Standardized Displacement Us(in) for Ky/Ka = 0.02	0.1	0.5	(2) Displ. Factor	(3) Permanent Deformation Dr (in) for Ky/Ka = 0.02	0.1	0.5	(4) Normaliz. Factor F	(5) Normalized Perm. Deform. Dn (non-dimens.) for Ky/Ka = 0.02	0.1	0.5
1	230.9	55.6	1.9	0.275505	63.614	15.318	0.523	61.378	1.03643	0.24957	0.00853
1	138.2	41.6	1.38	0.546901	75.582	22.751	0.755	255.800	0.29547	0.08894	0.00295
4	294.3	74.8	2.37	0.150301	44.234	11.243	0.356	164.355	0.26913	0.06840	0.00217
4	268.7	85.3	2.09	0.136220	36.602	11.620	0.285	56.264	0.65054	0.20652	0.00506
5	192.9	70.1	3.61	0.244430	47.151	17.135	0.882	420.354	0.11217	0.04076	0.00210
5	366.2	136.2	3.1	0.133829	49.008	18.228	0.415	22.036	2.22397	0.82716	0.01883
8	143.5	41	2.7	0.288650	41.421	11.835	0.779	115.884	0.35744	0.10213	0.00673
8	157.9	31.4	1.7	0.512259	80.886	16.085	0.871	74.919	1.07965	0.21470	0.01162
9	167.7	53	5.2	0.686899	115.193	36.406	3.572	24.520	4.69799	1.48476	0.14567
9	187	52.3	3.2	0.289135	54.068	15.122	0.925	262.486	0.20599	0.05761	0.00352
15	125.8	23.6	1.07	0.024770	3.116	0.585	0.027	9.541	0.32661	0.06127	0.00278
18	164.7	36.5	0.65	0.140444	23.131	5.126	0.091	185.273	0.12485	0.02767	0.00049
21	115.7	22.6	0.66	0.532234	61.579	12.028	0.351	13.512	4.55724	0.89018	0.02600
25	94.6	23.8	1.08	0.104754	9.910	2.493	0.113	24.186	0.40973	0.10308	0.00468
29	582.9	127.1	0.5	0.088813	51.769	11.288	0.044	237.456	0.21802	0.04754	0.00019
34	198.7	41.9	0.02	0.127893	25.412	5.359	0.003	52.764	0.48162	0.10156	0.00005
35	363	69.8	1.45	0.043584	15.821	3.042	0.063	12.907	1.22578	0.23570	0.00490
37	100.6	26.3	0.73	0.125357	12.611	3.297	0.092	41.090	0.30691	0.08023	0.00223
48	398	126.1	1.26	0.303797	120.911	38.309	0.383	328.102	0.36852	0.11676	0.00117
51	172	38.6	1.47	0.329857	56.735	12.732	0.485	62.606	0.90623	0.20338	0.00775
54	247.7	60.7	2.88	0.173687	43.022	10.543	0.500	56.292	0.76427	0.18729	0.00889
54	215.9	58	0.31	0.215868	46.606	12.520	0.067	24.586	1.89562	0.50925	0.00272
56	223.3	50.7	0.17	0.074256	16.581	3.765	0.013	49.988	0.33170	0.07531	0.00025
57	210.1	62	1.55	0.234954	49.364	14.567	0.364	32.591	1.51466	0.44697	0.01117
57	284.2	87.7	1.46	0.214307	60.906	18.795	0.313	29.647	2.05436	0.63395	0.01055
58	237.6	53.3	1.28	0.137326	32.629	7.319	0.176	59.279	0.55042	0.12347	0.00297
59	479.9	85.6	0.99	0.058126	27.895	4.976	0.058	7.775	3.58766	0.63993	0.00740
62	231.2	63.9	2.77	0.201078	46.489	12.849	0.557	48.078	0.96695	0.26725	0.01158
65	155.9	34.7	0.39	0.186379	29.056	6.467	0.073	18.453	1.57462	0.35048	0.00394
72	117.7	49.3	0.64	0.444157	52.277	21.897	0.284	112.384	0.46517	0.19484	0.00253
75	207.2	48.8	2.17	0.313643	64.987	15.306	0.681	47.030	1.38181	0.32545	0.01447
78	179.5	36.2	2.18	0.359060	64.451	12.998	0.783	33.799	1.90691	0.38457	0.02316
81	505.5	63.2	3.27	0.016358	8.269	1.034	0.053	195.780	0.04224	0.00528	0.00027
83	228.3	64.3	1.75	0.178639	40.783	11.487	0.313	75.674	0.53893	0.15179	0.00413
86	306.8	62.2	2.36	0.244258	74.938	15.193	0.576	45.615	1.64284	0.33307	0.01264
88	276	117.5	4.62	0.222876	61.514	26.188	1.030	27.562	2.23186	0.95016	0.03736
89	181.4	44.3	0.18	0.260140	47.189	11.524	0.047	6.304	7.48535	1.82801	0.00743
98	218.9	21.3	0.14	0.169647	37.136	3.613	0.024	12.434	2.98658	0.29061	0.00191
103	605.1	161	2.95	0.020421	12.357	3.288	0.060	15.542	0.79508	0.21155	0.00388
104	180.1	36.7	1.21	0.029466	5.307	1.081	0.036	3.799	1.39682	0.28464	0.00938
105	338.5	55.8	1.49	0.069958	23.681	3.904	0.104	15.756	1.50294	0.24775	0.00662
106	204.1	53.9	4.07	0.060208	12.289	3.245	0.245	28.030	0.43840	0.11578	0.00874
107	257.9	78.3	0.94	0.160825	41.477	12.593	0.151	71.515	0.57997	0.17608	0.00211
112	154.8	32.1	1.99	0.264979	41.019	8.506	0.527	135.514	0.30269	0.06277	0.00389
114	287.2	110.1	2.51	0.149279	42.873	16.436	0.375	51.910	0.82591	0.31662	0.00722
115	351.6	71.4	1.2	0.304211	106.960	21.721	0.365	47.550	2.24941	0.45679	0.00768

TABLE 4 NON-DIMENSIONAL NORMALIZED PERMANENT DEFORMATIONS, Dn

Caltech File #	(1) Standardized Displacement Us(in) for Ky/Ka = 0.02	0.1	0.5	(2) Displ. Factor	(3) Permanent Deformation Dr (in) for Ky/Ka = 0.02	0.1	0.5	(4) Normaliz. Factor F	(5) Normalized Perm. Deform. Dn (non-dimens.) for Ky/Ka = 0.02	0.1	0.5
121	253.1	67.4	2.64	0.206666	52.307	13.929	0.546	35.496	1.47363	0.39242	0.01537
131	244.7	38.7	0.34	0.135461	33.147	5.242	0.046	28.253	1.17324	0.18555	0.00163
137	285.7	122.7	0.56	0.325313	92.942	39.916	0.182	40.090	2.31832	0.99565	0.00454
141	183.3	57.3	1.76	0.187916	34.445	10.768	0.331	115.082	0.29931	0.09356	0.00287
142	204.5	54.2	1.29	0.043494	8.894	2.357	0.056	19.141	0.46469	0.12316	0.00293
143	331.8	93.2	4.25	0.016298	5.408	1.519	0.069	7.545	0.71666	0.20130	0.00918
144	254.9	72.9	6.46	0.046691	11.902	3.404	0.302	68.107	0.17475	0.04998	0.00443
145	227.7	97.3	3.23	0.735155	167.395	71.531	2.375	115.945	1.44375	0.61694	0.02048
148	185	62.2	2.22	0.230749	42.689	14.353	0.512	60.004	0.71143	0.23920	0.00854
166	166.2	49.1	3.79	0.128641	21.380	6.316	0.488	32.433	0.65921	0.19475	0.01503
176	183	59.4	1.19	0.441986	80.883	26.254	0.526	634.995	0.12738	0.04135	0.00083
185	440.3	128.3	6.79	0.025392	11.180	3.258	0.172	30.023	0.37238	0.10851	0.00574
186	405.2	54.3	1.26	0.083845	33.974	4.553	0.106	20.759	1.63655	0.21931	0.00509
187	498	187.3	8.67	0.014560	7.251	2.727	0.126	16.186	0.44795	0.16848	0.00780
188	200.5	26.4	0.34	0.213183	42.743	5.628	0.072	24.889	1.71738	0.22613	0.00291
192	110.9	33.3	0.54	0.324455	35.982	10.804	0.175	584.681	0.06154	0.01848	0.00030
198	174.5	34.1	1.92	0.201501	35.162	6.871	0.387	22.563	1.55839	0.30453	0.01715
217	294	88.1	1.6	0.168847	49.641	14.875	0.270	75.512	0.65739	0.19699	0.00358
221	231.7	63.5	1.73	0.022685	5.256	1.441	0.039	13.695	0.38380	0.10518	0.00287
223	327.4	71.4	1.86	0.025619	8.388	1.829	0.048	7.146	1.17383	0.25599	0.00667
233	257.6	66.5	1.68	0.344585	88.765	22.915	0.579	124.159	0.71493	0.18456	0.00466
233	371	89.2	2.58	0.135724	50.353	12.107	0.350	41.913	1.20139	0.28885	0.00835
236	372.1	77.6	1.94	0.090735	33.762	7.041	0.176	22.801	1.48072	0.30880	0.00772
239	255.9	63.5	2.48	0.209793	53.686	13.322	0.520	30.172	1.77936	0.44154	0.01724
239	297.7	54.3	1.49	0.191215	56.925	10.383	0.285	27.154	2.09633	0.38237	0.01049
241	160.7	52.4	1.42	0.311507	50.059	16.323	0.442	43.464	1.15174	0.37555	0.01018
241	221.8	50.4	1.75	0.234917	52.105	11.840	0.411	11.172	4.66397	1.05980	0.03680
244	191.8	45.6	1.69	0.189670	36.379	8.649	0.321	27.594	1.31834	0.31343	0.01162
246	198.4	57.2	1.49	0.204652	40.603	11.706	0.305	31.172	1.30254	0.37553	0.00978
251	189.6	34.8	0.18	0.156967	29.761	5.462	0.028	53.957	0.55156	0.10124	0.00052
253	280.2	64.5	1.44	0.128549	36.019	8.291	0.185	22.449	1.60448	0.36934	0.00825
255	206.4	61.5	0.69	0.347329	71.689	21.361	0.240	66.854	1.07231	0.31951	0.00358
261	200.1	56.5	0.83	0.289261	57.881	16.343	0.240	53.009	1.09191	0.30831	0.00453
262	100.8	47.4	1.46	0.816070	82.260	38.682	1.191	36.234	2.27025	1.06756	0.03288
262	118.6	42	1.57	0.696780	82.638	29.265	1.094	42.609	1.93945	0.68682	0.02567
265	200.1	51.7	0.43	0.223622	44.747	11.561	0.096	9.069	4.93423	1.27486	0.01060
266	175.6	60.2	0.74	0.299585	52.607	18.035	0.222	31.933	1.64744	0.56478	0.00694
267	157.9	40.3	0.7	0.277113	43.756	11.168	0.194	123.662	0.35384	0.09031	0.00157
267	218.9	58.6	0.25	0.261315	57.202	15.313	0.065	7.971	7.17646	1.92115	0.00820
312	108.4	9.2	0	0.051510	5.584	0.474	0.000	5.282	1.05718	0.08972	0.00008

NOTES: (1) Standardized Displacement According to Franklin and Chang (1977)
(2) Factor Converting the Standardized Displacement Into Actual Permanent Deformation From Franklin and Chang (1977)
(3) Actual Permanent Deformation From Integration of Time-Histories by Franklin and Chang (1977)
(4) F = (Neq*Ka*T^2)
(5) Dn = Dr/F

Peak Ground Acceleration / Number of Equivalent Cycles / Damage State	1 - 5	5 - 10	10 - 15	15 - 20	20 - 25
	0.0g ≤ A < 0.05g				
NO/MINOR (<1')					
HEAVY (1' - 4')					
CATASTROPHIC (>4')					
	0.05g ≤ A < 0.1g				
NO/MINOR (<1')					
HEAVY (1' - 4')					
CATASTROPHIC (>4')					
	0.1g ≤ A < 0.15g				
NO/MINOR (<1')			0.55		
HEAVY (1' - 4')			0.25		
CATASTROPHIC (>4')			0.20		
	0.15g ≤ A < 0.2g				
NO/MINOR (<1')					
HEAVY (1' - 4')					
CATASTROPHIC (>4')					
	0.2g ≤ A < 0.25g				
NO/MINOR (<1')					
HEAVY (1' - 4')					
CATASTROPHIC (>4')					
	A ≥ 0.25g				
NO/MINOR (<1')					
HEAVY (1' - 4')					
CATASTROPHIC (>4')					

TABLE 5 TYPICAL DAMAGE PROBABILITY MATRIX FOR MODE 1

Peak Ground Acceleration / ΔN_{eq} or ΔM / Damage State	A < 0.1g	0.10g ≤ A < 0.15g					0.15g ≤ A < 0.2g					0.2g ≤ A < 0.25g					A ≥ 0.25g				
No Flow Failure																					
Flow Failure																					

TABLE 6 TYPICAL DAMAGE PROBABILITY MATRIX FOR MODE 2

Peak Ground Acceleration / Magnitude	ANNUAL NUMBER OF EVENTS, $\lambda \times 10^{-4}$					
	0.0g≤A<0.05g	0.05g≤A<0.1g	0.1g≤A<0.15g	0.15g≤A<0.2g	0.2g≤A<0.25g	A≥0.25g
$4.33 \leq M < 5.0$	1467.50	41.22	7.87	2.67	1.07	1.25
$5.0 \leq M < 5.5$	392.80	18.51	4.17	1.25	0.55	0.64
$5.5 \leq M < 6.0$	163.30	12.04	2.54	0.98	0.37	0.46
$6.0 \leq M < 6.5$	68.19	7.22	1.86	0.73	0.36	0.44
$6.5 \leq M < 6.8$	12.90	1.72	0.67	0.21	0.12	0.18
TOTAL	2113.69	80.71	17.11	5.84	2.47	2.97

TABLE 7 SEISMIC HAZARD ANALYSIS RESULTS FOR THE EXAMPLE SITE

Peak Ground Acceleration / Number of Cycles	ANNUAL NUMBER OF EVENTS, λ X 10^{-4}					
	0.0g≤A<0.05g	0.05g≤A<0.1g	0.1g≤A<0.15g	0.15g≤A<0.2g	0.2g≤A<0.25g	A≥0.25g
$1 \leq N_{eq} < 2$	1467.50	41.22	7.87	2.67	1.07	1.25
$2 \leq N_{eq} < 3$	392.80	18.51	4.17	1.25	0.55	0.64
$3 \leq N_{eq} < 5$	163.30	12.04	2.54	0.98	0.37	0.46
$5 \leq N_{eq} < 8$	68.19	7.22	1.86	0.73	0.36	0.44
$8 \leq N_{eq} < 11$	12.90	1.72	0.67	0.21	0.12	0.18
TOTAL	2113.69	80.71	17.11	5.84	2.47	2.97

TABLE 8 SEISMIC HAZARD ANALYSIS RESULTS FOR THE EXAMPLE SITE

NUMBER OF CYCLES	MAGNITUDE	PEAK GROUND ACCELERATION														
		0.0g ≤ A < 0.05g			0.05g ≤ A < 0.10g			0.10g ≤ A < 0.15g			0.15g ≤ A < 0.20g			A ≥ 0.20g		
		k_y(g)	k_a(g)	k_y/k_a	k_y(g)	k_a(g)	k_y/k_a	k_y(g)	k_a(g)	k_y/k_a	k_y(g)	k_a(g)	k_y/k_a	k_y(g)	k_a(g)	k_y/k_a
1 - 2	4.3-5.5	0.123	0.034	6.26	0.198	0.096	2.06	0.152	0.154	0.99	0.067	0.204	0.33	0	0.234	0
2 - 3	5.0-5.5	0.123	0.034	6.26	0.195	0.096	2.03	0.137	0.154	0.89	0	0.204	0	0	0.234	0
3 - 5	5.5-6.0	0.123	0.034	6.26	0.188	0.096	1.96	0.106	0.154	0.69	0	0.204	0	0	0.234	0
5 - 8	6.0-6.5	0.123	0.034	6.26	0.182	0.096	1.90	0.037	0.154	0.24	0	0.204	0	0	0.234	0
8-11	6.5-6.8	0.123	0.034	6.26	0.170	0.096	1.77	0	0.154	0	0	0.204	0	0	0.234	0

TABLE 9 VALUES OF k_y/k_a FOR EACH ACCELERATION AND MAGNITUDE RANGE (Example Problem)

Peak Ground Acceleration / Magnitude	PORE PRESSURE RATIO , R_u				
	0.0g≤A<0.05g	0.05g≤A<0.1g	0.1g≤A<0.15g	0.15g≤A<0.2g	0.2g≤A<0.25g
4.33 - 5.0	0	0.05	0.2	0.48	1.0
5.0 - 5.5	0	0.06	0.25	1.0	1.0
5.5 - 6.0	0	0.08	0.35	1.0	1.0
6.0 - 6.5	0	0.10	0.58	1.0	1.0
6.5 - 6.8	0	0.14	1.0	1.0	1.0

TABLE 10 PORE PRESSURE RATIO R_u, VS. GROUND ACCELERATION AND MAGNITUDE

TABLE 11 INPUT PARAMETERS TO THE COMPUTER PROGRAM (EXAMPLE SITE)

Accel. Range	Neq Range	Mean of Ky (g)	Accel. Ka (g)	Period T	Dn=Dr/Ka*Neq*T^2 Dr=2'	Dr=10'
	1-2	0.2130	0.0340	0.3150	12.2739	61.3695
	2-3	0.2130	0.0340	0.3150	7.3643	36.8217
.0g-.05g	3-5	0.2130	0.0340	0.3150	4.6027	23.0136
	5-8	0.2130	0.0340	0.3150	2.8324	14.1622
	8-11	0.2130	0.0340	0.3150	1.9380	9.6899
	1-2	0.1980	0.0960	0.3800	2.9871	14.9353
	2-3	0.1950	0.0960	0.3800	1.7922	8.9612
.05g-.1g	3-5	0.1880	0.0960	0.3800	1.1201	5.6007
	5-8	0.1820	0.0960	0.3800	0.6893	3.4466
	8-11	0.1700	0.0960	0.3800	0.4716	2.3582
	1-2	0.1514	0.1540	0.4450	1.3578	6.7891
	2-3	0.1369	0.1540	0.4450	0.8147	4.0735
.1g-.15g	3-5	0.1065	0.1540	0.4450	0.5092	2.5459
	5-8	0.0401	0.1540	0.4450	0.3133	1.5667
	8-11	0.0000	0.1540	0.4450	0.2144	1.0720
	1-2	0.0670	0.2040	0.5100	0.7804	3.9020
	2-3	0.0000	0.2040	0.5100	0.4682	2.3412
.15g-.2g	3-5	0.0000	0.2040	0.5100	0.2926	1.4632
	5-8	0.0000	0.2040	0.5100	0.1801	0.9005
	8-11	0.0000	0.2040	0.5100	0.1232	0.6161
	1-2	0.0000	0.2340	0.5700	0.5446	2.7232
	2-3	0.0000	0.2340	0.5700	0.3268	1.6339
.2g-.25g	3-5	0.0000	0.2340	0.5700	0.2042	1.0212
	5-8	0.0000	0.2340	0.5700	0.1257	0.6284
	8-11	0.0000	0.2340	0.5700	0.0860	0.4300
	1-2	0.0000	0.2660	0.6350	0.3861	1.9303
	2-3	0.0000	0.2660	0.6350	0.2316	1.1582
>.25g	3-5	0.0000	0.2660	0.6350	0.1448	0.7239
	5-8	0.0000	0.2660	0.6350	0.0891	0.4455
	8-11	0.0000	0.2660	0.6350	0.0610	0.3048

NOTES:

Standard Deviation of (Ky)=Sigma(Ky)=0.06

Standard Deviation of (T)=Sigma(T)=0.08

Peak Ground Acceleration / Number of Equivalent Cycles / Damage State	1 - 2	2 - 3	3 - 5	5 - 8	8 - 11
	0.0g ≤ A < 0.05g				
NO/MINOR (<2')	1.0	1.0	1.0	1.0	1.0
HEAVY (2' - 10')	0	0	0	0	0
CATASTROPHIC (>10')	0	0	0	0	0
	0.05g ≤ A < 0.1g				
NO/MINOR (<2')	1.0	1.0	1.0	1.0	1.0
HEAVY (2' - 10')	0	0	0	0	0
CATASTROPHIC (>10')	0	0	0	0	0
	0.1g ≤ A < 0.15g				
NO/MINOR (<2')	0.998	0.991	0.952	0.801	0.703
HEAVY (2' - 10')	0.002	0.006	0.025	0.070	0.096
CATASTROPHIC (>10')	0	0.003	0.023	0.129	0.201
	0.15g ≤ A < 0.2g				
NO/MINOR (<2')	0.858	0.729	0.702	0.680	0.664
HEAVY (2' - 10')	0.094	0.149	0.126	0.100	0.084
CATASTROPHIC (>10')	0.048	0.122	0.172	0.220	0.252
	0.2g ≤ A < 0.25g				
NO/MINOR (<2')	0.735	0.702	0.677	0.656	0.642
HEAVY (2' - 10')	0.160	0.138	0.113	0.090	0.077
CATASTROPHIC (>10')	0.105	0.160	0.210	0.254	0.281
	A ≥ 0.25g				
NO/MINOR (<2')	0.706	0.676	0.654	0.635	0.623
HEAVY (2' - 10')	0.153	0.126	0.101	0.081	0.068
CATASTROPHIC (>10')	0.141	0.198	0.245	0.284	0.309

TABLE 12 DAMAGE PROBABILITY MATRIX FOR MODE 1 (Example Problem)

Peak Ground Acceleration / Number of Cycles / Damage State	A < 0.1g	0.10g ≤ A < 0.15g					0.15g ≤ A < 0.2g					0.2g ≤ A < 0.25g					A ≥ 0.25g				
	1-11	1-2	2-3	3-5	5-8	8-11	1-2	2-3	3-5	5-8	8-11	1-2	2-3	3-5	5-8	8-11	1-2	2-3	3-5	5-8	8-11
No Flow Failure	1.0	.993	.981	.952	.698	.032	.849	.032	.032	.032	.032	.032	.032	.032	.032	.032	.032	.032	.032	.032	.032
Flow Failure	0	.007	.019	.048	.302	.968	.151	.968	.968	.968	.968	.968	.968	.968	.968	.968	.968	.968	.968	.968	.968

TABLE 13 DAMAGE PROBABILITY MATRIX FOR MODE 2 (Example Problem)

Peak Ground Acceleration / Number of Equivalent Cycles / Combined Damage State	1 - 2	2 - 3	3 - 5	5 - 8	8 - 11
	0.0g ≤ A < 0.05g				
OS	1.0	1.0	1.0	1.0	1.0
HS	0	0	0	0	0
C/F	0	0	0	0	0
	0.05g ≤ A < 0.1g				
OS	1.0	1.0	1.0	1.0	1.0
HS	0	0	0	0	0
C/F	0	0	0	0	0
	0.1g ≤ A < 0.15g				
OS	0.991	0.972	0.906	0.559	0.022
HS	0.002	0.006	0.024	0.049	0.003
C/F	0.007	0.022	0.070	0.392	0.975
	0.15g ≤ A < 0.2g				
OS	0.728	0.023	0.022	0.022	0.021
HS	0.080	0.005	0.004	0.003	0.003
C/F	0.192	0.972	0.974	0.975	0.976
	0.2g ≤ A < 0.25g				
OS	0.023	0.022	0.022	0.021	0.021
HS	0.005	0.004	0.004	0.003	0.002
C/F	0.972	0.974	0.974	0.976	0.977
	A ≥ 0.25g				
OS	0.023	0.022	0.021	0.020	0.020
HS	0.005	0.004	0.003	0.003	0.002
C/F	0.972	0.974	0.976	0.977	0.978

TABLE 14 DAMAGE PROBABILITY MATRIX FOR COMBINED MODES (Example Problem)

SEISMIC RISK				
Damage State	Permanent Deformation	Annual Number of Events (x 10^{-3})	Annual Probability	Probability in 50 Years
No or Minor	Less than 2 feet	221.903	0.9996	98.14%
Heavy	2 to 10 feet	0.165	0.165×10^{-3}	0.81%
Catastrophic	Greater than 10 feet	0.211	0.211×10^{-3}	1.05%

TABLE 15 SEISMIC RISK RESULTS FOR MODE 1 (Example Problem)

SEISMIC RISK			
Post-Earthquake Stability (State)	Annual Number of Events (x 10^{-3})	Annual Probability of Exceedence	Probability in 50 Years
Survival	221.259	0.999	95.0%
Failure	1.020	0.001	5.0%

TABLE 16 SEISMIC RISK RESULTS FOR MODE 2 (Example Problem)

SEISMIC RISK (Combined)				
Damage State	Consequence	Annual Number of Events (x 10^{-3})	Annual Probability	Probability in 50 Years
OS	No or Minor Damage	221.174	0.9989	94.63%
HS	Heavy Damage	0.044	0.043×10^{-3}	0.21%
C/F	Failure	1.060	1.060×10^{-3}	5.16%

TABLE 17 SEISMIC RISK RESULTS FOR COMBINED MODES (Example Problem)

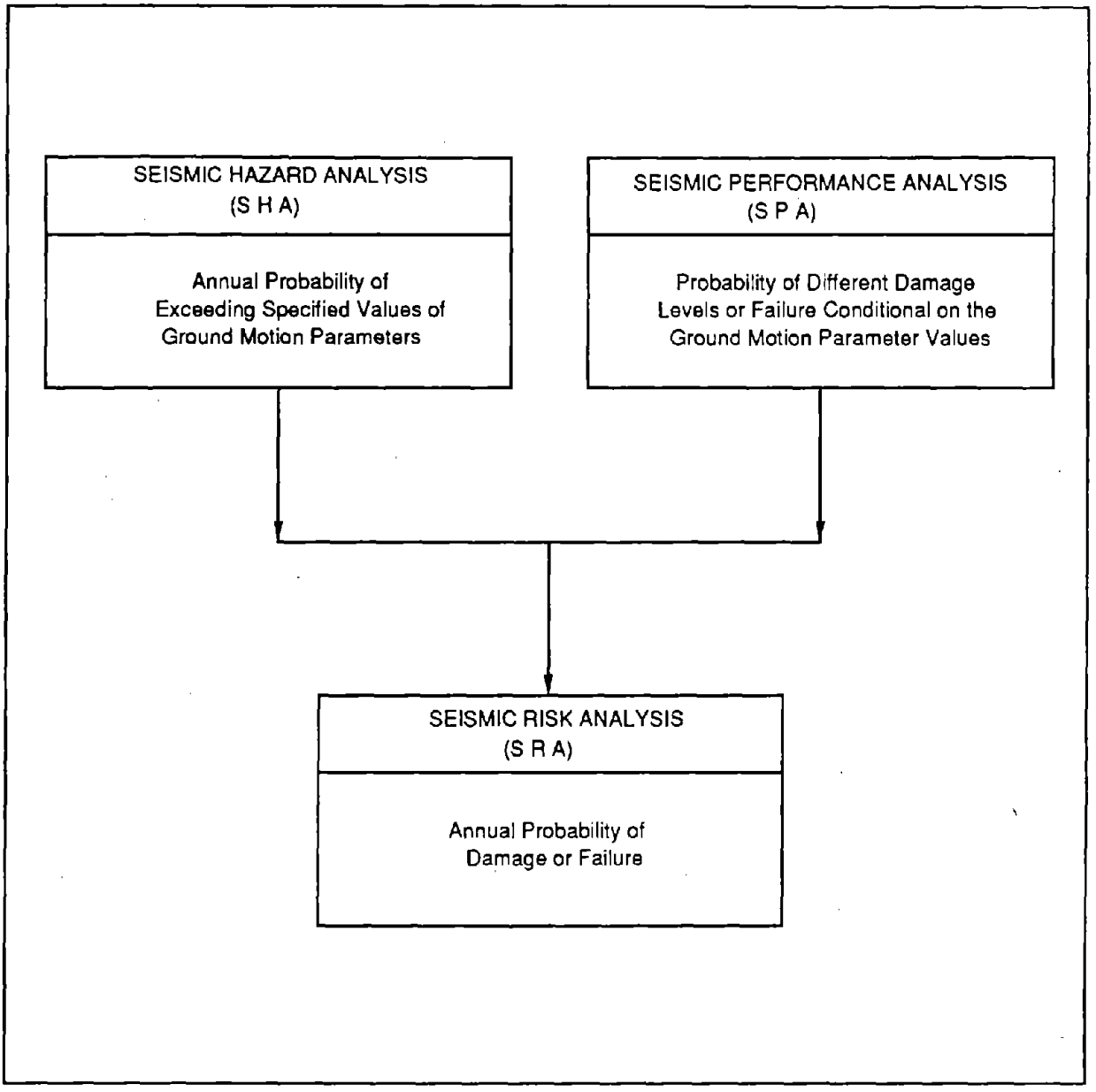

FIGURE 1 SCHEMATIC REPRESENTATION OF SEISMIC RISK ANALYSIS

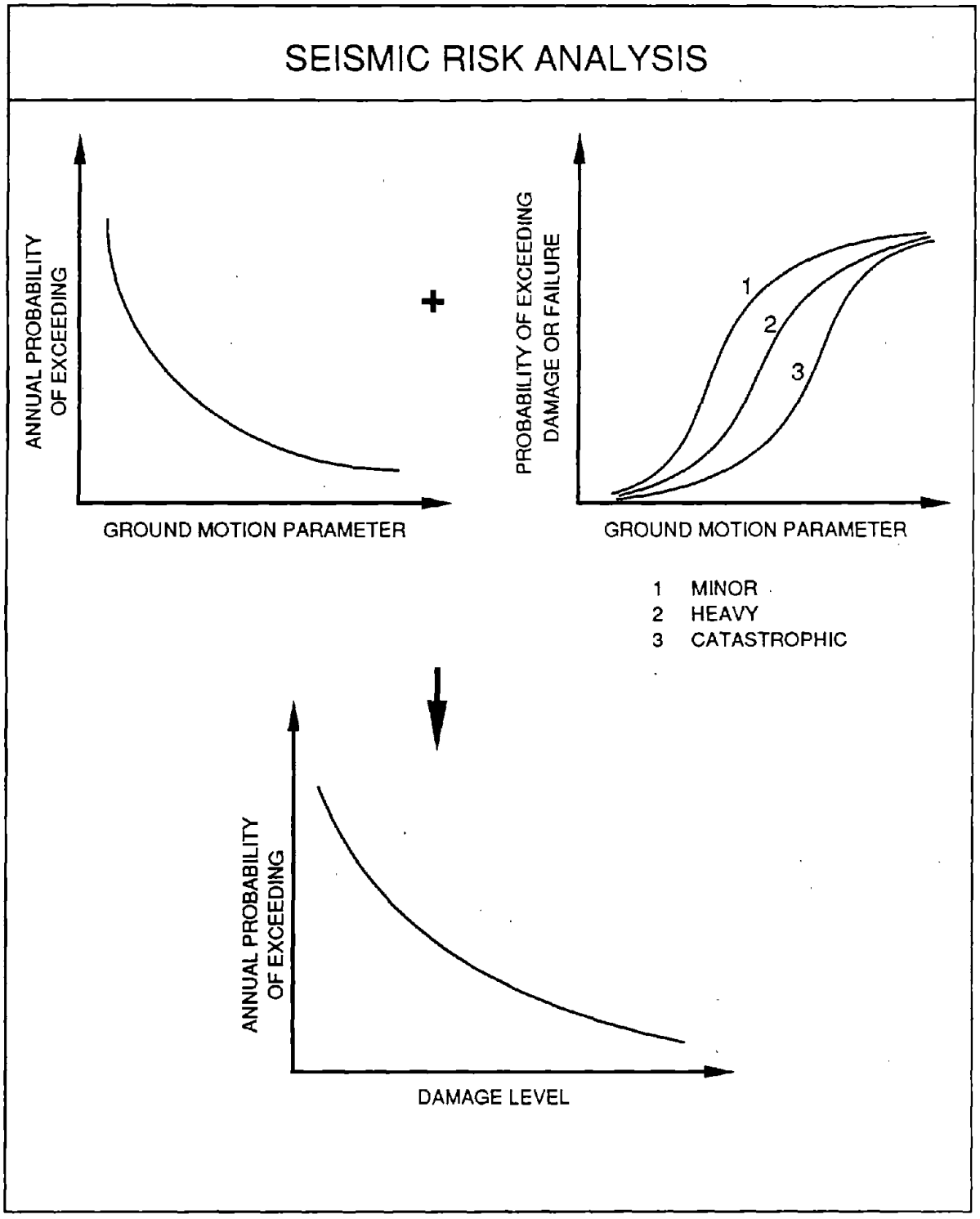

FIGURE 2 STEPS INVOLVED IN SEISMIC RISK ANALYSIS

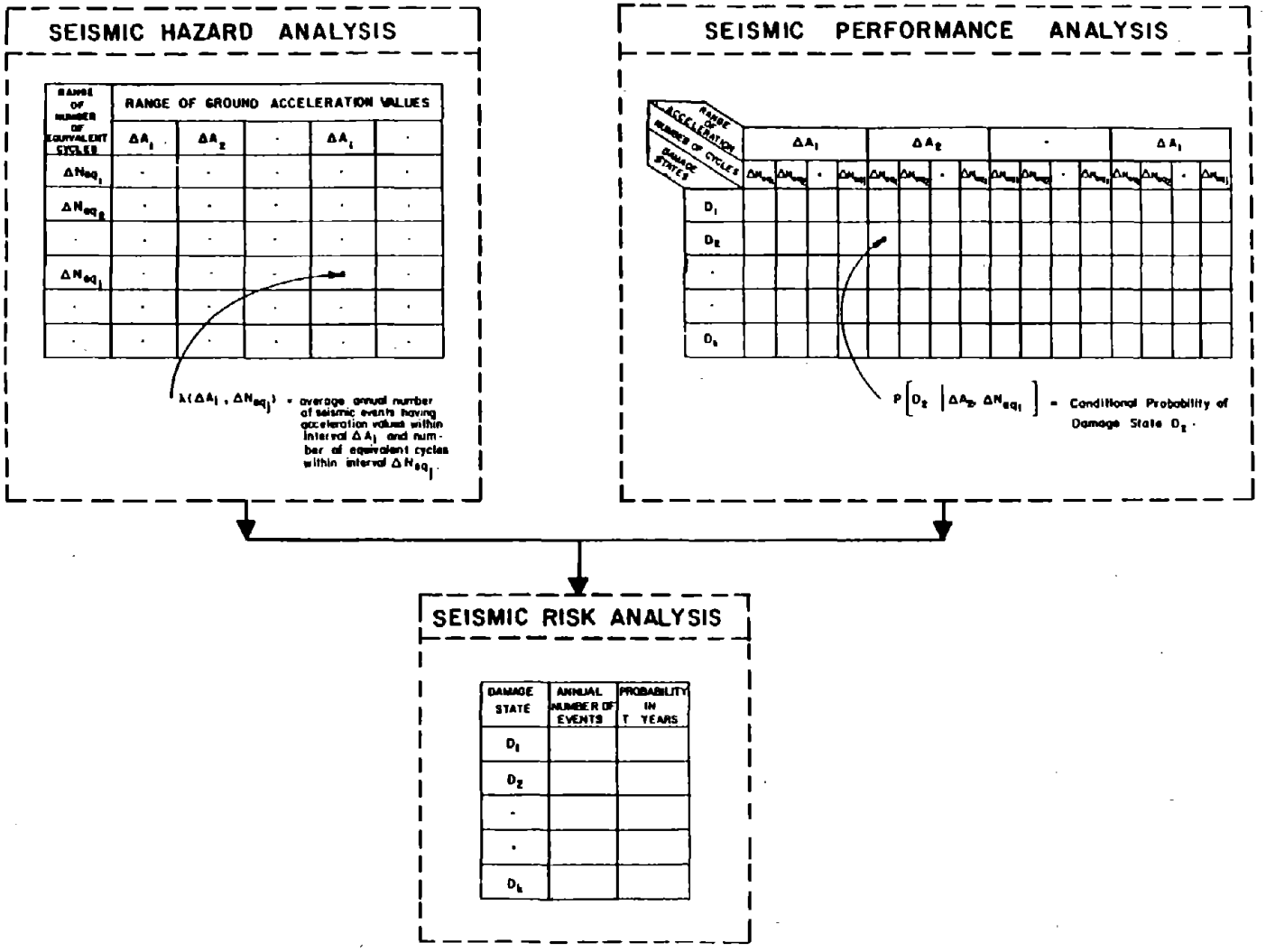

FIGURE 3 MATRIX REPRESENTATION OF THE INTEGRATED SEISMIC RISK ANALYSIS PROPOSED

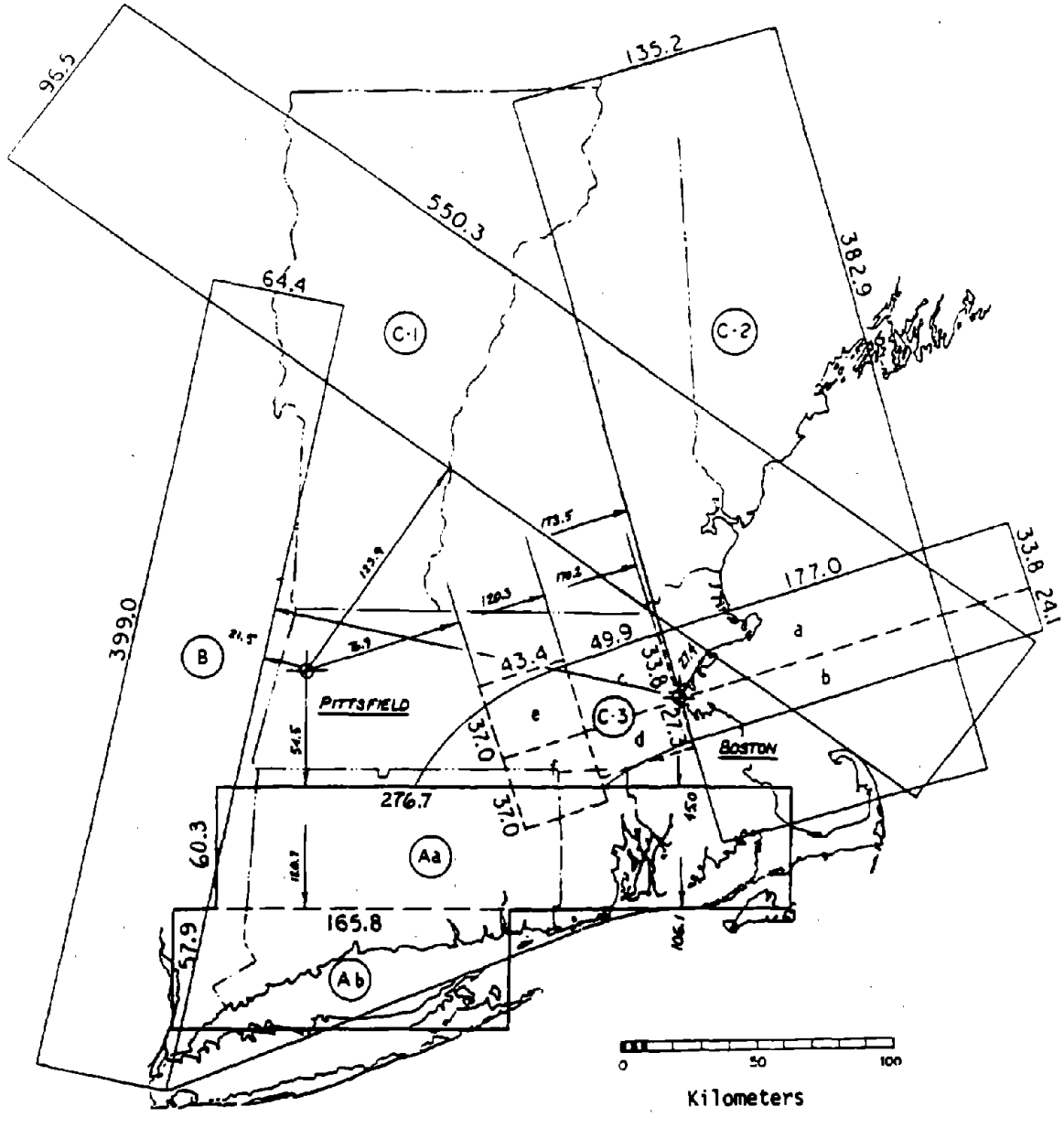

FIGURE 4 SEISMIC SOURCE ZONES FOR BOSTON AREA (EXAMPLE PROBLEM)

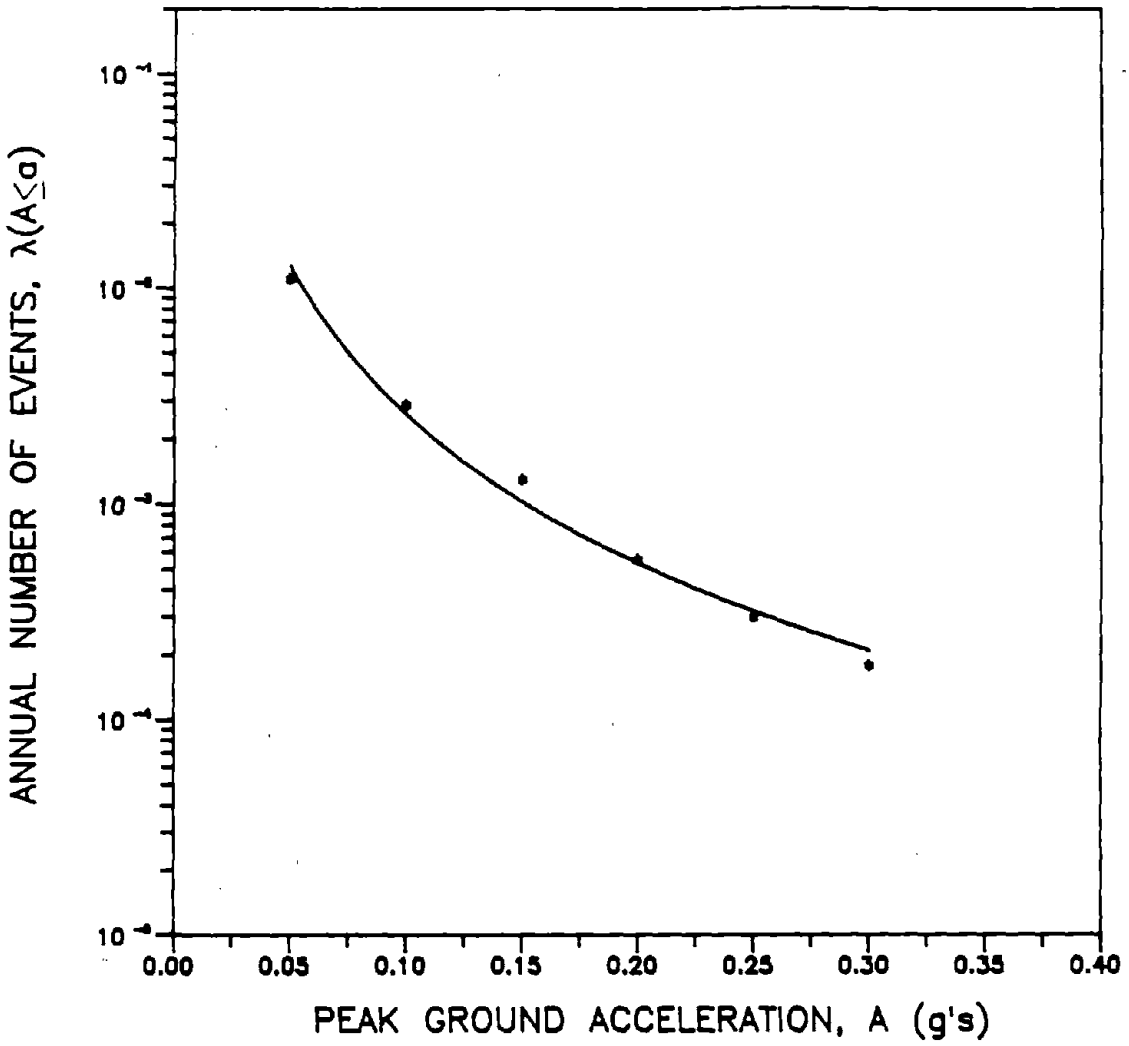

FIGURE 5 ANNUAL NUMBER OF EVENTS, $\lambda(A \leq a)$ FOR BOSTON AREA

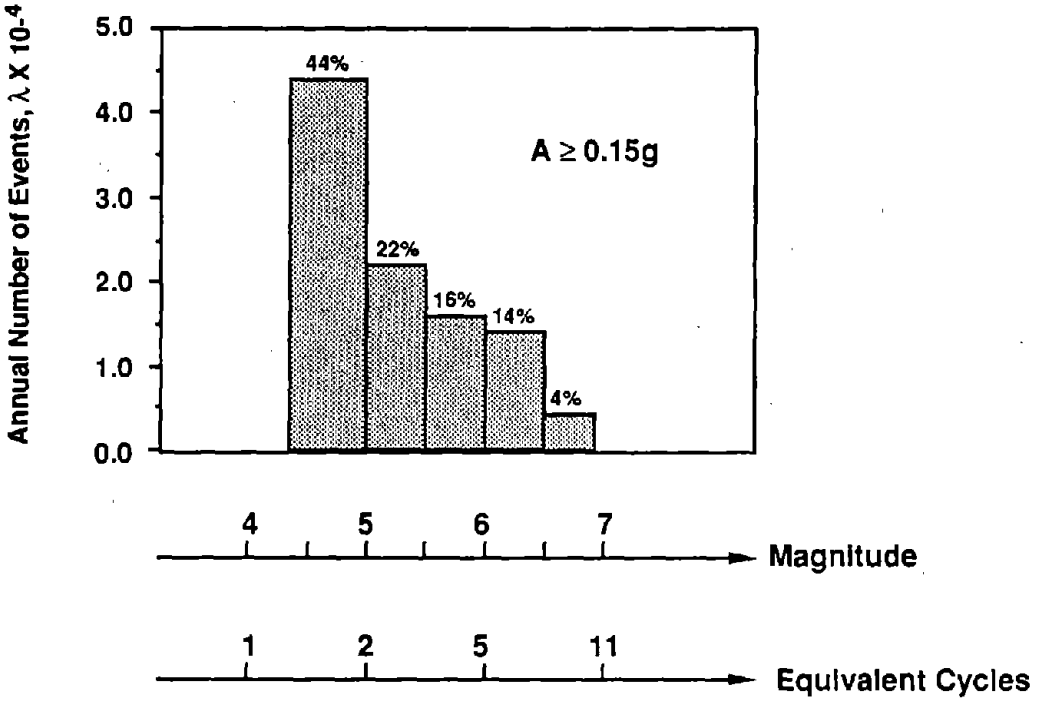

FIGURE 6 HISTOGRAM OF ANNUAL NUMBER OF EVENTS AS A FUNCTION OF MAGNITUDE AND NUMBER OF EQUIVALENT CYCLES

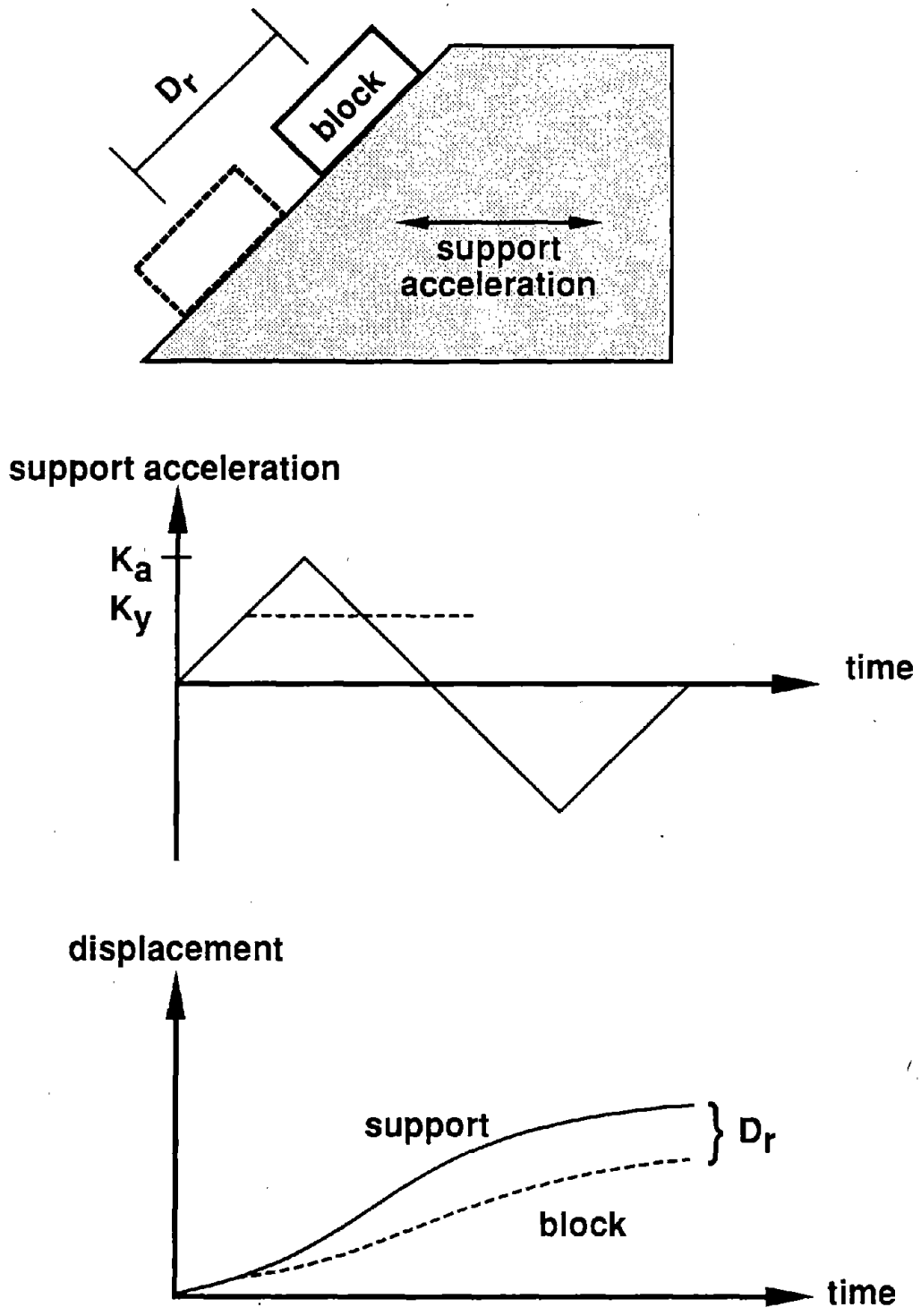

FIGURE 7 SLIDING BLOCK REPRESENTATION OF RELATIVE DISPLACEMENT FOR TRIANGULAR BASE EXCITATION

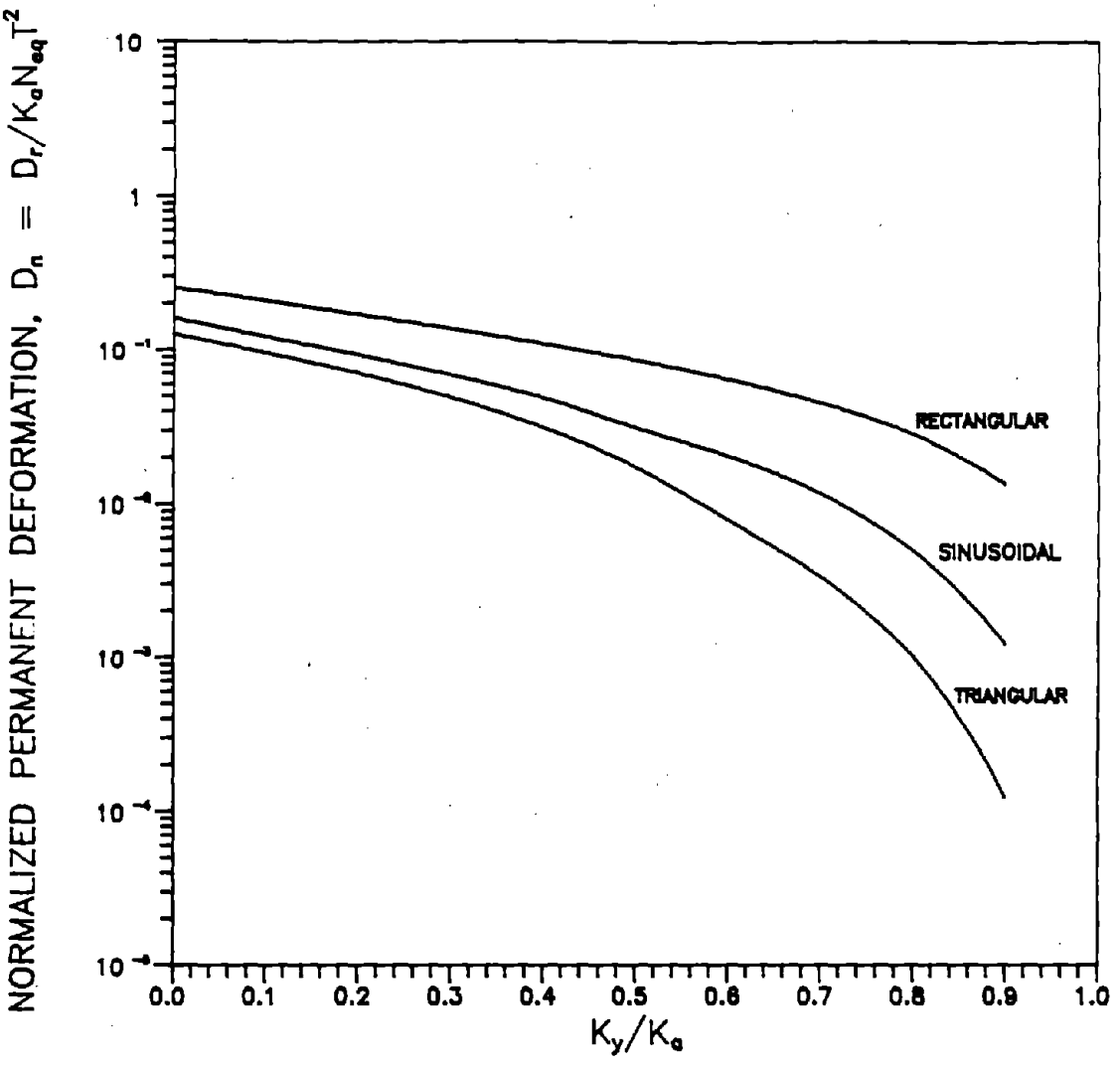

FIGURE 8 NORMALIZED PERMANENT DEFORMATION VS. K_y/K_a FOR 3 SIMPLE BASE MOTIONS CONSIDERED

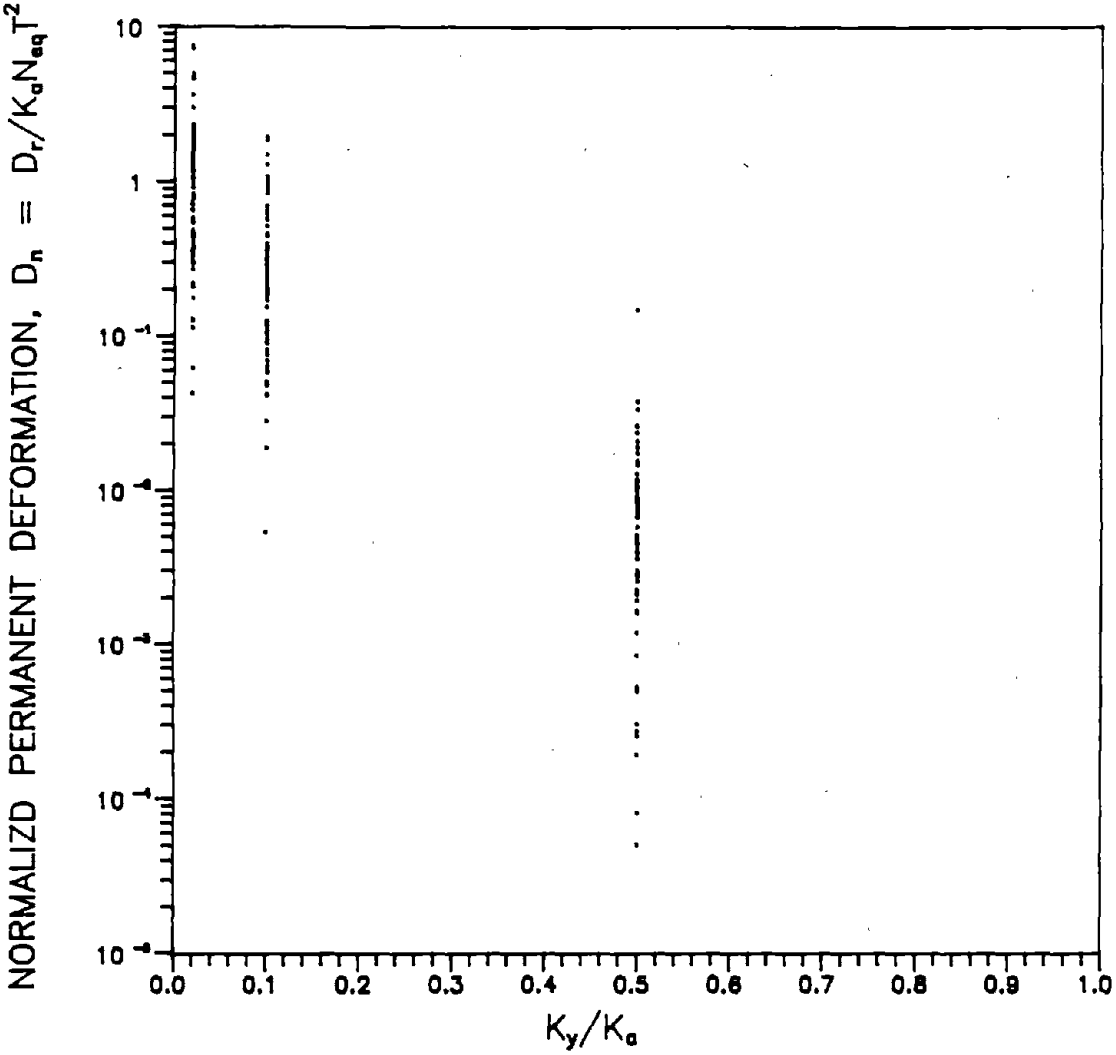

FIGURE 9 NORMALIZED PERMANENT DEFORMATIONS FROM 86 GROUND MOTION RECORDS VS. K_y/K_a

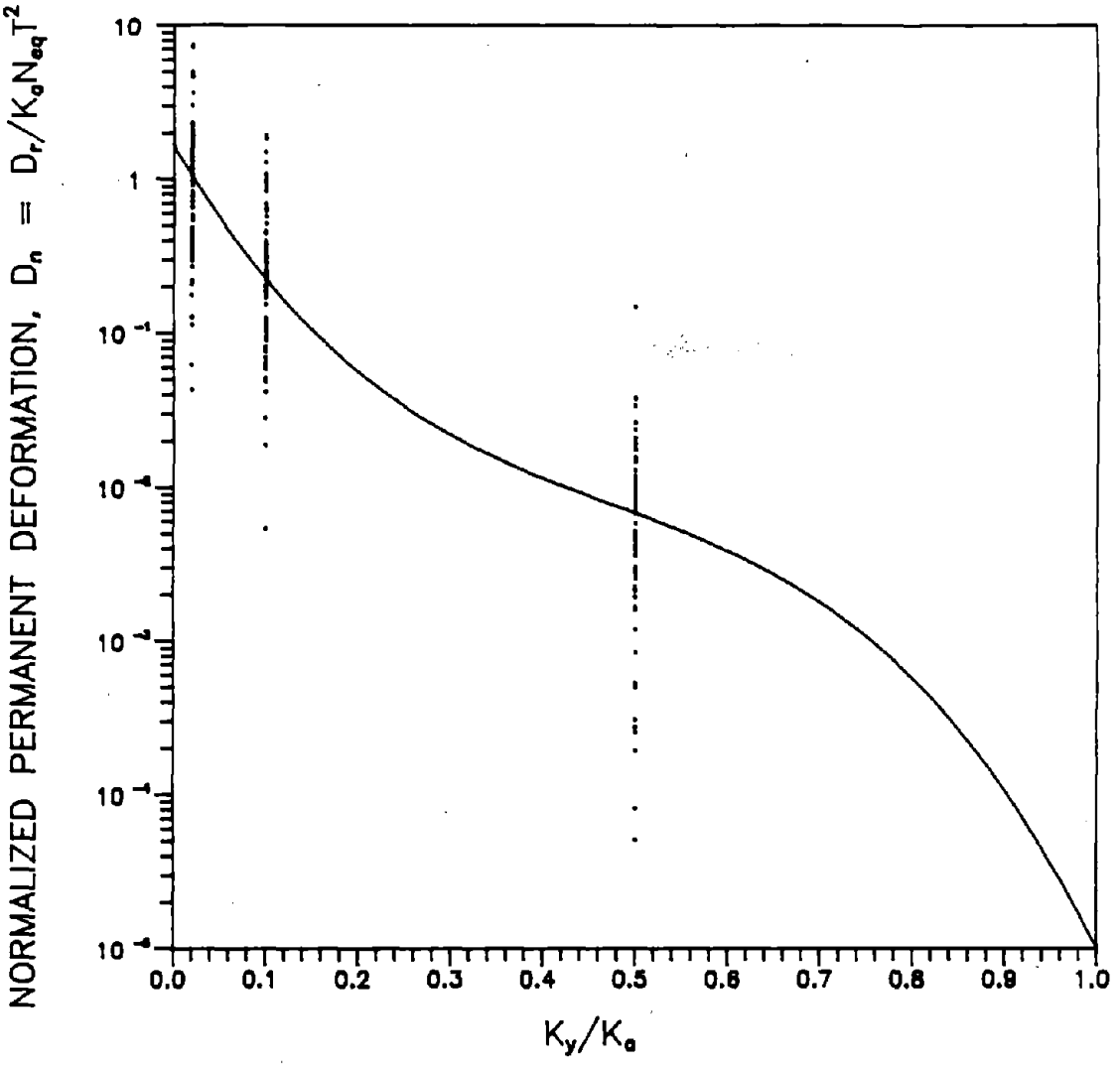

FIGURE 10 FUNCTION FOR NORMALIZED PERMANENT DEFORMATION BASED ON ACTUAL EARTHQUAKE RECORDS

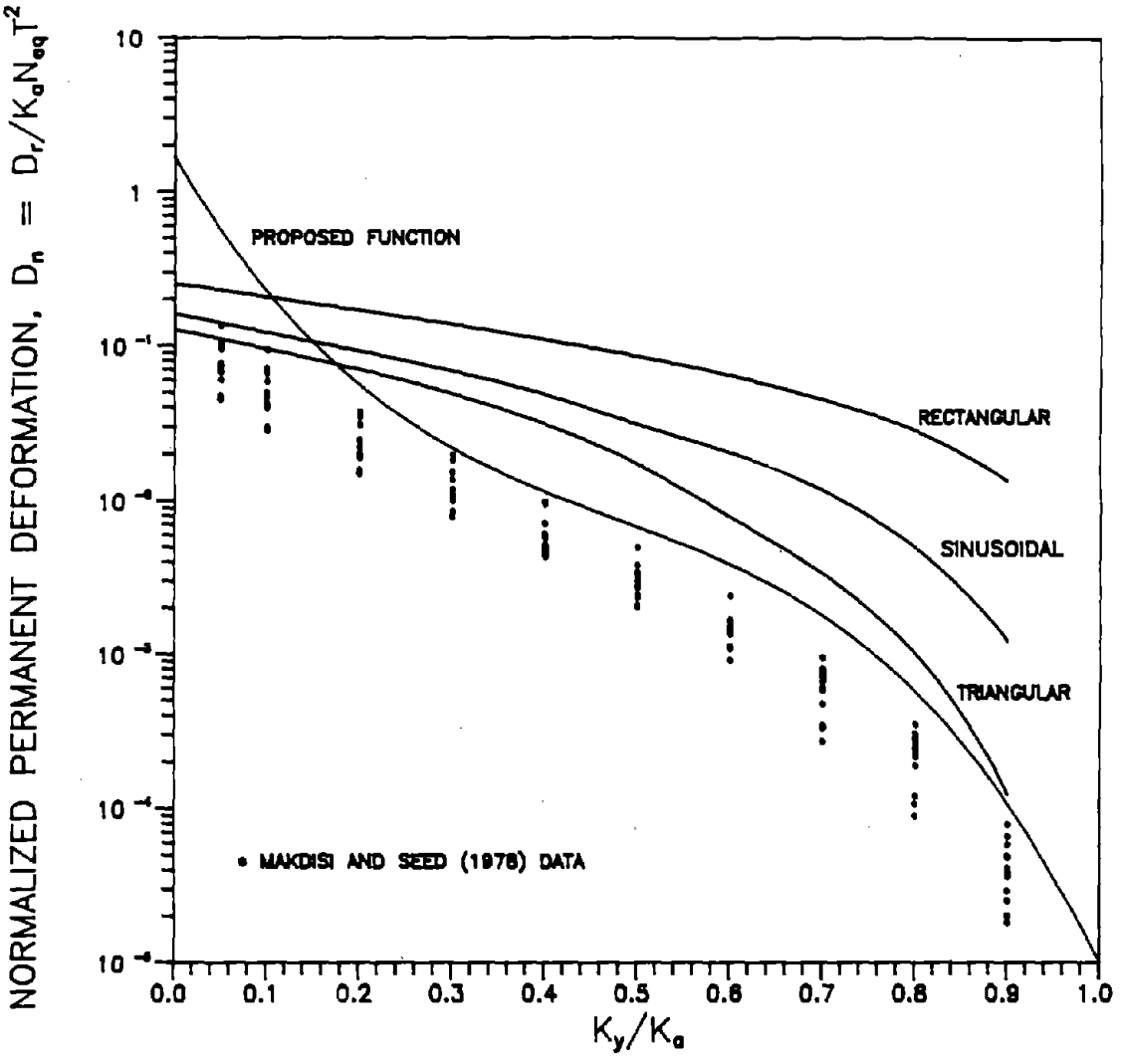

FIGURE 11 NORMALIZED PERMANENT DEFORMATION VS. K_y/K_o (COMPARISON OF THE PROPOSED DEFORMATION FUNCTION MAKDISI AND SEED DATA AND 3 SIMPLE BASE MOTIONS)

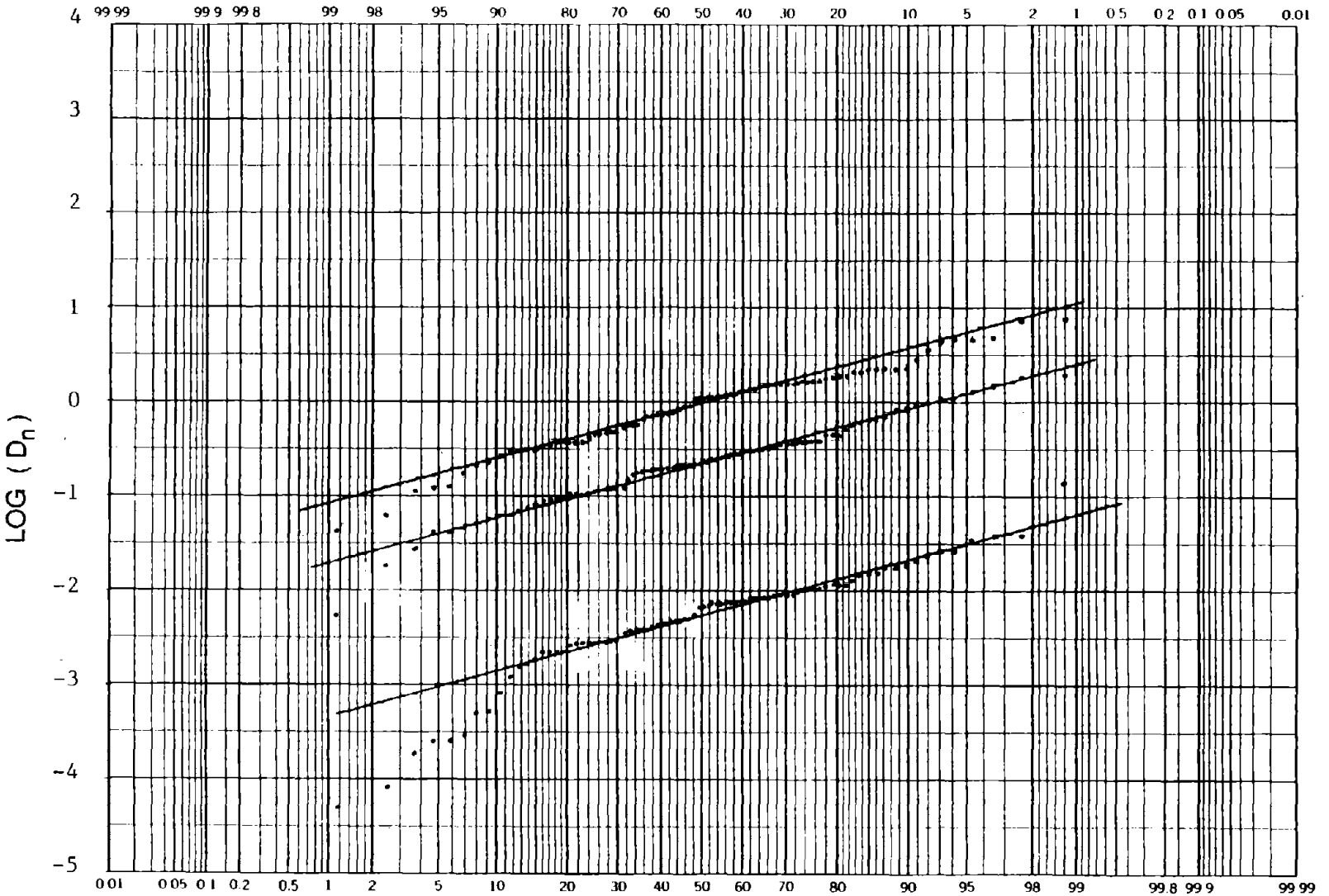

FIGURE 12 LOG OF NORMALIZED PERMANENT DEFORMATION, LOG (D_n), ON NORMAL PROBABILITY PAPER

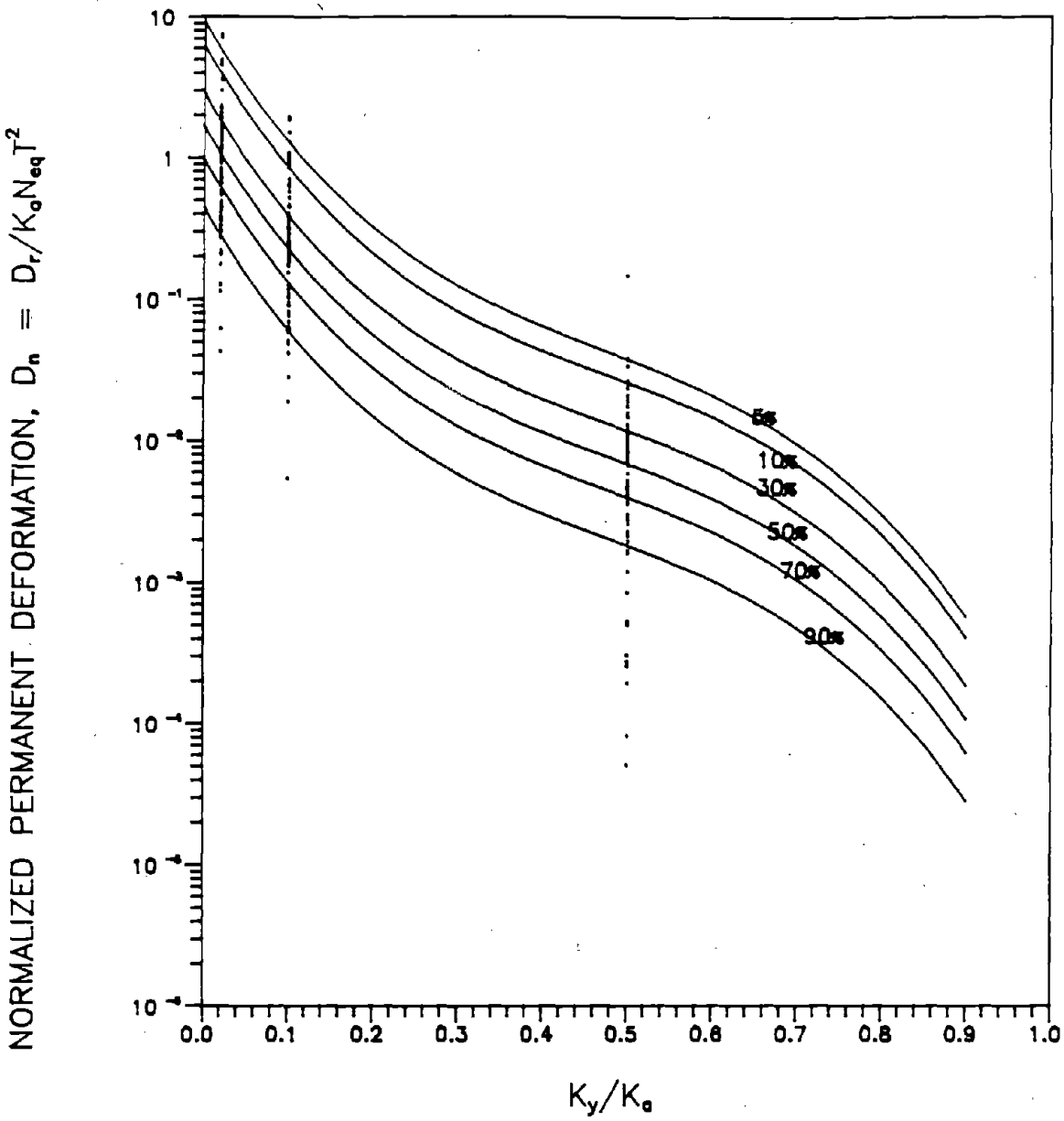

FIGURE 13 PROBABILITIES OF EXCEEDING D_n DUE TO THE SCATTER IN THE DATA (UNCERTAINTY ON THE PROPOSED FUNCTION ONLY)

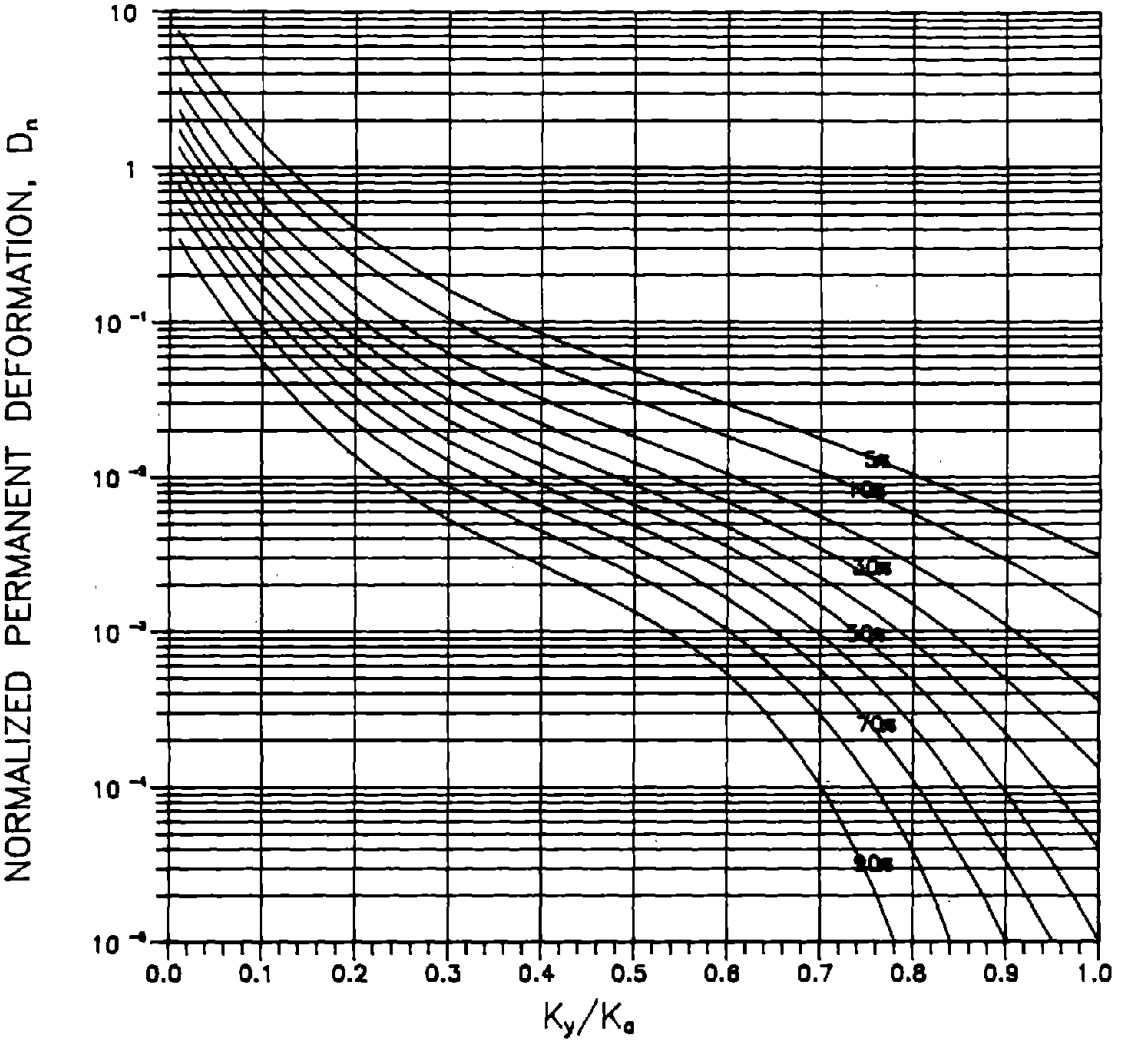

FIGURE 14 PROBABILITY CONTOURS OF NORMALIZED PERMANENT DEFORMATION VS. K_y/K_a

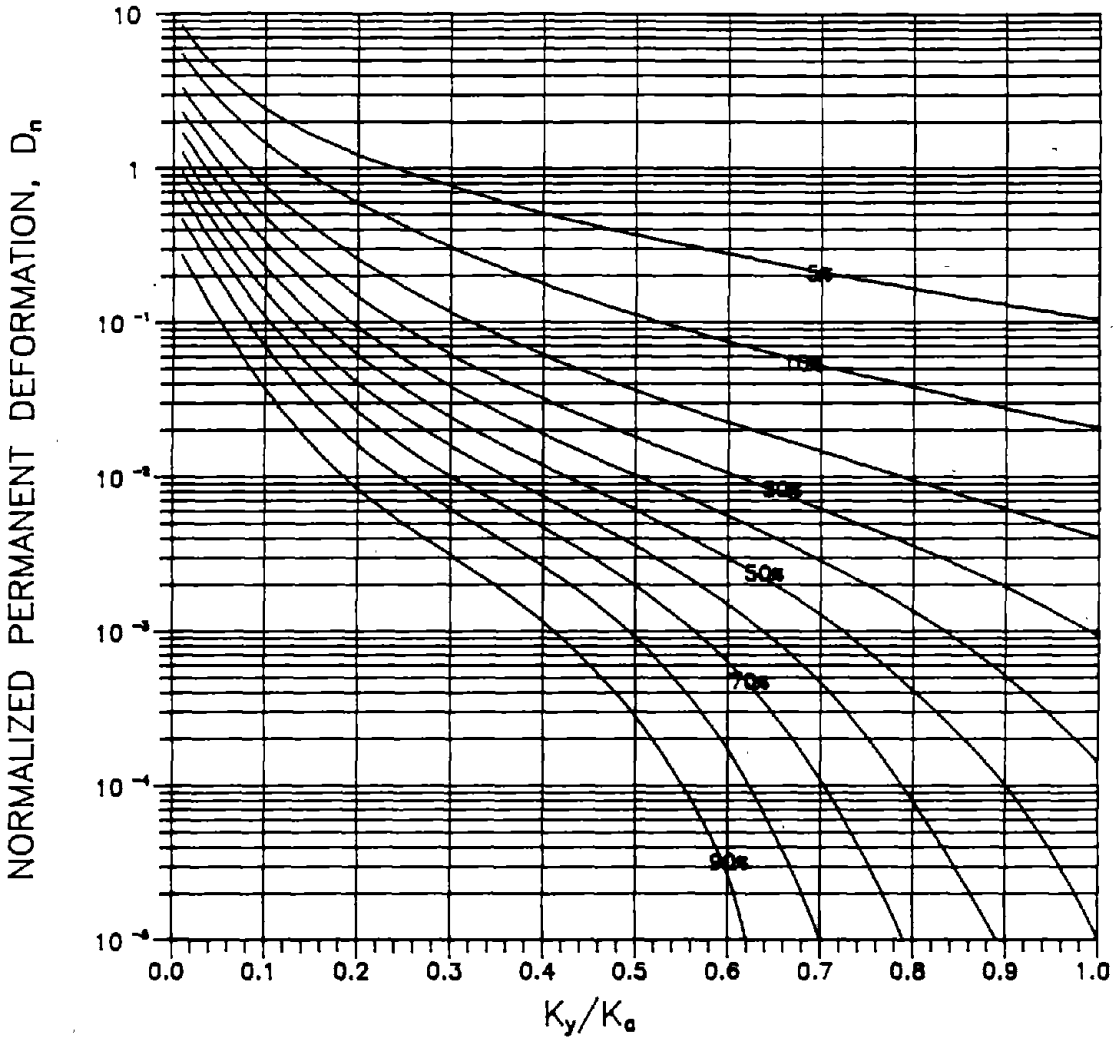

FIGURE 15 PROBABILITY CONTOURS OF NORMALIZED PERMANENT DEFORMATION VS. K_y/K_a

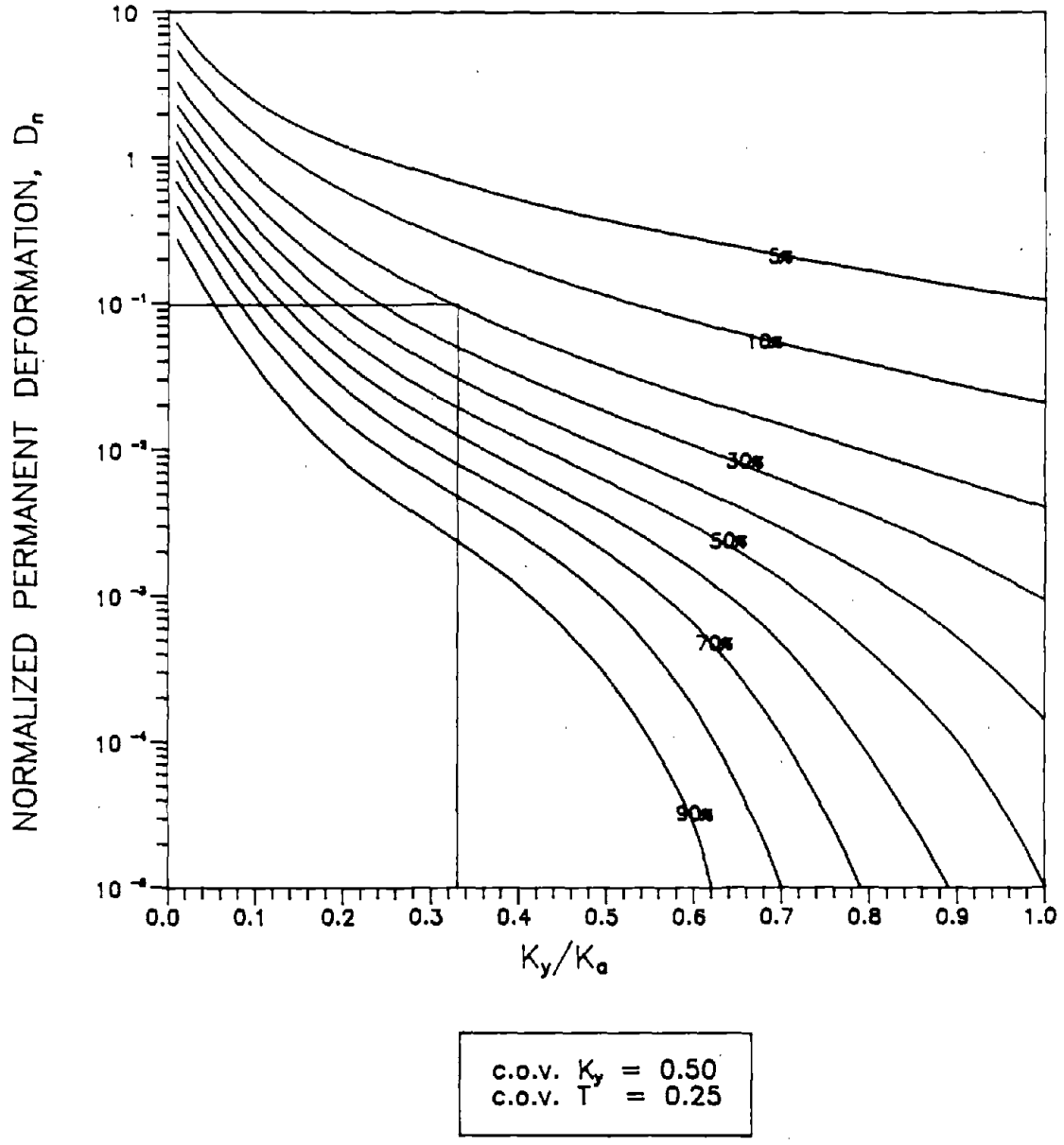

FIGURE 16 PROBABILITY CONTOURS OF NORMALIZED PERMANENT DEFORMATION VS. K_y/K_a (Example Application)

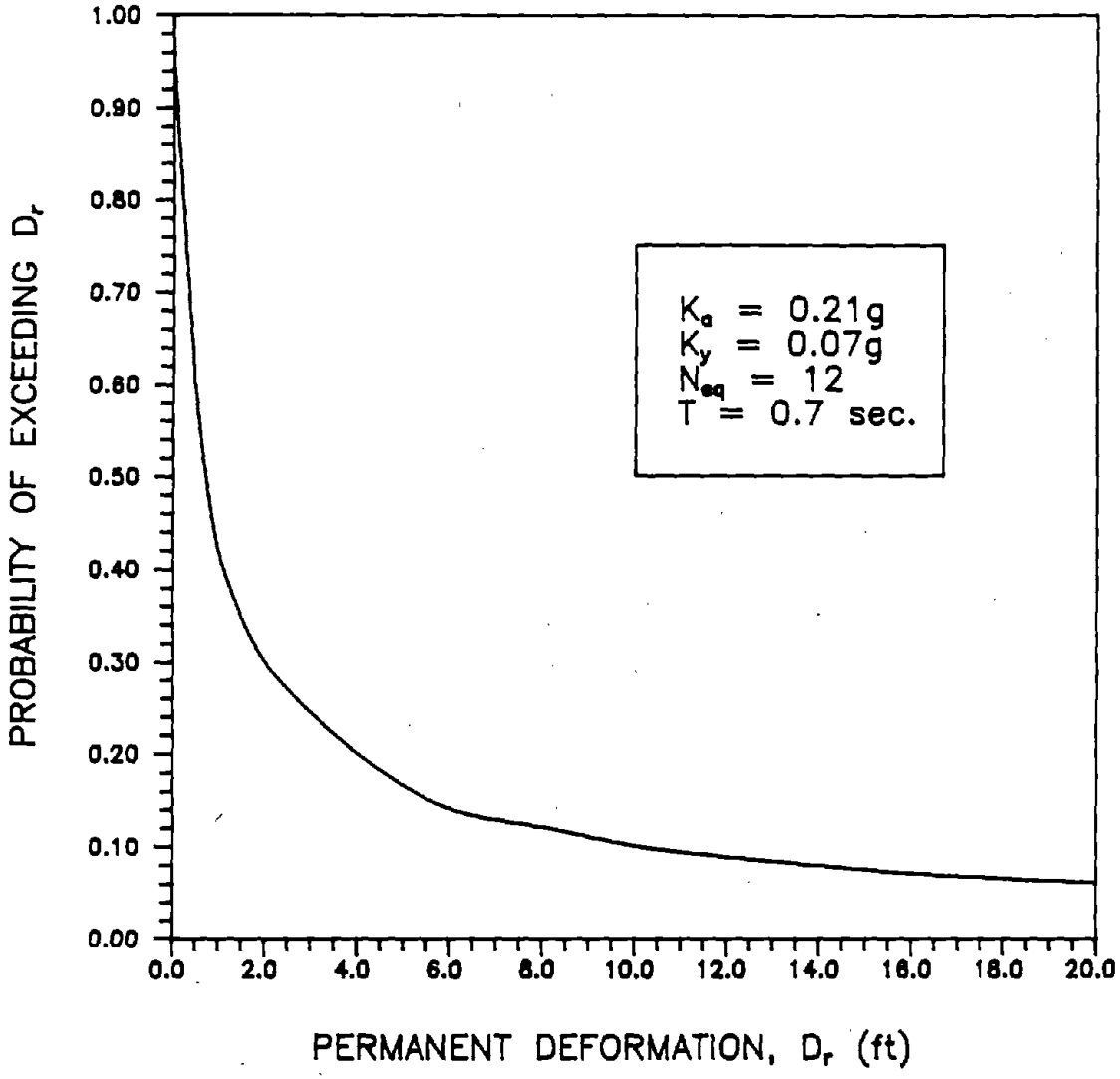

FIGURE 17 PROBABILITY OF EXCEEDING D_r VS. PERMANENT DEFORMATION

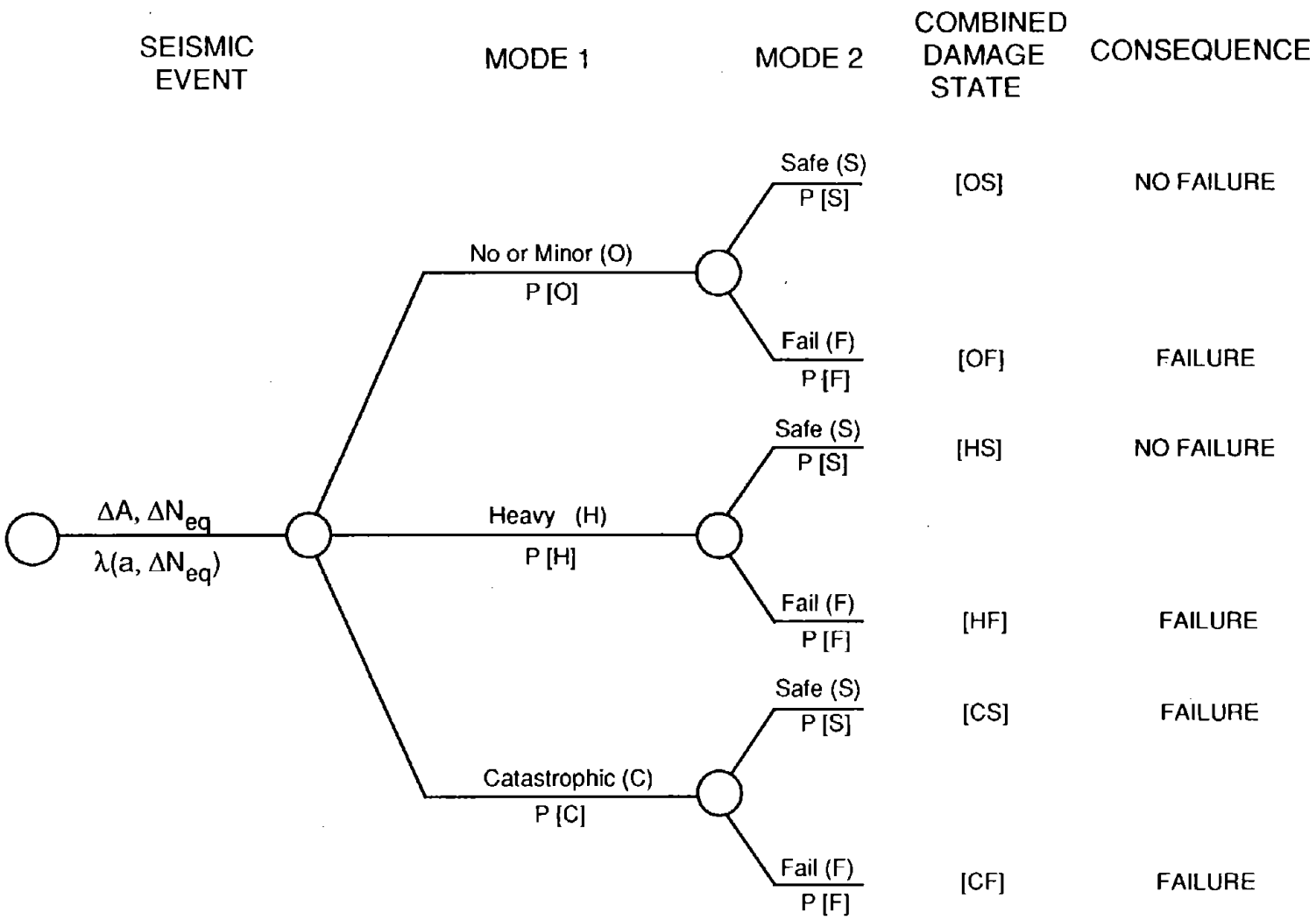

FIGURE 18 EVENT TREE OF THE SEISMIC PERFORMANCE ANALYSIS

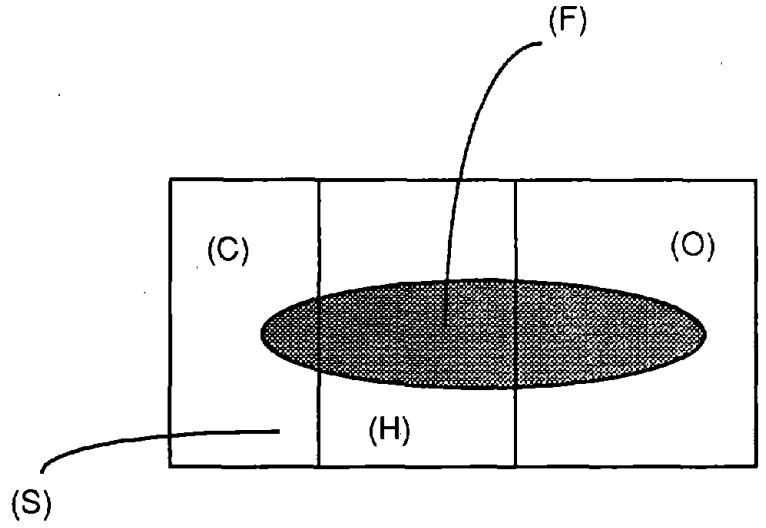

FIGURE 19 a VENN DIAGRAM ILLUSTRATION OF COMBINED OUTCOMES OF MODES CONSIDERED

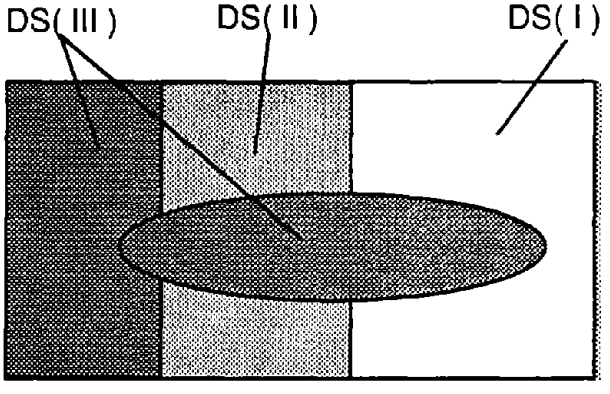

FIGURE 19 b CORRESPONDING DAMAGE STATES DEFINED

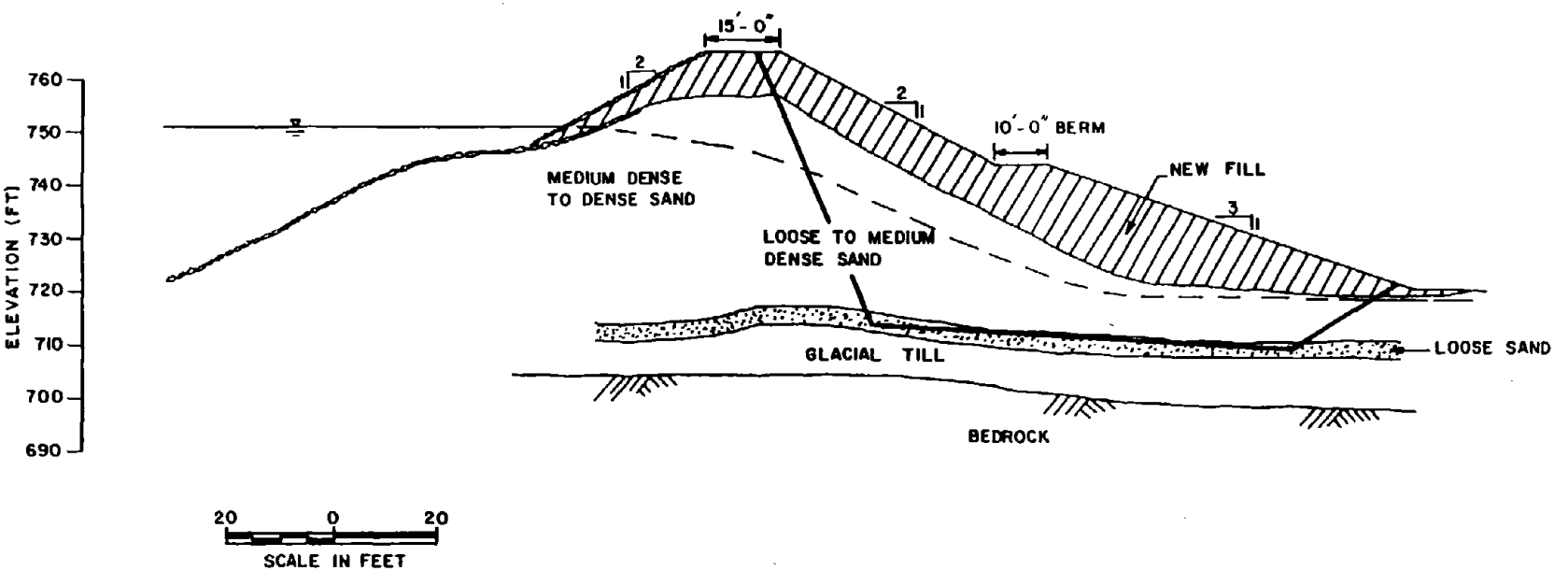

FIGURE 20 CROSS-SECTION OF THE DAM CONSIDERED IN THE EXAMPLE PROBLEM

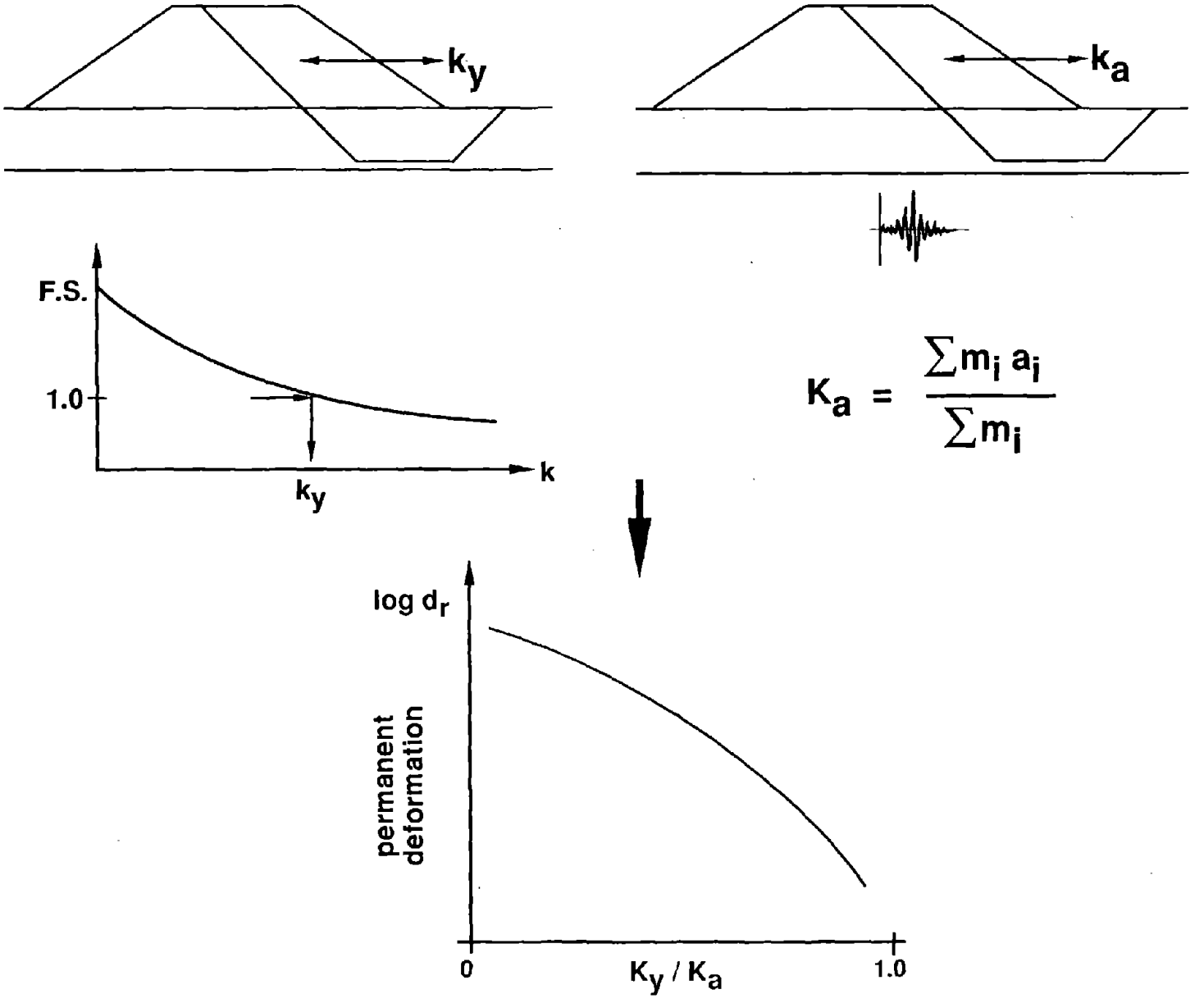

FIGURE 21 STEPS INVOLVED IN THE SEISMIC PERFORMANCE ANALYSIS OF AN EARTH DAM

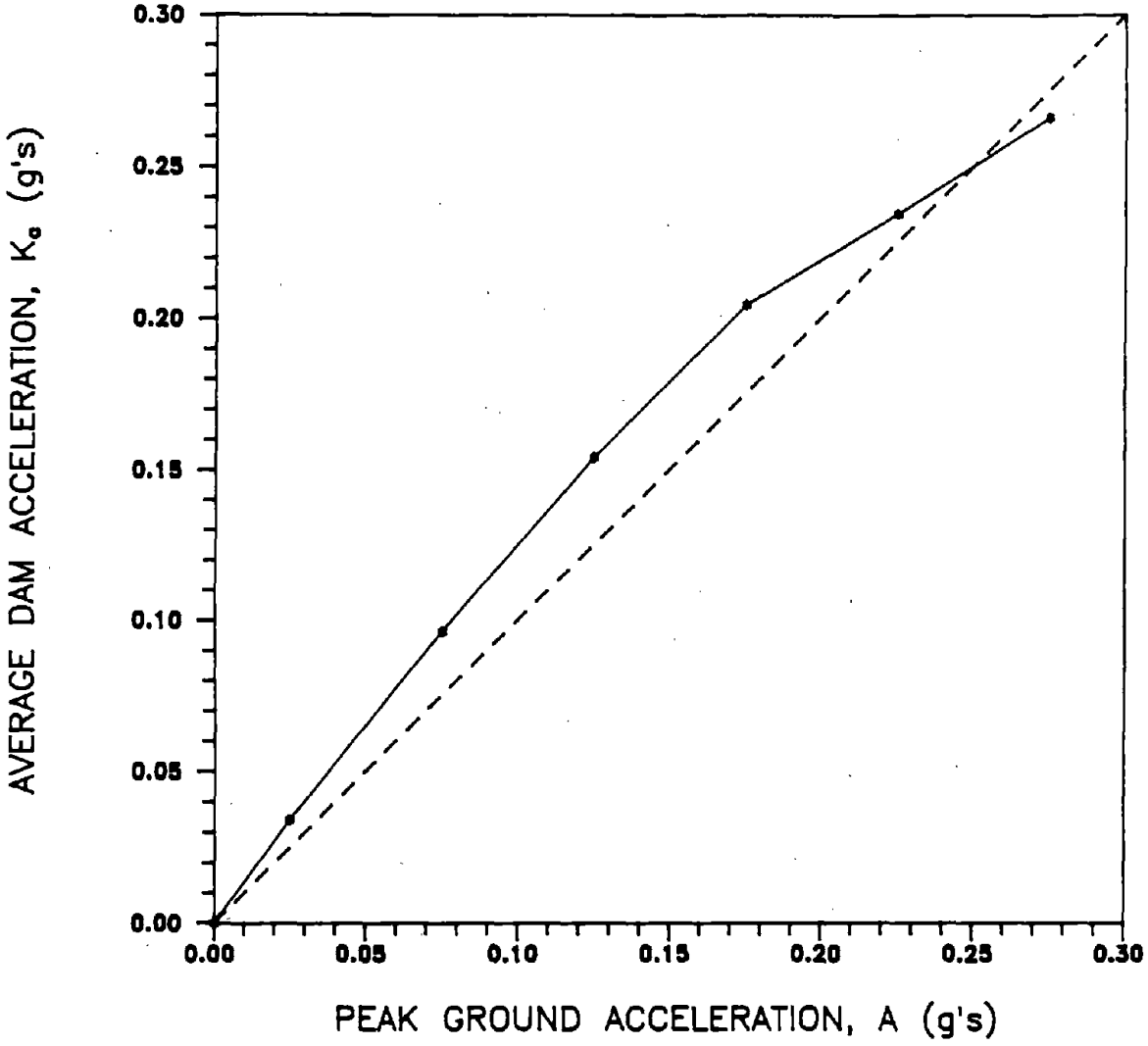

FIGURE 22 AVERAGE LATERAL ACCELERATION OF THE DAM, K_a VS. PEAK GROUND ACCELERATION, A

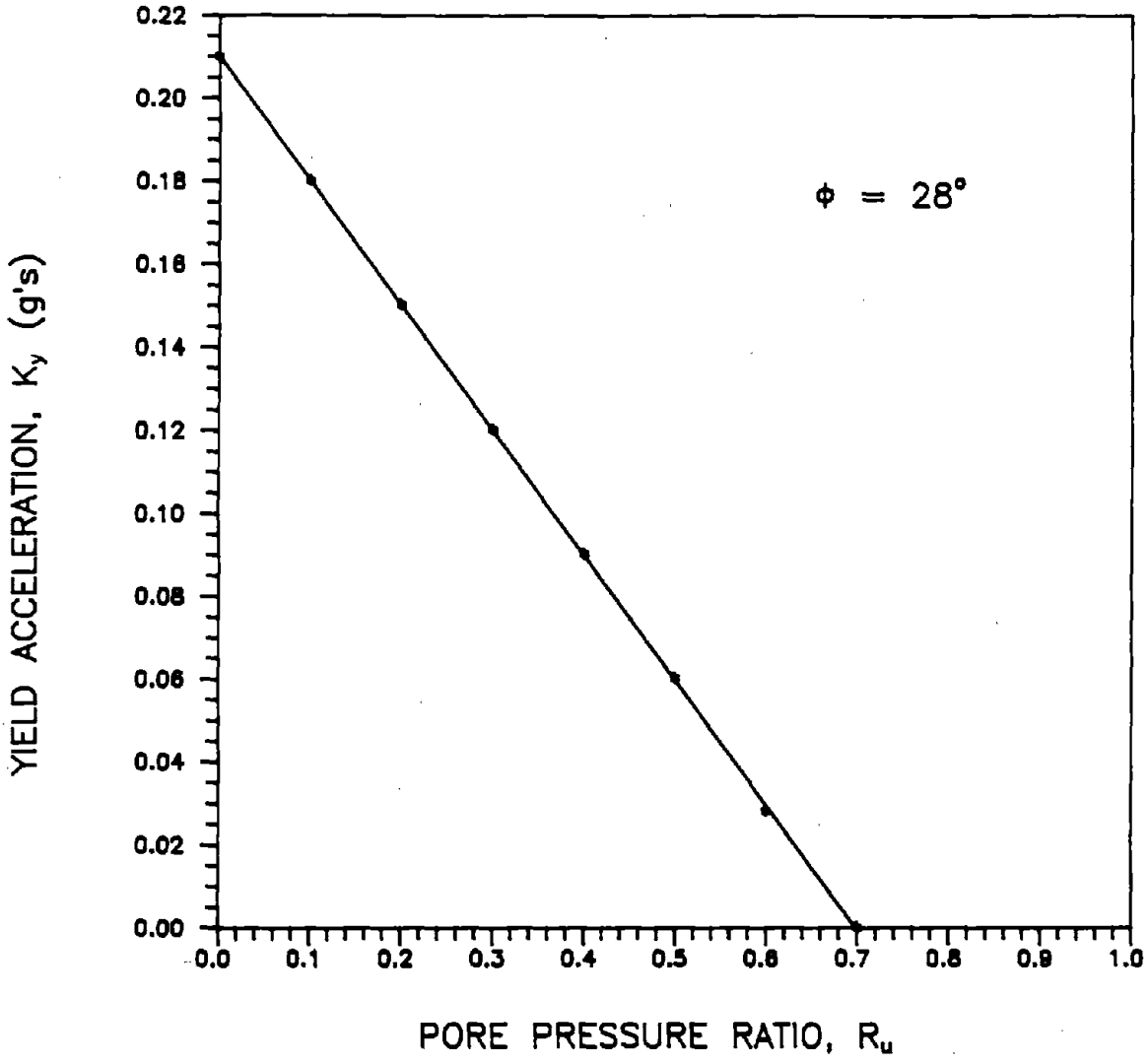

FIGURE 23 YIELD ACCELERATION, K_y VS. PORE PRESSURE RATIO, R_u

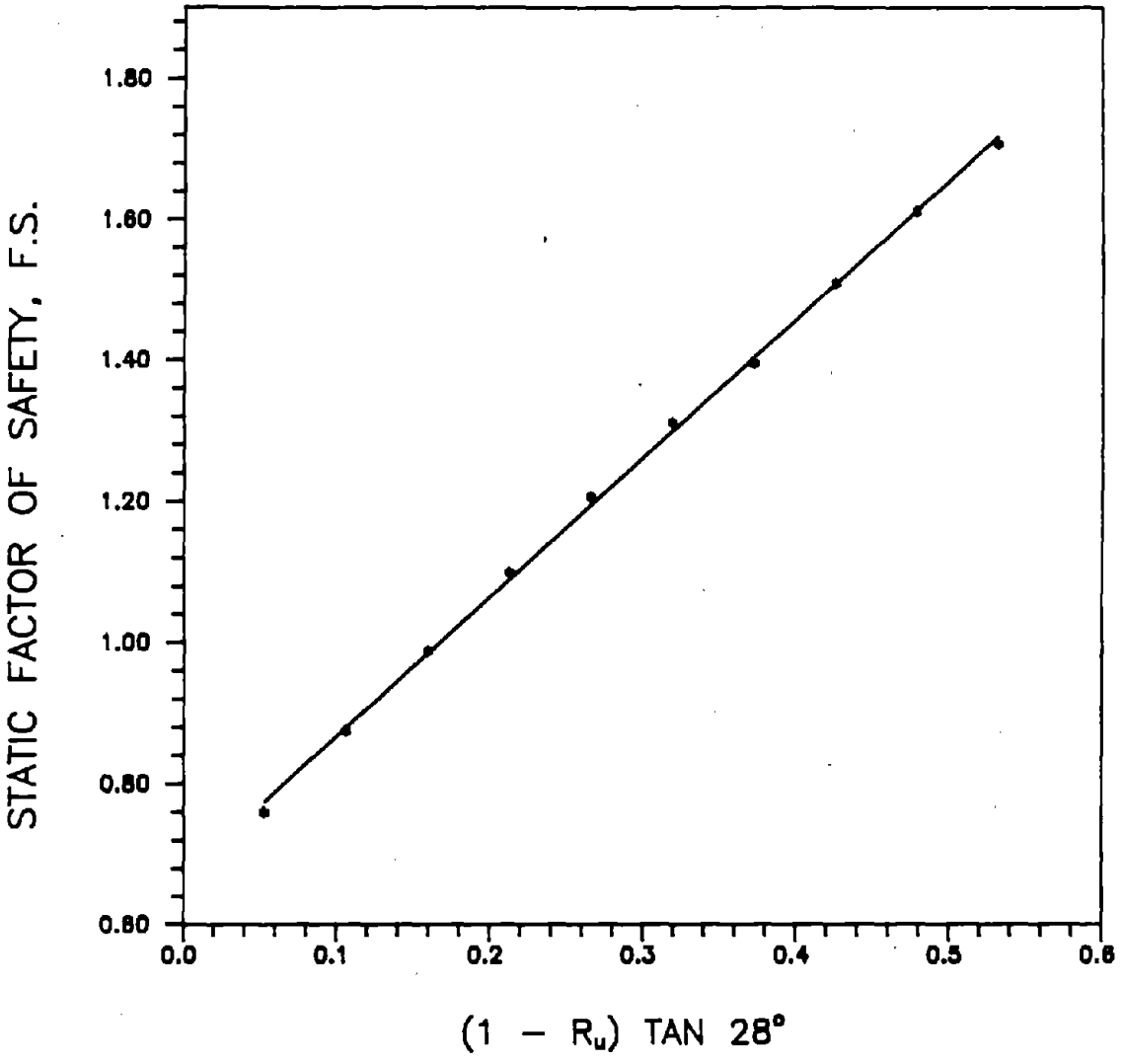

FIGURE 24 STATIC FACTOR OF SAFETY VS. PORE PRESSURE RATIO, R_u

APPENDIX A

MATHEMATICAL FORMULATION OF SEISMIC HAZARD ANALYSIS

The mathematical formulation developed for the calculation of $\lambda(a, \Delta M)$ where ΔM is the range of magnitude selected for the desired acceleration-magnitude distribution follows.

Conventional Approach

Figure A-1 shows a schematic outline of the major steps involved in a conventional Seismic Hazard Analysis. The conditional probability, $P[A \geq a \,|E]$, of acceleration A exceeding an assumed value 'a' given that an earthquake, E, will occur is obtained from Equation A-1.

$$P[A \geq a \,|E] = P[M \geq m \,|E] \tag{A-1}$$

where 'm' can be determined from an acceleration attenuation law. For reasons of simplicity in this presentation, if the attenuation law is assumed to be deterministic then 'm' can be obtained from Equation A-2.

$$a = b_1 e^{b_2 m} (R + 25)^{-b_3} \tag{A-2}$$

hence;

$$m = \ln\left[\frac{a}{b_1}(R + 25)^{b_3}\right]^{\frac{1}{b_2}} \tag{A-3}$$

The complementary cumulative distribution function for earthquake magnitude can be expressed by Equation A-4.

$$P[M \geq m \mid E] = \frac{\bar{\lambda}(m)}{\bar{\lambda}(m_o)} \qquad \text{(A-4)}$$

where $\bar{\lambda}(m)$ gives the annual number of earthquakes with magnitudes equal to or greater than 'm' per unit area of source zone, and $\bar{\lambda}(m_o)$ designates the annual number of earthquakes occurring within a unit area of source zone and exceeding a minimum magnitude of interest, m_o.

Cornell and Vanmarcke (1969) proposed a magnitude-frequency relationship that considers both upper and lower bounds on earthquake magnitudes. Their proposed complementary cumulative probability distribution function is given by Equation A-5.

$$P[M \geq m \mid E] = 1 - K(m)_{m_o - m_{max}}(1 - e^{-\beta(m-m_o)}) \qquad m_o \leq m < m_i \qquad \text{(A-5)}$$

where

$$K(m)_{m_o - m_{max}} = [1 - e^{-\beta(m_{max}-m_o)}]^{-1}$$

β = magnitude - frequency parameter

and

m_{max} = maximum "credible" magnitude.

Employing the complementary distribution function of Equation A-5

$$P[A \geq a \mid E] = P[M \geq m \mid E] = 1 - K(m)_{m_o - m_{max}} (1 - e^{-\beta(m-m_o)}) \qquad \text{(A-6)}$$

where

$$m = \ln\left[\frac{a}{b_1}(R + 25)^{b_3}\right]^{\frac{1}{b_2}}$$

Combining Equations A-1 and A-4 yields

$$\bar{\lambda}(a) = P[A > a \mid E]\,\bar{\lambda}(m_o) \qquad \text{(A-7)}$$

where $\lambda(a)$ is the total number of events causing acceleration to exceed the value 'a' per unit area of source. Integrating Equation A-7 over all the area sources yields

$$\lambda(a) = \int_{\text{all area sources}} \left[1 - K(m)_{m_o - m_{max}}\left(1 - e^{-\beta(m-m_o)}\right)\right] \bar{\lambda}(m_o)\, d(\text{area}) \qquad \text{(A-8)}$$

Limitation of Conventional Formulation

Since the integration shown in Equation A-8 is performed over the entire area of source zones having varying distances from the site of interest, the contributions to the total number of events, $\lambda(a)$, come from events of different magnitudes. Typically, the integration shown in Equation A-8 is carried out with the use of a computer program. The

mathematical formulations used in currently available computer programs do not permit (in the progress of the integration) determination of the magnitude-distribution of the events with acceleration exceeding 'a'. To determine the distribution over M, a modification in the conventional mathematical formulation was introduced.

Modified Seismic Hazard Analysis

The purpose of the modification introduced herein is to determine how many of $\lambda(a)$ events are from earthquakes with magnitudes from m_o to m_i, and m_i to m_{max}. The exact formulation of this new approach to Seismic Hazard Analysis follows:

$$\lambda(a)_{m_o - m_i} = \lambda(m)_{m_o - m_i} = R(m)_{m_o - m_{max}} (\lambda_{m_o - m_{max}}) - \lambda_{m_i - m_{max}} \qquad \text{(A-9)}$$

where

$\lambda(m)_{m_o - m_i}$ = number of events causing magnitude to exceed m, but ranging between m_o and m_i. Thus if $m > m_i$, $\lambda(m) = 0$.

$R(m)_{m_o - m_{max}} = 1 - K(m)_{m_o - m_{max}} (1 - e^{-\beta(m-m_o)})$

$\lambda_{m_o - m_{max}}$ = total number of events causing magnitude to exceed m_o but less than m_{max}

$\lambda_{m_i - m_{max}}$ = total number of events causing magnitude to exceed m_i but less than m_{max}

Further manipulation of Equation A-9 yields,

$$\lambda(m)_{m_o - m_i} = R(m)_{m_o - m_{max}} (\lambda_{m_o - m_{max}}) - R(m_i)_{m_o - m_{max}} (\lambda_{m_o - m_{max}})$$

$$= -K(m)_{m_o - m_{max}} (\lambda_{m_o - m_{max}})[1 - e^{-\beta(m-m_o)}]$$

$$+ K(m)_{m_o - m_{max}} (\lambda_{m_o - m_{max}})[1 - e^{-\beta(m_i - m_o)}]$$

$$= K(m)_{m_o - m_{max}} (\lambda_{m_o - m_{max}})[e^{-\beta(m - m_o)} - e^{-\beta(m_i - m_o)}] \quad \text{(A-10)}$$

The solution of Equation A-9 (or Equation A-10) in the form that is presented requires the use of a computer or introduction of major modifications in a currently available program. A closer examination of Equation A-9 reveals that existing computer programs could be used to solve Equation A-9 provided that the computer is "fooled" by reading in appropriately modified values of certain parameters required. The resulting outcome of the analysis is identical to that which would have been obtained from Equation A-9.

Proposed Solution

Equation A-11 is selected as a substitute for Equation A-9 and

$$\lambda(m)_{m_o - m_i} = R(m)_{m_o - m_i} \lambda_{m_o - m_i} \quad \text{(A-11)}$$

where

$$R(m)_{m_o - m_i} = 1 - K(m)_{m_o - m_i} [1 - e^{-\beta(m - m_o)}]$$

$$K(m)_{m_o - m_i} = [1 - e^{-\beta(m_i - m_o)}]^{-1}$$

and

$\lambda_{m_o - m_i}$ = total number of events causing magnitude to exceed m_o but less than m_i.

$$= K(m)_{m_o - m_{max}} \lambda_{m_o - m_{max}} [1 - e^{-\beta(m_i - m_o)}]$$

To justify the validity of Equation A-11 as a replacement for Equation A-8, the following

manipulations are performed on Equation A-11.

$$\lambda(m)_{m_o - m_i} = [1 - K(m)_{m_o - m_i}(1 - e^{-\beta(m-m_o)})][K(m)_{m_o - m_{max}} \lambda_{m_o - m_{max}}[1 - e^{-\beta(m_i-m_o)}]$$
$$= K(m)_{m_o - m_{max}} \lambda_{m_o - m_{max}}[e^{-\beta(m-m_o)} - e^{-\beta(m_i-m_o)}] \quad \text{(A-12)}$$

It is noted that Equation A-12 and A-10 are identical. Therefore, Equation A-11 can be used as a substitute for Equation A-9 in the Seismic Hazard Analysis. The advantage of using Equation A-11 is that its form is exactly identical to the equation used in conventional computer programs (Equation A-9). However, the values of the parameters are quite different. Thus, by reading in the appropriately modified values of the parameters needed by the computer program, Equation A-11 can be solved conveniently using the computer program coded by Schumacker and Whitman (1978).

Procedure for Modified Seismic Hazard Analysis

To obtain the number of earthquakes causing acceleration to exceed 'a' and having magnitudes between m_o and a selected value m_i, the following parameter modifications would be required.

(a) maximum "credible" magnitude to be read into the computer would be m_i

(b) number of events causing magnitude to exceed m_o to be read into computer program would be equal to:

$$\lambda_{(m_o)}\left[\frac{1 - e^{-\beta(m_i - m_o)}}{1 - e^{-\beta(m_{max} - m_o)}}\right]$$

With the use of these modified parameters, the results of the computer analysis will

correspond to $\lambda(a)_{m_o - m_i}$, total number of events causing acceleration to exceed 'a' and having magnitudes greater than m_o but less than m_i. By selecting various values of m_i it is possible to generate a histogram of events $\lambda(a, \Delta M)$ for various intervals of magnitude as shown in Figure A-2.

Since direct relationship is assumed between magnitudes and associated number of equivalent cycles, the results obtained could be used to generate the same type of histogram for corresponding ranges of N_{eq}, $\lambda(a, \Delta N_{eq})$. This is also shown in Figure A-2.

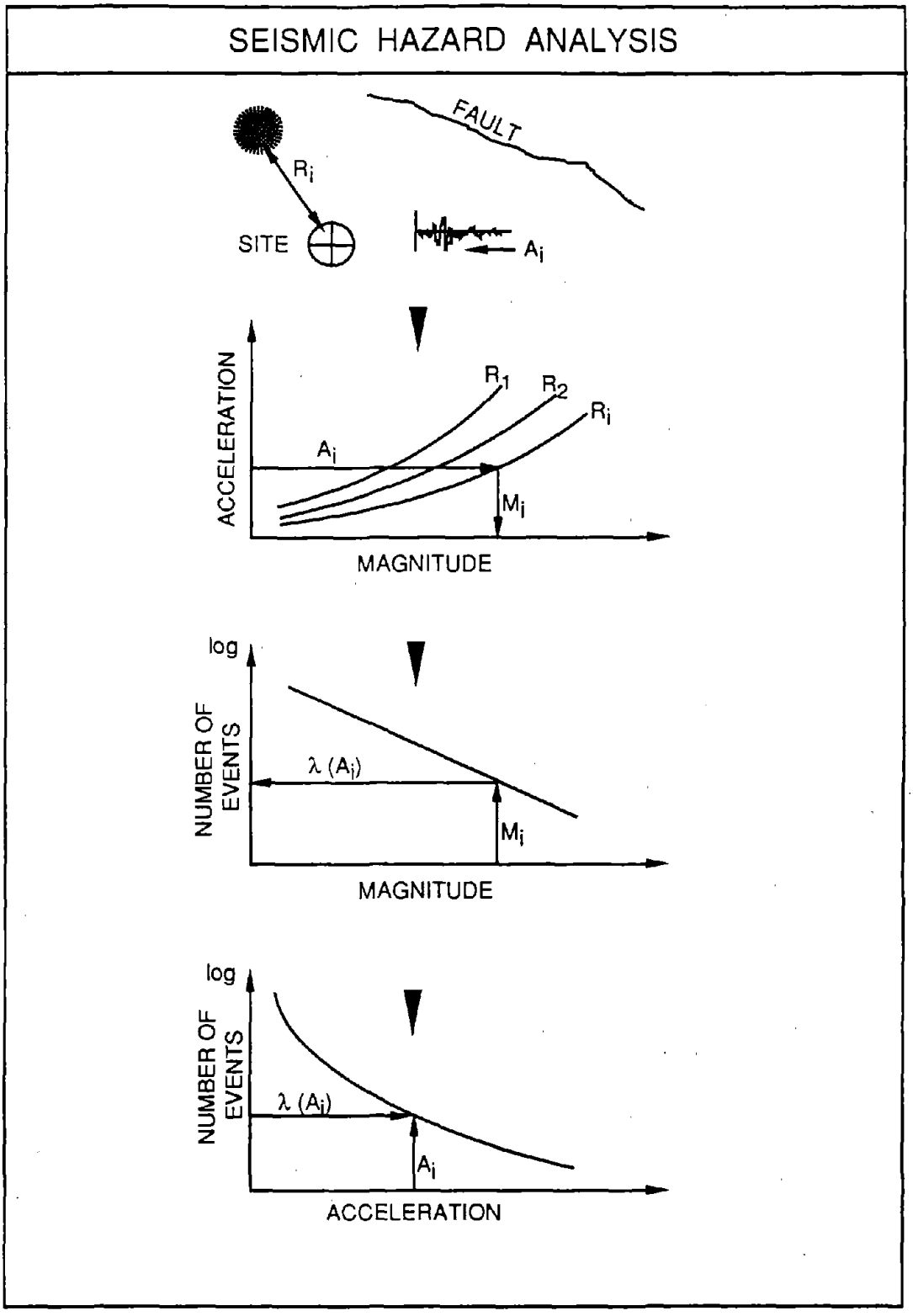

FIGURE A-1 PROCEDURES INVOLVED IN SEISMIC HAZARD ANALYSIS

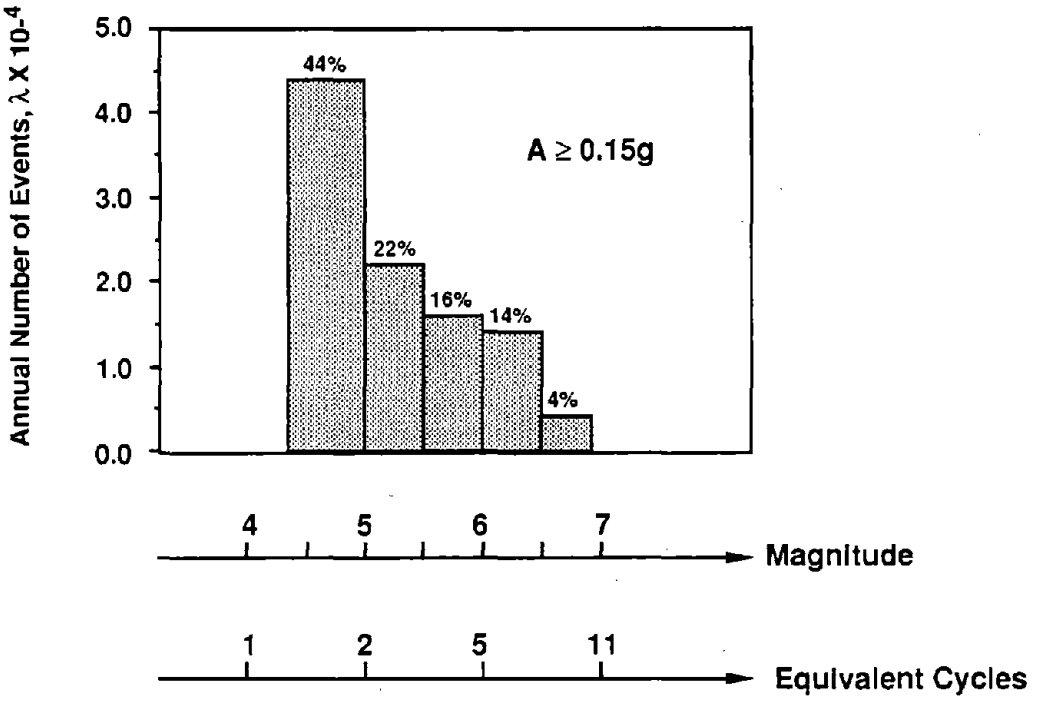

FIGURE A-2 HISTOGRAM OF ANNUAL NUMBER OF EVENTS AS A FUNCTION OF MAGNITUDE AND NUMBER OF EQUIVALENT CYCLES

APPENDIX B

RELATIONSHIP BETWEEN EARTHQUAKE MAGNITUDE AND NUMBER OF EQUIVALENT CYCLES

The application to earth dams of the Seismic Hazard Analysis described in this report requires a relationship between equivalent number of cycles and earthquake magnitude. In general this relationship is expressed as following

$$N_{eq} = f(s,M) \qquad \text{(B-1)}$$

where

M = earthquake magnitude

and s = acceleration or stress ratio (constant) = a_{av}/a_{peak}

The results of the research conducted by Asturias and Dobry (1982), Haldar and Tang (1979), Lee & Chan (1972), and data from earthquake studies do not indicate any correlation between N_{eq} and epicentral distance, fault to site distance, component of motion, or near surface ground conditions. To establish the relationship between M, N_{eq} and s, a statistical analysis was made by Singh (1984) using the equivalent number of cycles calculated for 57 earthquakes by Lee & Chen (1972) and for s = 0.65, 0.75, and 0.85. This relationship is shown in Equation B-2.

$$\ln N_{eq} = -1.73 + 0.46 - 3.61 \ln s \qquad \text{(B-2)}$$

The uncertainty present in this relationship was calculated and the standard deviation of $\ln N_{eq}$ given by Equation B-1 was estimated to be $\sigma_{\ln N_{eq}} = 0.39$. Equation B-2 can

therefore be used to estimate N_{eq} based on M and s for a desired confidnece level. Seed & Idriss (1975) suggested that when s = 0.65, the number of equivalent cycles for Richter magnitudes of 7.0, 7.5, and 8.0 is 10, 20, and 30 cycles, respectively.

Haldar & Tang (1981) proposed a statistical relationship similar to Equation B-2. They suggested that the intensity of the uniform stress be taken to be 75% of the maximum stress (i.e. s = 0.75). The relationship proposed by Haldar and Tang is:

$$E[N_{eq} | M = m] = 106.1 - 36.4m + 3.3m^2 \quad \text{for } m \geq 5.0 \qquad \text{(B-3)}$$

and the corresponding variance, $Var(N_{eq} | M) = 29.1$

The most commonly used method for calculating number of equivalent cycles is based on an equivalent rule for recorded cycles derived from a representative cyclic strength curve of sands, and described by Lee & Chan (1972).

Klohn et. al. (1978) have extracted the following table proposed by Seed (1976) that provides a means of estimating the number of "significant cycles" of shaking with peak acceleration equal to 65 percent of the maximum acceleration for a given magnitude earthquake.

Richter Magnitude	Significant Cycles		
	Lower 15%	Mean	Upper15%
5.0	2	4	5
5.5	2	4	5
6.0	3	4	6
6.5	4	6	9
7.0	6	10	15
7.5	8	15	24
8.0	11	22	33

In a more recent publication Seed et. al. (1983) presented the following table that relates N_{eq} to magnitude, M.

Magnitude (1)	Number of represnetative cycles at 0.65 τ_{max} (2)
8-1/2	26
7-1/2	15
6-3/4	10
6	5-6
5-1/4	2-3

For the example application of Integrated Seismic Risk Analysis described in Section VI, relationship proposed by Seed et. al. (1983) was used to establish the N_{eq} intervals for each

selected magnitude interval. These intervals are tabulated below.

TABLE FOR N_{eq} AND M RANGES

Magnitude Range	Number of Equivalent Cycles Range
4.33 - 5.0	1 - 2
5.0 - 5.5	2 - 3
5.5 - 6.0	3 - 5
6.0 - 6.5	5 - 8
6.5 - 6.8	8 - 11

APPENDIX C

SEISMIC DATA AND PROCEDURES IN SHA

In carrying out the Seismic Hazard Analysis for the example site (Boston area) the seismic source maps proposed by Cornell and Merz (1974), and Tong et al (1975), shown in Figure 4 was utilized and the sources used are identified as following

Seismic Sources	Total # of Events/ Year	I_{max} (MMI)	M_{max}
A_1	0.03809	8.3	6.53
A_2	0.02191	8.3	6.53
B	6/250 = 0.024	8.3	6.53
C-1	33/250 = 0.132	8.7	6.8
Background	$(8x10^{-7})(R^2\pi)/mi^2 = 0.00628$	6.3	5.2

where R is taken to be 50 miles or 80 km., and I_{max} is referred to as "maximum intensity of the interset."

Gutenberg and Richter (1954) developed the following relationship between magnitudes and intensities

$$M_{max} = 1 + (2/3)I_{max} \qquad \text{(C-1)}$$

where I_{max} is the epicentral intensity for all the sources mentioned. The minimum intensity of interest, I_0, was assumed to equal 5.0. Thus, based on Equation C-1 the minimum magnitude of interest, m_0, was 4.33.

Seismic Hazard Analysis requires utilization of an acceleration attenuation law. In this study, the attenuation law proposed by Donovan (1973-worldwide) was used. It is expressed as

$$a_g = 1320\, e^{0.58M}\, (R + 25)^{-1.52}; \qquad \sigma_{\ln a_g} = 0.84 \qquad \text{(C-2)}$$

where a_g is the peak ground acceleration in gals

R is the epicentral distance in km.

$\sigma_{\ln a_g}$ is the standard deviation of natural logarithm of a_g.

The computer program MITRISK developed by Schumacker and Whitman (1978) was used to compute the probabilities of joint occurrence of acceleration and magnitude or equivalent number of cycles as descirbed in Appendix A. The results are discussed in Seciton VI of this report.

APPENDIX D

PROCEDURES FOR ESTIMATION OF PERMANENT DEFORMATION

Estimation of earthquake-induced permanent deformation can be made using Newmark's sliding block model shown in Figure 7. In this approach, a rigid-plastic interface property is assumed such that if the acceleration of the block exceeds a limiting acceleration k_y, then sliding of the block relative to the base will occur.

Sinusoidal Pulse

In Figure D-1 the motions of the block for a sinusoidal excitation of the base are illustrated. The derivation of the mathematical expression for the permanent deformation, D_r, follows. The equations of motion for the base are:

$$A = k_a \sin\left(\frac{2\pi t}{T}\right) \tag{D-1}$$

$$V = k_a \frac{T}{2\pi}\left[1 - \cos\left(\frac{2\pi t}{T}\right)\right] \tag{D-2}$$

$$D = k_a \left(\frac{T}{2\pi}\right)^2 \left[\frac{2\pi t}{T} - \sin\left(\frac{2\pi t}{T}\right)\right] \tag{D-3}$$

Solving for t_y (from Equation D-1)

$$\frac{t_y}{T} = \frac{1}{2\pi} \sin^{-1}\left(\frac{k_y}{k_a}\right) \tag{D-4}$$

Solving for t_f (using Equation D-2 and Figure D-1)

$$V_{t_f} = \frac{k_a T}{2\pi}\left[1 - \cos\left(\frac{2\pi t_f}{T}\right)\right] \quad \text{for the base} \quad \text{(D-5)}$$

$$V_{t_f} = V_y + k_y(t_f - t_y) = \frac{k_a T}{2\pi}\left[1 - \cos\left(\frac{2\pi t_y}{T}\right)\right] + k_a \sin\left(\frac{2\pi t_y}{T}\right)(t_f - t_y) \quad \text{for the block} \quad \text{(D-6)}$$

Considering that at time $t = t_f$ the velocity of the block and the base will be equal and they will move together, the right hand sides of Equations D-5 and D-6 are set equal resulting:

$$\left(\frac{k_y}{k_a}\right)\frac{t_f}{T} + \frac{1}{2\pi}\cos\left(\frac{2\pi t_f}{T}\right) = \frac{1}{2\pi}\sqrt{1 - \left(\frac{k_y}{k_a}\right)^2} + \frac{k_y}{k_a}\left(\sin^{-1}\frac{k_y}{k_a}\right)\frac{1}{2\pi} \quad \text{(D-7)}$$

Equation D-7 shows that the solution for t_f is implicit and is a function of k_y/k_a. Following an iterative technique, values of t_f/T were evaluated as a function of k_y/k_a as shown in Figure D-2.

Solving Equation D-3 for the displacement of the base at $t = t_f$ gives:

$$d_{t_f} = k_a\left(\frac{T}{2\pi}\right)^2\left[\frac{2\pi t_f}{T} - \sin\left(\frac{2\pi t_f}{T}\right)\right] \quad \text{for the base} \quad \text{(D-8)}$$

The displacement of the block at time t_f can be expressed as

$$d_{t_f} = d_y + \Delta d_{(t_f - t_y)} \quad \text{(D-9)}$$

where

$$\Delta d_{(t_f - t_y)} = V_y(t_f - t_y) + \frac{1}{2} k_y(t_f - t_y)^2$$

and d_y, V_y, and k_y are obtained from Equations D-1 through D-3 by substituting $t = t_f$ into Equation D-9, resulting in the following expression for the permanent deformation of the block:

$$D_r = k_a\left(\frac{Tt_y}{2\pi}\right) - \left[k_a\left(\frac{T}{2\pi}\right)^2 \sin\left(\frac{2\pi t_y}{T}\right)\right] + k_a\frac{T}{2\pi}\left[1 - \cos\left(\frac{2\pi t_y}{T}\right)\right](t_f - t_y) - \frac{k_y}{2}(t_f - t_y)^2 \qquad \text{(D-10)}$$

Finally, normalizing the permanent deformation of Equation D-10, with respect to k_a, and square of period, T, results in the following expression.

$$D_n = \frac{D_r}{k_a T^2} = 4\pi^2\left[\sin\left(\frac{2\pi t_y}{T}\right) - \sin\left(\frac{2\pi t_f}{T}\right) + 2\pi\cos\left(\frac{2\pi t_y}{T}\right)\left(\frac{t_f}{T} - \frac{t_y}{T}\right) - \frac{k_y}{2k_a}(2\pi)^2\left(\frac{t_f}{T} - \frac{t_y}{T}\right)^2\right] \qquad \text{(D-11)}$$

where

$$D_r = d_{tf_{base}} - d_{tf_{block}}$$

Note that since t_y/T and t_f/T are function of only k_y/k_a, the normalized permanent deformation per cycle of motion, D_n, is also a function of only k_y/k_a.

Triangular Pulse

Referring to Figure D-3 (a) and (b), equations of motion for the triangular pulse are as following

For the range $0 \leq t \leq T/4$

$$A_1 = 4k_a t/T \quad \text{(D-12)}$$

$$V_1 = 2k_a t^2/T \quad \text{(D-13)}$$

$$D_1 = 2k_a t^3/3T \quad \text{(D-14)}$$

For the range $T/4 \leq t \leq 3T/4$

$$A_2 = 2k_a - 4k_a t/T \quad \text{(D-15)}$$

$$V_2 = 2k_a t - (2k_a t^2/T) - (k_a T/4) \quad \text{(D-16)}$$

$$D_2 = k_a t^2 - 2k_a t^3/3T - k_a Tt/4 + k_a T^2/48 \quad \text{(D-17)}$$

For the range $3T/4 \leq t \leq T$

$$A_3 = 4k_a t/T - 4k_a \quad \text{(D-18)}$$

$$V_3 = (2k_a t^2/T) - 4k_a t + 2k_a T \quad \text{(D-19)}$$

$$D_3 = (2k_a t^3/3T) - 2k_a t^2 + 2k_a Tt - 13k_a T^2/24 \quad \text{(D-20)}$$

From Figure D-3 (a) and Equation D-13

$$k_y/t_y = k_a/(T/4) \quad \text{or} \quad t_y = (k_y/k_a)(T/4) \quad \text{(D-21)}$$

$$V_{t_y} = V_{1@t_y} = 2k_a t_y^2/T \qquad \text{(D-22)}$$

where

k_y = yield acceleration of the block

T = predominant period of the motion

k_a = peak ground acceleration

t_y = time needed for acceleration of base to reach yield acceleration

Let

$$k_y/k_a = R$$

then according to Equations D-21 and D-22

$$t_y = RT/4$$

$$V_{t_y} = k_a R^2 T/8$$

Consequently, the velocity of the block, V_b, at the time $t > t_y$ will be

$$V_b = V_{t_y} + k_y (t - t_y) \qquad \text{(D-23)}$$

when the pulse reverses its direction (see Figure D-3 (a)) the velocity of the base starts to decrease and at time $t \geq t_f$ the block and the base move together.

i.e. $V_b = V_2$

where V_2 is defined by Equation D-16.

$$V_{t_y} + k_y (t - t_y) = 2k_a t - (2k_a t^2/T) - (k_a T/4) \quad \text{(D-24)}$$

The time after which the block and the base move together, t_f, can be calculated from Equation D-24 as following:

$$k_a R^2 T/8 + k_y (t_f - t_y) = (2k_a t_f) - (2k_a t_f^2/T) - (k_a T/4) \quad \text{(D-25)}$$

Dividing Equation D-25 by the quantity $(k_a T/8)$ and rearranging yields

$$16 (t_f/T)^2 + (8R - 16)(t_f/T) + (2 - R^2) = 0 \quad \text{(D-26)}$$

Equation D-26 explicitly defines the values of t_f/T for all the values of $R = k_y/k_a$.

The permanent deformation between the block and the base, D_r, is obtained from Equation D-27.

$$D_r = d_{t_{f\,base}} - d_{t_{f\,block}} \quad \text{(D-27)}$$

where $d_{t_{f\,base}}$ and $d_{t_{f\,block}}$ are the displacements of the base and the block, respectively, at time $t = t_f$, and are calculated from the following expressions using Equations D-14 and D-17.

$$d_{t_{f\,base}} = \left[k_a t_f^2 - \frac{2k_a t_f^3}{3T} - \frac{k_a T\, t_f}{4} + \frac{k_a T^2}{48} \right] \quad \text{(D-28)}$$

and

$$d_{t_{f\,block}} = d_{t_y} + \int_{t_y}^{t_f} V_t\,dt \qquad \text{(D-29)}$$

$$= \frac{2k_a t_y^3}{3T} + \left[\frac{2k_a t_y^2 t_f}{T} + k_y t_f^2 - 2k_y t_y t_f - \frac{2k_a t_y^3}{T} + k_y t_y^2\right]$$

where d_{t_y} is the permanent deformation of the block (and the base) at time $t = t_y$, calculated from Equation D-14, and V_{t_f} is the velocity of the block at time t_f. From Figure D-3

$$V_{t_f} = V_{t_y} + k_y(t_f - t_y) \qquad \text{(D-30)}$$

Substituting the right hand side of Equations D-28 and D-29 into Equation D-27, and dividing through by $k_a T^2$, the normalized permanent deformation between the base and the block, D_n, for triangular pulse can be expressed as an explicit function of R as following

$$D_n = \frac{D_r}{k_a T^2} = -\frac{1}{24}R^3 + \frac{3}{8}\frac{t_f}{T}R^2 - \frac{t_f^2}{T^2}R + \left[\frac{1}{48} - \frac{t_f}{4T} + \frac{t_f^2}{T^2} - \frac{2t_f^3}{3T^3}\right] \qquad \text{(D-31)}$$

The above formulation for the normalized permanent deformation of a triangular pulse is valid for the range where $t_f \leq 3T/4$. For the range where $t_f \geq 3T/4$, Equation D-26 becomes

$$16\,(t_f/T)^2 - 8(4 + R)(t_f/T) + (R + 16) = 0 \qquad \text{(D-32)}$$

This equation allows the calculation of values of t_f/T for any given value of R. Again, for this range the permanent deformation of the block can be calculated from Equation D-20 as

following

$$d_{t_f\,base} = \left[\frac{2k_a t_f^3}{3T} - 2k_a t_f^2 + 2k_a T t_f - \frac{13}{24} k_a T^2 \right] \qquad \text{(D-33)}$$

The equation for permanent deformation of the block remains the same as the previous case (i.e. Equation D-20). For the range where $t_f \geq 3T/4$, the relative permanent deformation normalized with respect to k_a and T^2 becomes

$$D_n = \frac{D_r}{k_a T^2} = -\frac{1}{24}R^3 + \frac{3\,t_f}{8T}R^2 - \frac{t_f^2}{T^2}R + \left[-\frac{13}{24} + \frac{2t_f}{T} - \frac{2t_f^2}{T^2} + \frac{2t_f^3}{3T^3} \right] \qquad \text{(D-34)}$$

Rectangular Pulse

The velocities of the base, V_b, and the block, V, for a rectangular motion can be calculated from the acceleration curve of Figure D-4 at time $t = t_f$ as following

$$V_b = k_y t_f \tag{D-35}$$

$$V = (k_a T/2) - k_a(t_f - T/2) \tag{D-36}$$

Equating V_b to V yields:

$$t_f = k_a T/(k_a + k_y) \tag{D-37}$$

The permanent deformation, D_r, associated with this time ($t = t_f$) is the difference in the area under the velocity curves shown in Figure D-4. Thus,

$$D_r = t_f (k_a - k_y) T/4 \tag{D-38}$$

Combining Equations D-34 and D-35 yields the following expression for D_n, the normalized permanent deformation, for one cycle of rectangular pulse.

$$D_n = \frac{D_r}{T^2 k_a} = \frac{1}{4}\left(\frac{1 - \frac{k_y}{k_a}}{1 + \frac{k_y}{k_a}}\right) = f\left(\frac{k_y}{k_a}\right) \tag{D-39}$$

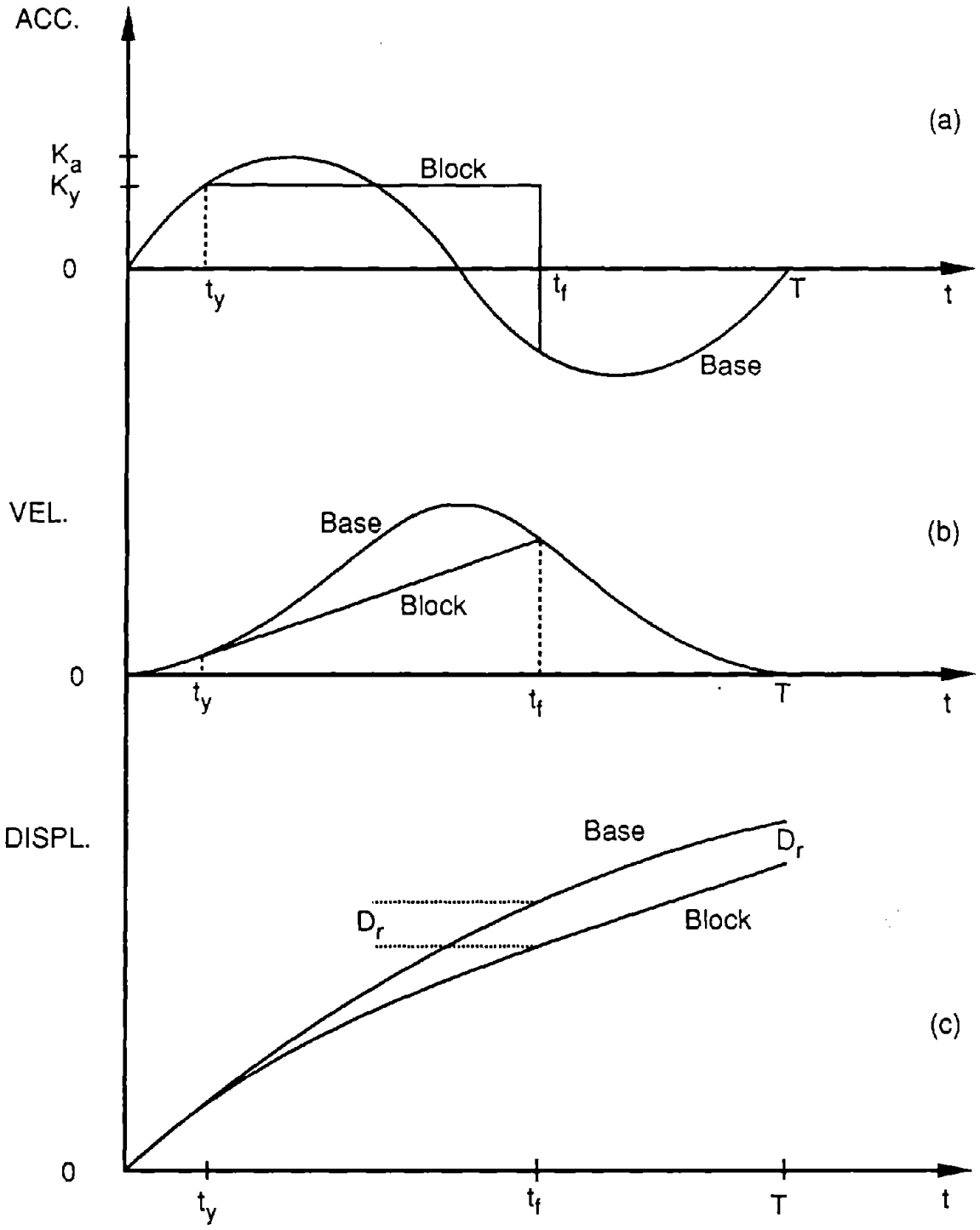

FIGURE D-1 PERMANENT DEFORMATION FOR SINUSOIDAL BASE EXCITATION

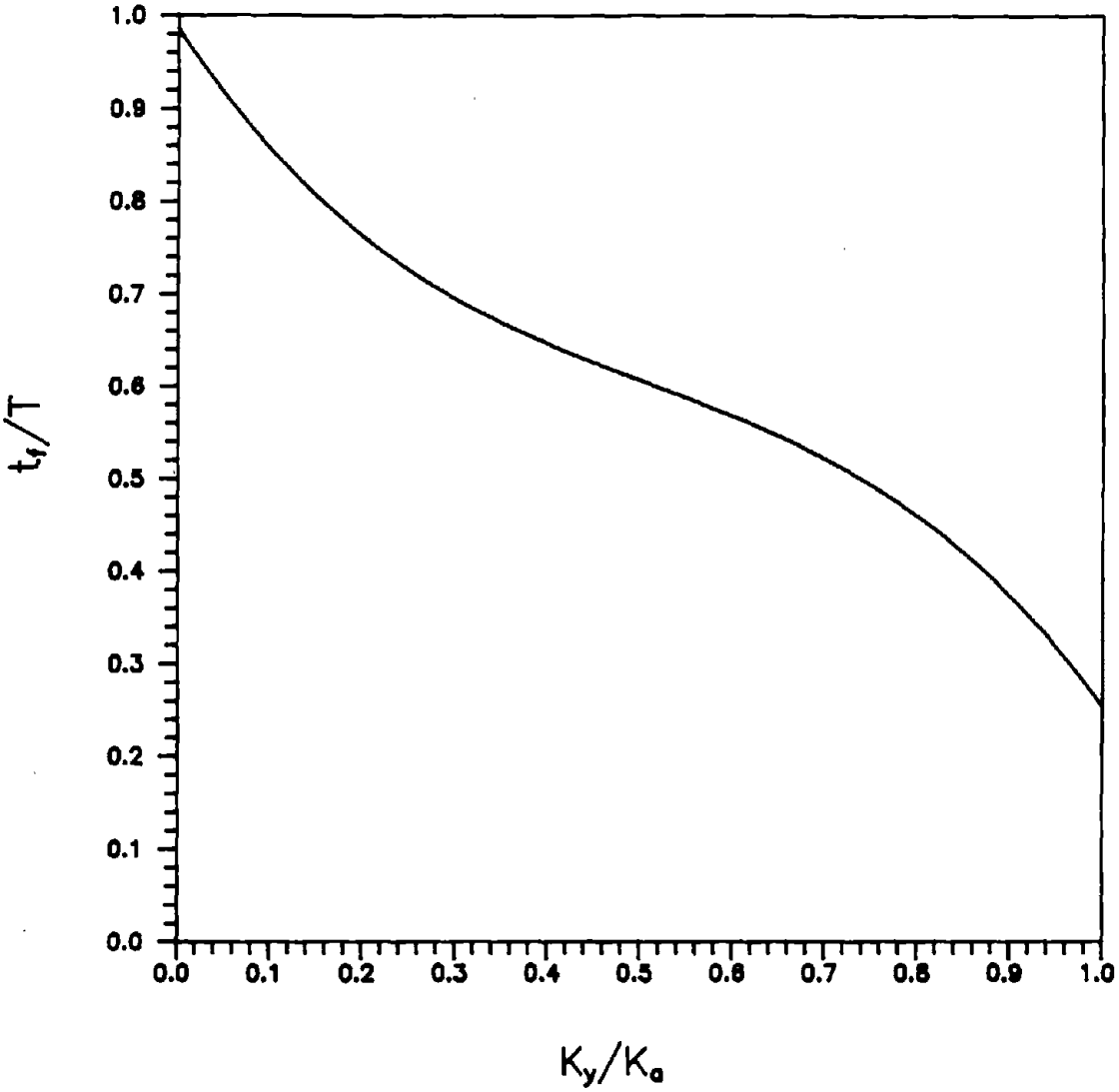

FIGURE D–2 t_f/T vs. K_y/K_a FOR SINUSOIDAL BASE EXCITATION

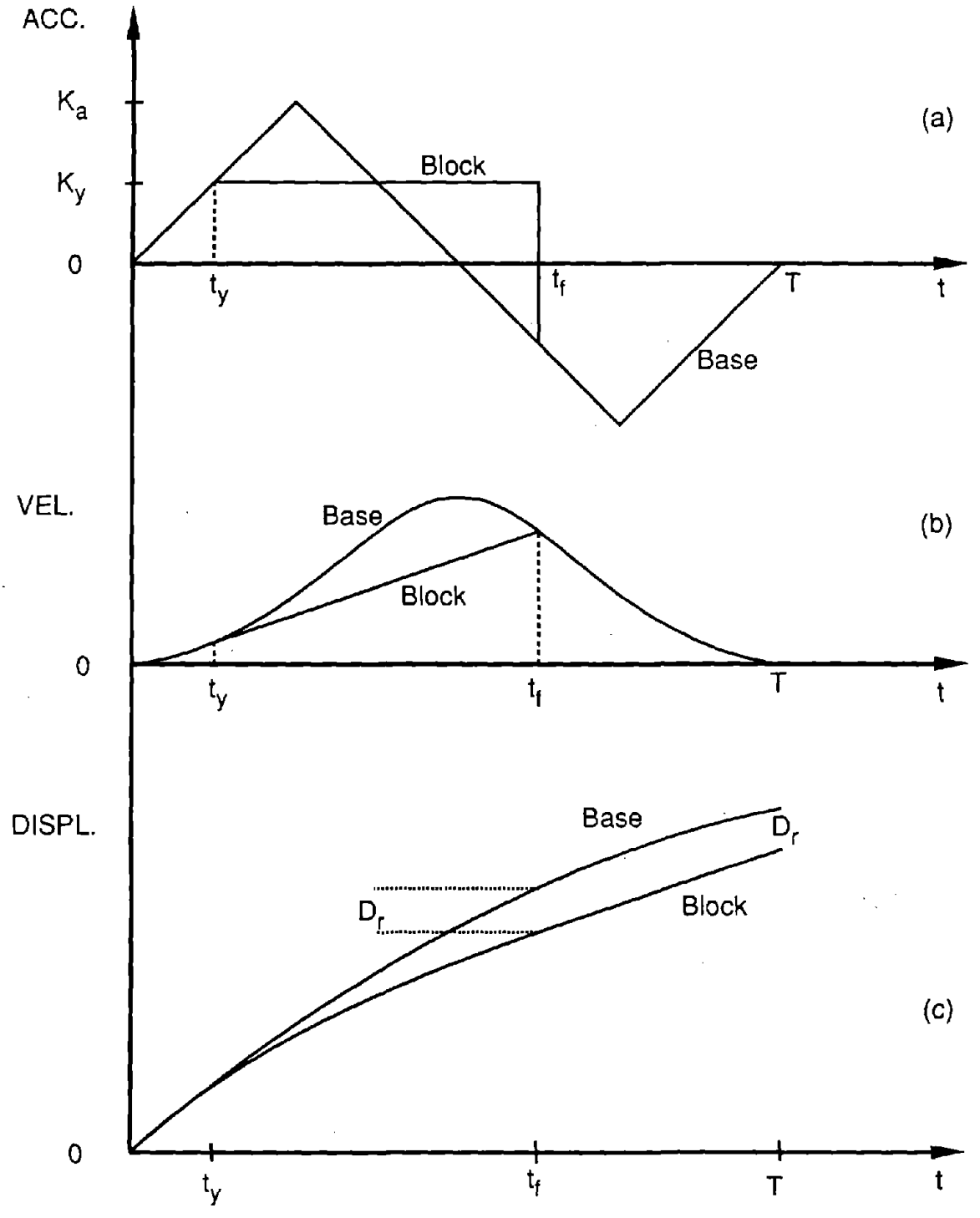

FIGURE D-3 PERMANENT DEFORMATION FOR TRIANGULAR BASE EXCITATION

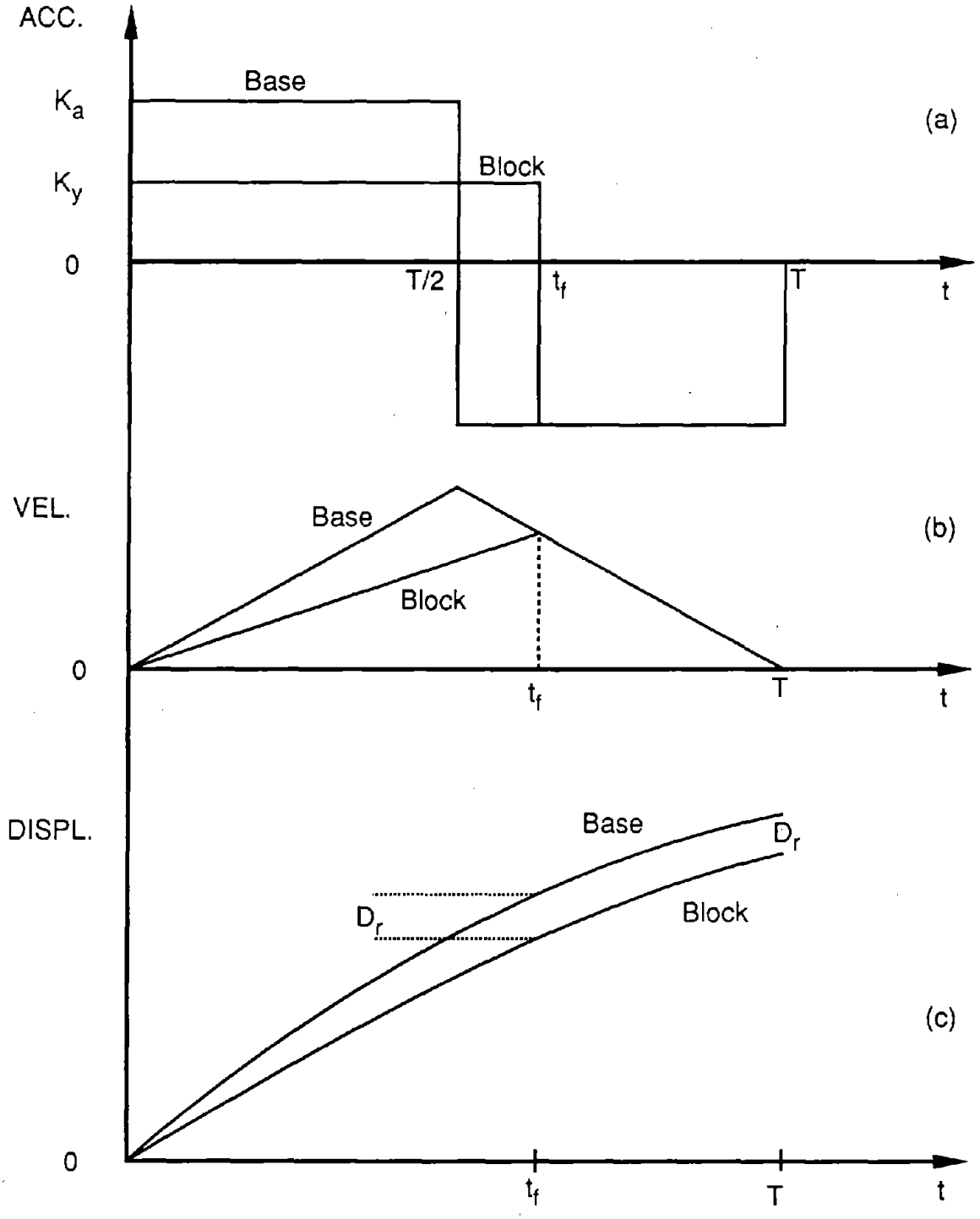

FIGURE D-4 PERMANENT DEFORMATION FOR RECTANGULAR BASE EXCITATION

APPENDIX E

PERFORMANCE ANALYSIS AND PROGRAM NIMPED

E-1 Mathematical Formulations

An analytical model was developed to calculate the probability of exceeding any specified value of permanent deformation. The model involves the expression

$$\log D_r = g(K_y/K_a) + S\,\xi_{D_n} + 2\log T + \log(K_a.N_{eq}) \qquad \text{(E-1)}$$

where

D_r = permanent deformation

K_y = yield acceleration of the cross-section of the dam

K_a = actual acceleration of the cross-section of the dam

S = random variable reflecting scatter of the available data about the above relationship resulting from the inherently random nature of seismic motions

ξ_{D_n} = the standard deviation of $\log D_n$

T = the predominant period of the motion of the dam cross-section

N_{eq} = number of equivalent uniform cycles for the motion of the dam cross-section

T, S, N_{eq}, K_y and K_a are random variables. $X = S\,\xi_{D_n}$ is a random variable that accounts for the uncertainty introduced into the above relationship due to the inherently random

nature of seismic ground motions. ξ_{D_n} is the value of the standard deviation of the normal random variate $X = S\,\xi_{D_n}$. Therefore, S is the standard normal variate. Treating X as normally distributed is justified by probability plots of the available data, discussed in Section IV-1.4.

The seismic performance analysis requires calculation of the probability of the permanent deformation of the dam exceeding some pre-specified value, given the maximum acceleration and the number of equivalent cycles of the motion of the dam (i.e., $P[D_r > d_r \mid K_a = k_a , N_{eq} = n_{eq}]$. This can be formally calculated by performing the following integration, provided that the probability density functions for each of the random variables are known.

$$P[D_r > d_r \mid k_a, n_{eq}] = \int_{\frac{k_y}{k_a}=-\infty}^{+\infty} \left\{ \int_{t=-\infty}^{+\infty} \left[\int_{s=s_1}^{+\infty} f_{\left(S \mid T, \frac{K_y}{k_a}\right)}\left(s \mid t, \frac{k_y}{k_a}\right) ds \right] f_{\left(T \mid \frac{K_y}{k_a}\right)}\left(t \mid \frac{k_y}{k_a}\right) dt \right\} f_{\frac{K_y}{k_a}}\left(\frac{k_y}{k_a}\right) d\frac{k_y}{k_a} \qquad \text{(E-2)}$$

where

$$s_1 = \frac{\log d_r - \log(k_a n_{eq}) - g\left(K_y/k_a\right) - 2\log T}{\xi_{D_n}} \qquad \text{(E-3)}$$

The region of integration is defined by

$$g(K_y/K_a) + S\,\xi_{D_n} + 2\log T + \log(k_a\, n_{eq}) > \log d_r \qquad \text{(E-4)}$$

or alternatively by

$$S > s_1$$

$$S > \frac{\log d_r - \log(k_a\, n_{eq}) - g\left(K_y/k_a\right) - 2\log T}{\xi_{D_n}} \qquad \text{(E-5)}$$

This can be visualized by inspecting Figure E-1. A three-dimensional cartesian coordinate system is used to represent the relationship between the random variables, T, S, and K_y, and to represent their probability density functions. The surface shown represents all the combinations of values of S, T, and K_y that give $D_r = d_r$. All the points above the surface represent combinations giving $D_r > d_r$ and all the points below the surface represent combinations giving $D_r < d_r$. The probability density functions assumed in this study for each of these three random variables are shown below and to the left of the coordinate system. By definition, the probability density function of K_y gives the probability of $k_{ya} < K_y < k_{yb}$, which is equal to the area under the probability density function between k_{ya} and k_{yb}. Similarly, the probability of $t_a < T < t_b$ equals the area beneath the probability density function of T between t_a and t_b. The probability that both $k_{ya} < K_y < k_{yb}$ and $t_a < T < t_b$ is equal to the product of the above two areas. Furthermore, the probability that both $k_{ya} < K_y < k_{yb}$ and $t_a < T < t_b$, and also $D_r > d_r$ is equal to the product of the above two areas and the area under the probability density function of S within the region $S > s_1$. If these computations are performed for all the possible combinations of ranges Δk_y and Δt, which are indicated by the grid on the three-dimensional surface, and then their

results are summed up, the final summation is the probability that $D_r > d_r$. This series of computations is what the above integration represents. The integration can be performed analytically, in which Δk_y and Δt are made to approach zero in the limit. Alternatively, the integration can be performed to a high degree of accuracy by numerical means, which was done in this study. Specifically, integration with respect to the random variable, S, was performed by 16 point Gauss Quadrature. The integrations with respect to T and K_y were performed by setting Δk_y and Δt to reasonably small values and then performing the above described computations and summation. A computer program was written for this purpose. It is called Numerical Integration Methodology for the Probabilistic Evaluation of Deformation or NIMPED for short. The listing of the program is given in Section E-2.

The random variables T and K_y were taken to be normally distributed. However, the negative tail of each of these distributions was truncated and it was assumed that the probability of the random variable taking on the value zero is equal to the truncated negative area. This was necessary due to the fact that the surface defined by Equations E-4 and E-5 is not defined for negative values of T and K_y.

It is reasonable to take the random variable S as normally distributed due to the fact that probability plots of the available data indicated that the $\log D_n$ is normally distributed for any given ratio k_y/k_a. This is illustrated by the plots of $\log D_n$ versus frequency of exceedance in Figure 12 in Section IV-1.4. In addition, the nearly equal slopes of these plots suggests that the standard deviation of $\log D_n$, or i.e. ξ_{D_n}, is independent of k_y/k_a.

The calculated probability, $P[D_r > d_r]$, is conditioned upon the values of the random variables N_{eq} and K_a being equal to two specific values, designated by n_{eq} and k_a, respectively. A description of the calculation of the probability of the joint occurrence of

N_{eq} and K_a being within specified ranges is given in Section IV.

E-2 Program NIMPED

Program NIMPED computes the probability of exceeding a specified level of earthquake-induced permanent deformation of an earth dam.

The program runs on IBM-PC or compatibles, and requires an input file named NIMPED.DAT. To run the program just type NIMPED. The output from the program is stored in a file named NIMPED.OUT.

User's Guide for NIMPED

The following is the format for the input data in NIMPED.DAT.

Line 1 (Free Format, data separated by commas or single spaces)

MIUKY = mean value of the yield acceleration of the cross-section of the dam, K_y, in g's.

SIGMAK = standard deviation of K_y, σ_{K_y}., in g's.

KA = acceleration of the cross-section of the dam, K_a, in g's.

NEQ = number of uniform cycles of motion for the dam, N_{eq}, in cycles.

MIUT = mean value of the predominant period of the seismic motion, T, in seconds.

SIGMAT = standard deviation of T, σ_T, in seconds.

SIGMAM = standard deviation of the function $\log D_n = g(K_y/K_a)$, use $\sigma_{\log D_n} = 0.45$.

UR = specified permanent deformation, probability of exceedence of which is to be computed, d_r, in units of length.

Line 2 (Free Format)

NDR = Number of intervals of K_y/K_a used in the numerical integration. (100 to 200)

RMIN = Minimum value of K_y/K_a used in the numerical integration. (Generally equal to zero)

RMAX = Maximum value of K_y/K_a used in the numerical integration. (Generally equal to 1.0)

Line 3 (Free Format)

NDT = Number of intervals of T used in the numerical integration. (100 to 200)

TMIN = Minimum value of T used in the numerical integration. (Generally equal to zero)

TMAX = Maximum value of T used in the numerical integration. (Generally equal to the mean of T plus 3 to 4 standard deviation of T)

Output File NIMPED.OUT

The output of the program NIMPED consists of the listing of the following parameters and results.

MIUKY = mean value of the yield acceleration of the cross-section of the dam, K_y, in g's.

SIGMAK = standard deviation of K_y, σ_{K_y}., in g's.

KA = acceleration of the cross-section of the dam, K_a, in g's.

NEQ = number of uniform cycles of motion for the dam, N_{eq}, in cycles.

MIUT = mean value of the predominant period of the seismic motion, T, in seconds.

SIGMAT = standard deviation of T, σ_T, in seconds.

UR = specified permanent deformation, probability of exceedence of which is to be computed, d_r, in units of length.

MIUR = Mean value of K_y/K_a .

DISP = Normalized permanent deformation = $D_n = d_r/(k_a N_{eq} T^2)$

TPROB = Probabilty of exceeding the value of the specified permanent deformation d_r.

Listing of the computer program NIMPED along with a sample input and output files follow.

```
C      PROGRAM  NIMPED
C      (Numerical Integration Methodology for Probabilistic
C       Evaluation of Deformations)
C*********************************************************************
C     THIS PROGRAM CALCULATES PROBABILITY OF EXCEEDING A CERTAIN LEVEL
C     OF PERMANENT DEFORMATION OF AN EARTH DAM USING NUMERICAL
C     INTEGRATION TECHNIQUES FOR MULTIVARIATE FUNCTION
C*********************************************************************
C*********************************************************************
C     NOMENCLATURE
C
C  MIUKY  = Ky = MEAN VALUE OF YIELD ACCELERATION
C  SIGMAK = STANDARD DEVIATION OF Ky
C  KA     = Ka = AVERAGE DAM ACCELERATION
C  NEQ    = NUMBER OF EQUIVALENT UNIFORM CYCLES
C  UR     = Dr = ACTUAL DEFORMATION (IN UNITS OF LENGTH)
C  R      = Ky/Ka = RATIO OF YIELD ACCELERATION TO AVG. DAM ACCELERATION
C  SIGMAR = STANDARD DEVIATION OF R (=Ky/Ka)
C  MIUR   = MEAN VALUE OF R (=Ky/Ka)
C  NDR    = NUMBER OF INTERVALS OF R CONSIDERED
C  RMIN   = MINIMUM VALUE OF R CONSIDERED (OF INTEREST)
C  RMAX   = MAXIMUM VALUE OF R CONSIDERED (OF INTEREST)
C  DR     = LENGTH OF R INTERVALS
C  T      = PREDOMINANT PERIOD OF THE DAM CONSIDERED
C  MIUT   = MEAN VALUE OF T
C  SIGMAT = STANDARD DEVIATION OF T
C  NDT    = NUMBER OF INTERVALS OF T CONSIDERED
C  TMIN   = MINIMUM VALUE OF T CONSIDERED (OF INTEREST)
C  TMAX   = MAXIMUM VALUE OF T CONSIDERED (OF INTEREST)
C  DT     = LENGTH OF T INTERVALS
C  SIGMAM = STANDARD DEVIATION OF M
C  DP     = UR/(NEQ*KA) = PERMANENT DEFORMATION NORMALIZED WITH RESPECT TO
C           AVG. DAM ACCELERATION AND NUMBER OF EQUIVALENT CYCLES
C  SR     = STANDARD NORMAL VARIATE OF R
C  ST     = STANDARD NORMAL VARIATE OF T
C  GR     = A MATHEMATICAL EXPRESSION THAT RELATES NORMALIZED DEFORM. TO R
C  DFT    = VALUE OF PDF FOR STANDARD VARIATE OF T (i.e. ST)
C  S      = VARIABLE THAT PRESENTS THE UNCERTAINTY OF THE MODEL
C  DISP   = Dn = VALUE OF NORMALIZED DEFORMATION BEING EXCEEDED
C  TPROB  = TOTAL PROBABILITY OF EXCEEDENCE OF VALUE OF DISP
C*********************************************************************
C*********************************************************************
C
      IMPLICIT REAL*8(A-H,O-Z)
      REAL*8 MIUT,MIUR,MPROB,KA,NEQ,MIUKY
C
      JR=5
      JW=6
      PI=4.D0*DATAN(1.D0)
C
C*********************************************************************
C     THE LOOP BELOW WILL ALLOW TO INPUT AND PROCESS SEVERAL DATA SET IN
C     ONE FILE (ACTIVATE THE LOOP IF MORE THAN ONE DATA SET ARE INVOVED)
C*********************************************************************
C
C     DO 65 K=1,1000000
C
     OPEN (5,FILE='NIMPED.DAT')
      OPEN (6,FILE='NIMPED.OUT')
C
```

```
      READ(JR,*,END=70) MIUKY, SIGMAK, KA, NEQ, MIUT, SIGMAT,
     1                  SIGMAM, UR
C
      MIUR = MIUKY / KA
      SIGMAR = SIGMAK / KA
      DP = UR /(KA * NEQ)
C
C*********************************************************************
C     IN THE NEXT FEW LINES DR AND DT, LENGTH OF INTERVALS FOR R AND T,
C     RESPECTIVELY,CONSIDERED FOR INTEGRATION PURPOSES, ARE CALCULATED
C     BASED ON THEIR MAX. AND MIN. VALUES.
C*********************************************************************
C
      READ(JR,*) NDR, RMIN, RMAX
      IF(RMIN.LT.0.) RMIN = 0.0
      IF(RMAX.GT.1.) RMAX = 1.0
      DR = (RMAX-RMIN)/NDR
C
      READ(JR,*) NDT, TMIN, TMAX
      IF(TMIN.LT.0.) TMIN = 0.0
      DT = (TMAX-TMIN)/NDT
C
C*********************************************************************
C TRNCATION LEFT OF T = 0.0
C*********************************************************************
C
      R = 0.D0
      SR = (0.D0 - MIUR)/SIGMAR
      TRUNC = GAUSS(SR)
C
      GR = 0.2232064
C
      MPROB = 0.0
      T = TMIN - DT/2.
      DO 10 J=1,NDT
      T = T + DT
      ST = (T-MIUT)/SIGMAT
      DFT = DF(ST)/SIGMAT
C
      S = (DLOG10(DP) - 2*DLOG10(T) - GR) / SIGMAM
C
      AREA = 1.D0 - GAUSS(S)
C
      MPROB = MPROB + AREA*DFT*DT
  10  CONTINUE
C
      TPROB = MPROB * TRUNC
C
C*********************************************************************
C INTEGRATE FROM R = 0 TO R = (+)INFINITY
C*********************************************************************
C
      R = RMIN - DR/2.
      DO 30 I=1,NDR
      R = R + DR
      SR = (R - MIUR)/SIGMAR
      DFR = DF(SR)/SIGMAR
C
C*********************************************************************
C GR IS PART OF THE PERFORMANCE FUNCTION. GR DEPENDS ON
```

```
C R ALONE, AND THUS DOES NOT NEED TO BE IN THE T DO LOOP
C*********************************************************************
C
      GR = -11.482645*R**3 + 16.381141*R**2 - 10.121701*R
     ,      +0.2232064
C
C*********************************************************************
C INTEGRATE FROM T = 0 TO T = TMAX
C*********************************************************************
C
      MPROB = 0.D0
      T = TMIN - DT/2.
      DO 20 J=1,NDT
      T = T + DT
      ST = (T-MIUT)/SIGMAT
      DFT = DF(ST)/SIGMAT
C
C*********************************************************************
C 'INTEGRATE' FROM S = (-)INFINITY TO
C S = THE INVERSE FUNCTION OF R,T,LOGDP
C THIS GIVES THE CUMULATIVE PROBABILITY DISTRIBUTION OF S
C CONDITIONAL UPON R AND T
C*********************************************************************
C
      S = (DLOG10(DP) - 2*DLOG10(T) - GR) / SIGMAM
      AREA = 1.D0 - GAUSS(S)
C
C*********************************************************************
C CALCULATE THE CUMULATIVE PROBABILITY
C DISTRIBUTION OF S CONDITIONAL ON R ALONE
C*********************************************************************
C
      MPROB = MPROB + AREA*DFT*DT
  20  CONTINUE
C
C*********************************************************************
C CALCULATE THE CUMULATIVE PROBABILITY
C DISTRIBUTION OF S UNCONDITIONALLY, WHICH IS
C*********************************************************************
C
      TPROB = TPROB + MPROB*DFR*DR
  30  CONTINUE
C
      DISP = DP/MIUT**2
C
      WRITE(JW,*)'          MIUKY    = ', MIUKY
      WRITE(JW,*)'          SIGMAK   = ', SIGMAK
      WRITE(JW,*)'          KA       = ', KA
      WRITE(JW,*)'          NEQ      = ', NEQ
      WRITE(JW,*)'          MIUT     = ', MIUT
      WRITE(JW,*)'          SIGMAT   = ', SIGMAT
      WRITE(JW,*)'          UR       = ', UR
      WRITE(JW,*)'          MIUR     = ', MIUR
      WRITE(JW,*)'          DISP     = ', DISP
      WRITE(JW,*)'          TOTAL PROB. OF EXCEEDING = TPROB = ', TPROB
C
C 65  CONTINUE
C
  70  STOP
      END
```

```
C
C
C
C***********************************************************************
C***********************************************************************
C
      DOUBLE PRECISION FUNCTION DF(DX)
C
C***********************************************************************
C
C THIS FUNCTION COMPUTES THE VALUE OF PDF OF A NORMAL VARIABLE AT ANY
C POINT
C
      DOUBLE PRECISION DX,PI
      PI = 4.D0*DATAN(1.D0)
      DF = (1.D0/DSQRT(PI*2.D0))*DEXP(-0.5D0*DX**2)
      RETURN
      END
C
C
C
C***********************************************************************
C***********************************************************************
C
      DOUBLE PRECISION FUNCTION GAUSS(S)
C
C***********************************************************************
C
      DOUBLE PRECISION P(8),Q(9),S
C
C      THIS FUNCTION COMPUTES THE INTEGRAL OF THE STANDARD NORMAL
C      VARIABLE FROM (-) INFINITY TO THE UPPER LIMIT OF INTEGRATION, DP.
C
      DATA P(1),P(2),P(3),P(4),P(5),P(6),P(7),P(8)
     1  /0.88347894260849D+3, 0.15496793124037D+4,
     1   0.13471941340976D+4, 0.72304000277753D+3,
     1   0.25550049469496D+3, 0.59240010112914D+2,
     1   0.83765310814197D+1, 0.56418955944261D+0/
      DATA Q(1),Q(2),Q(3),Q(4),Q(5),Q(6),Q(7),Q(8),Q(9)
     1  /0.88347994260850D+3, 0.25465785458098D+4,
     1   0.33372213699893D+4, 0.26067120152651D+4,
     1   0.13335699756780D+4, 0.46028512369160D+3,
     1   0.10550025439769D+3, 0.14847012237523D+2,1.D0/
      DATA TOL /1.0E-8/
      Y=S/SQRT(2.)
C
        IF(ABS(Y).LT.TOL)THEN
            GAUSS=0.5
            RETURN
      ENDIF
C
      IF(Y.GT.8.)THEN
            GAUSS=1.
            RETURN
      ENDIF
C
      IF(Y.LT.-8.)THEN
            GAUSS=0.
            RETURN
      ENDIF
```

```
C
C      APPROXIMATE WITH RATIONAL FUNCTION
C
       Z=EXP(-Y*Y)
       YABS=ABS(Y)
       PNUM=P(8)
       DO 1 I=7,1,-1
1       PNUM=P(I)+YABS*PNUM
       QDEN=Q(9)
       DO 2 I=8,1,-1
2       QDEN=Q(I)+YABS*QDEN
       GAUSS=(PNUM/QDEN)*0.5*Z
       IF(S.GT.0.) GAUSS=1.0-GAUSS
C
       RETURN
       END

C*******************************************************************************
C*******************************************************************************
```

Example input data.
Filename = NIMPED.DAT

```
2.254,1.1270,6.762,12,0.7,0.175,0.45,4,
100,0,1,
100,0,4,
```

Example output.
Filename = NIMPED.OUT

```
MIUKY     =        2.25400000000000000
SIGMAK    =        1.12700000000000000
KA        =        6.76199999999999957
NEQ       =       12.00000000000000000
MIUT      =        0.69999999999999996
SIGMAT    =        0.17499999999999999
UR        =        4.00000000000000000
MIUR      =        0.33333333333333337
DISP      =        0.10060220479792038
TOTAL PROB. OF EXCEEDING = TPROB =        0.18818486207860316
```

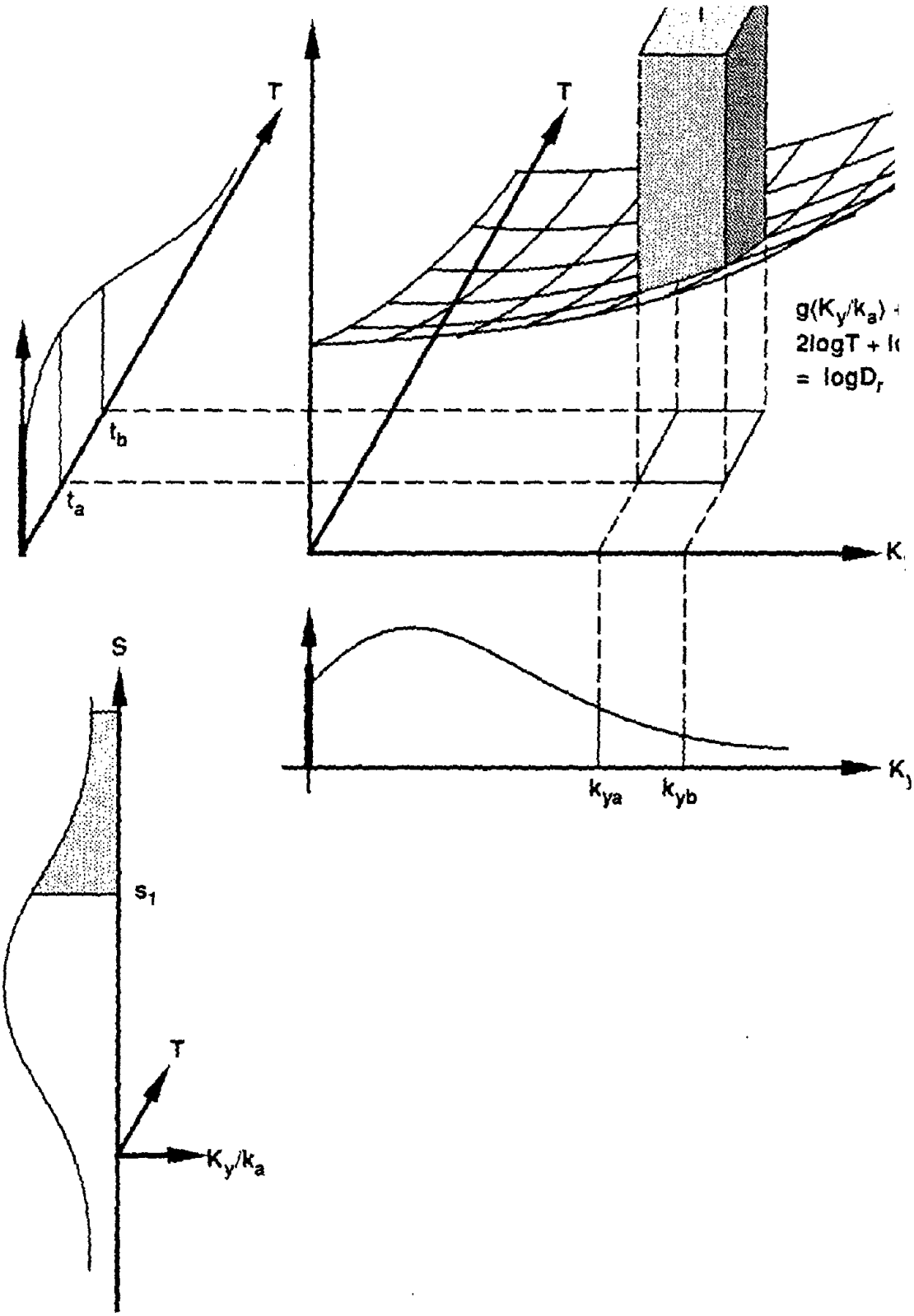

FIGURE E-1 SCHEMATIC REPRESENTATION OF THE DISTRIBUTIONS FOR T, S
K_y/k_a, AND THEIR JOINT PROBABILITY DENSITY FUNCTION

APPENDIX F

RELATIONSHIP BETWEEN UNCERTAINTIES IN K_y AND T

The standard deviations of T and K_y/K_a can be obtained based on statistical evaluation or subjective judgement by the investigator. This appendix describes one possible relationship between μ_{K_y} and μ_T, and between the $c.o.v._{K_y}$ and the $c.o.v._T$ for cohesionless soils and a similar relationship for cohesive soils where

μ_{K_y} = mean value of K_y

μ_T = mean value of T

$c.o.v._{K_y}$ = coefficient of variation of K_y

$c.o.v._T$ = coefficient of variation of T

These relationships apply to the case of an earth dam founded on a relatively rigid base

Cohesionless Soils

For cohesionless soils the following empirical relationships have been proposed among the shear modulus, G, the shear wave velocity, C_s, the mass density, ρ, and the predominant period, T, of a homogeneous soil layer of thickness H, on bedrock.

$$C_s = \sqrt{\frac{G}{\rho}} \qquad \text{(F-1)}$$

and

$$T = 4H/C_s \qquad \text{(F-2)}$$

Also Seed and Idriss (1970) proposed the following relationship

$$G = 1000\, K_2 \sqrt{\bar{\sigma}_m} \qquad \text{(F-3)}$$

where

K_2 = constant which is a function of relative density of cohesionless soil

$\bar{\sigma}_m$ = effective overburden pressure

Considering Equations F-1 through F-3 it follows that

$$T = \frac{4H\sqrt{\rho}}{\sqrt{1000\sqrt{\bar{\sigma}_m}}} (K_2)^{-\frac{1}{2}} \qquad \text{(F-4)}$$

The quantity

$$\frac{4H\sqrt{\rho}}{\sqrt{1000\sqrt{\bar{\sigma}_m}}}$$

is constant for a given soil at a given location. Therefore, Equation F-4 can be written as

$$T = C\,(K_2)^{-1/2} \qquad \text{(F-5)}$$

Considering the Taylor series expansion of Equation F-5, variances of T and K_2, can be related as follows

$$\text{Var}\,T = C^2\left(\frac{1}{4}\right)(K_2)^{-3}\text{Var}\,K_2 \qquad \text{(F-6)}$$

dividing both sides by μ_T^2

$$\frac{\text{Var}\,T}{\mu_T^2} = \frac{C^2}{4\mu_T^2}(K_2)^{-3}\,\text{Var}\,K_2 \qquad \text{(F-7)}$$

but if μ_T is replaced by the right hand side of the Equation (F-5), it results in

$$\frac{\text{Var}\,T}{\mu_T^2} = \frac{C^2}{4C^2(K_2)^{-1}}(K_2)^{-3}\,\text{Var}\,K_2 \qquad \text{(F-8)}$$

or

$$\frac{\text{Var}\,T}{\mu_T^2} = \frac{1}{4}\,\frac{\text{Var}\,K_2}{(K_2)^2} \qquad \text{(F-9)}$$

According to Seed and Idriss (1970) there is a relationship between K_2 and relative density D_r of cohesionless soils. A plot of their data, for small shear strains, indicates that this relationship is nearly a straight line; therefore, K_2 is linearly proportional to D_r. On the other hand Dunn et. al. (1980) have developed a relationship between D_r and the angle of internal friction ϕ, which can be approximated as a straight line. These plots are shown in Figures F-1 and F-2 respectively. In the range of interest, the angle of internal friction, ϕ, and its tangent are almost equal. (maximum difference is about 10% for the range considered.) The above mentioned relationships lead to the following conclusions:

$$c.o.v._T = \frac{1}{2} c.o.v._{K_2} \simeq \frac{1}{2} c.o.v._{D_r} \simeq \frac{1}{2} c.o.v._{\phi} \simeq \frac{1}{2} c.o.v._{\tan\phi} \qquad \text{(F-10)}$$

For the failure wedge considered in the example problem, as well as for a wide variety of stability problems, there exists a linear relationship between K_y and $\tan\phi$ (as shown in Figure F-3) suggesting that $c.o.v._{K_y} = c.o.v._{\tan\phi}$. From above mentioned relationships among different parameters and their variances it can be reasonably concluded that:

$$c.o.v._T \sim \frac{1}{2} c.o.v._{K_y} \qquad \text{(F-11)}$$

Cohesive Soils

For a cohesive soil Equation F-3 becomes

$$G = c\, S_u \qquad \text{(F-12)}$$

where S_u is the undrained shear strength of the soil and c is a constant. Equations F-1 and F-2 hold both for cohesive and cohesionless soils. Therefore

$$T = \frac{4H\sqrt{\rho}}{\sqrt{G}} = \frac{4H\sqrt{\rho}}{\sqrt{c}}\left(\frac{1}{\sqrt{S_u}}\right) \qquad \text{(F-13)}$$

Again the quantity

$$\frac{4H\sqrt{\rho}}{\sqrt{c}}$$

is constant and the only quantity changing (involved in uncertainty) is S_u. Thus, considering the variances of both sides in Equation F-13 and following the same steps as in cohesionless soils it can be shown that

$$c.o.v._T \sim \frac{1}{2} c.o.v._{S_u} \qquad \text{(F-14)}$$

Bolognesi (1980) has shown that for typical soil profiles, F.S. against slope instability is approximately linearly related to S_u. Hence, K_y which is related to F.S. can be assumed to be also linearly related to S_u. Thus,

$$c.o.v._T \sim \frac{1}{2} c.o.v._{K_y} \qquad \text{(F-15)}$$

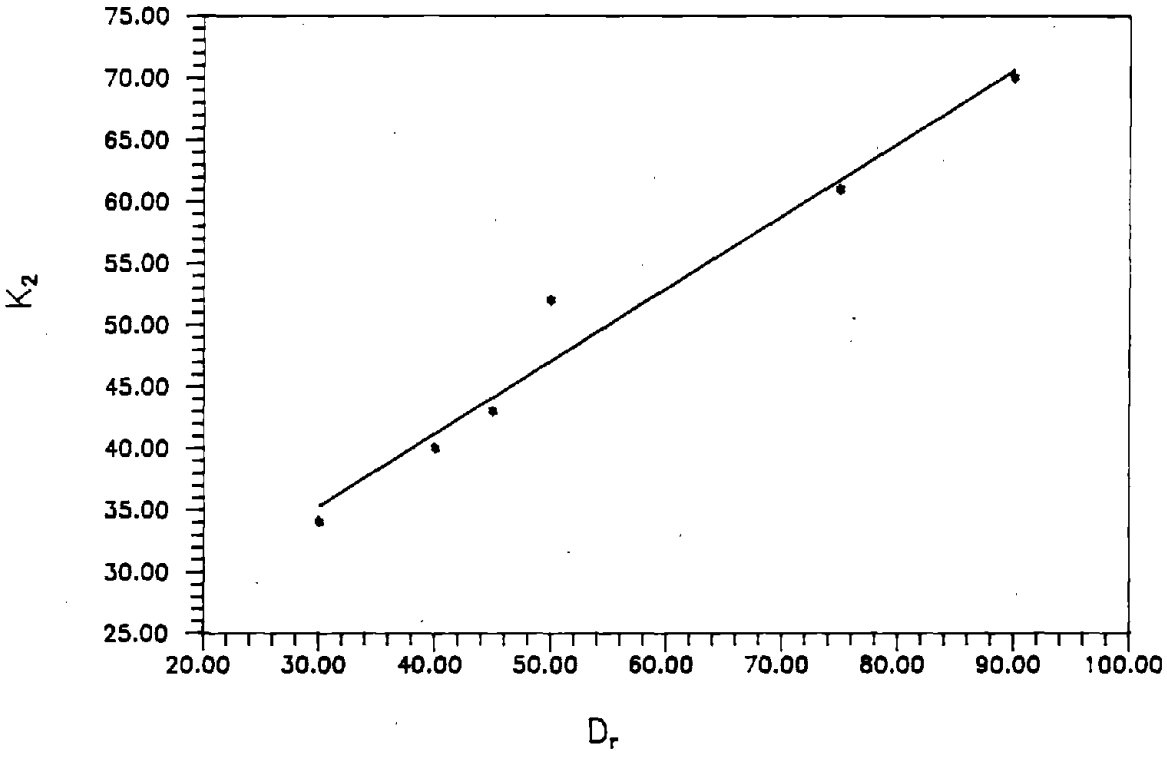

FIGURE F-1 K_2 VS. RELATIVE DENSITY, D_r FOR SANDS FOR SMALL STRAINS ($\gamma = 10^{-4}$)

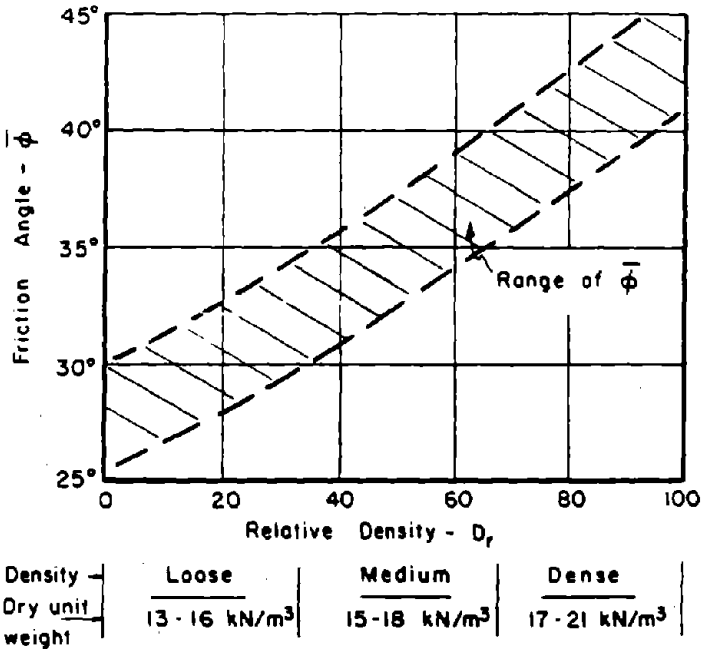

FIGURE F-2 ANGLE OF INTERNAL FRICTION, Φ, AS A FUNCTION OF RELATIVE DENSITY OF SANDS, D_r (DUNN et al 1980)

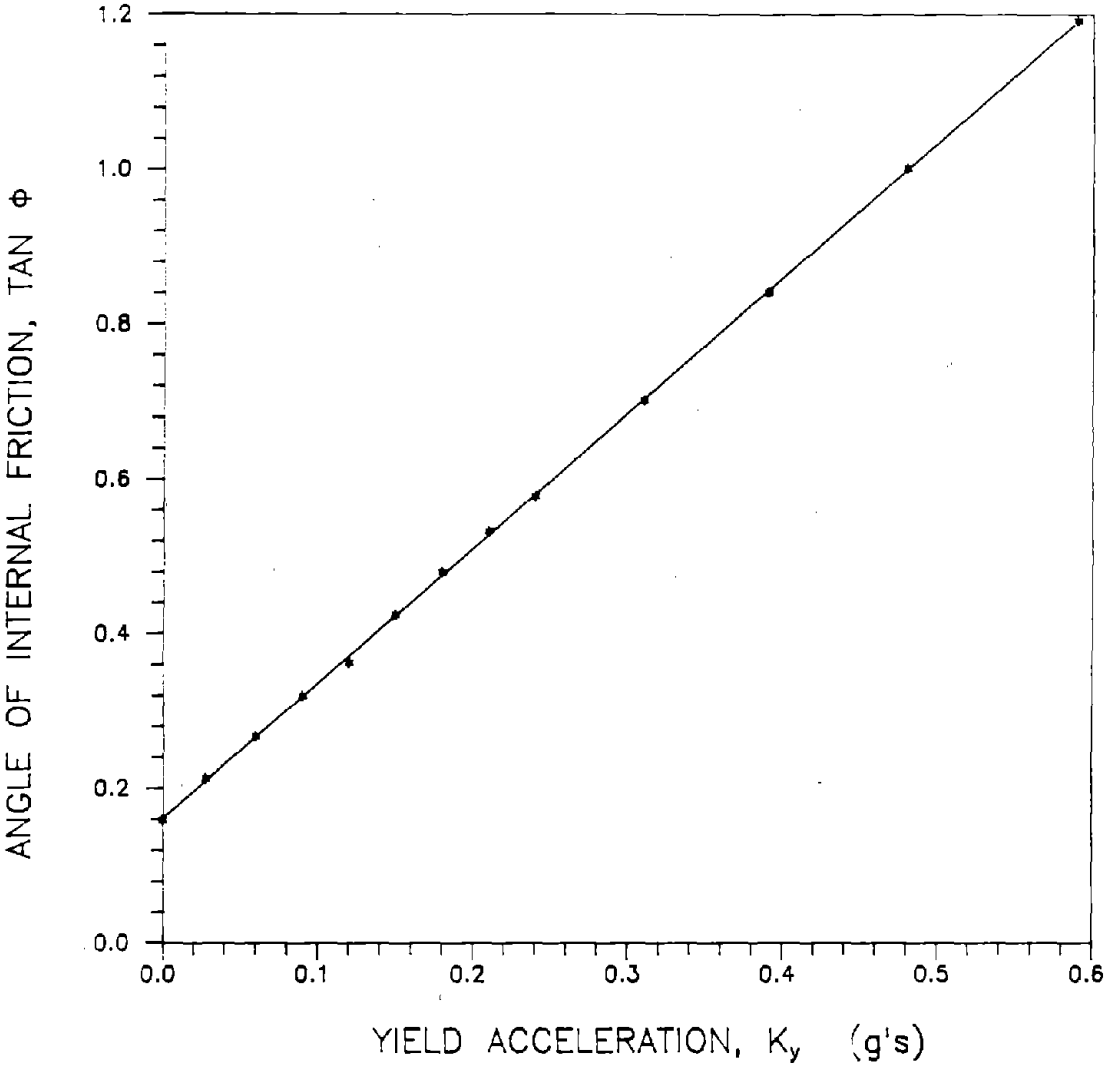

FIGURE F-3 TAN Φ VS. YIELD ACCELERATION, K_y , FOR THE EXAMPLE PROBLEM CONSIDERED